Report Prepared by:

Alberto A. Sagüés*
Jae Bong Lee*
Xiaoyuan Chang*
Howard Pickering[H]
Eric Nystrom[H]
William Carpenter*
S. C. Kranc*
Tonya Simmons*
Bruce Boucher*
Sherry Hierholzer*

*University of South Florida

HThe Pennsylvania State University

CORROSION OF EPOXY COATED REBAR IN FLORIDA BRIDGES

Final Report to Florida D.O.T.
WPI No. 0510603, State Job No. 99700-7556-010

Alberto A. Sagüés, P.I.
Department of Civil Engineering and Mechanics

College of Engineering
University of South Florida
Tampa, Florida 33620-5350
May, 1994

This electronic version was prepared 03/01/2002
Errata have been corrected in pages T1, T7 and T10

ACKNOWLEDGMENT

This report was prepared in cooperation with the State of Florida Department of Transportation (FDOT). The field investigations were performed jointly with personnel from the Corrosion Section of the Materials Office, Florida Department of Transportation, Gainesville, Florida. The Corrosion Section provided also valuable assistance in the preparation of concrete laboratory specimens and analysis of concrete samples. The opinions, findings and conclusions expressed in this publication are those of the authors and not necessarily those of the State of Florida Department of Transportation.

CONTENTS

TITLE PAGE i
ACKNOWLEDGMENT ii
CONTENTS 1
EXECUTIVE SUMMARY 4
1. INTRODUCTION 7
1.1 Background 7
1.2 Information needs critical to FDOT 8
1.3 Objectives of the project. 9
1.4 Approach. 9
2. METHODOLOGY - FIELD INVESTIGATIONS 11
2.1 Test site selection. 11
2.2 Site activities. 11
2.2.1 Visual examination and soundings 11
2.2.2 Rebar cover 11
2.2.3 Concrete Resistivity 12
2.2.4 Coring 12
2.2.5 Rebar sample extraction 12
2.2.6 Field coating adherence determination 13
2.2.7 Half-cell potentials 13
2.2.8 Macrocell Current Measurements 13
2.2.9 Mutual Resistance measurements 14
2.2.10 Polarization resistance 14
2.3 Laboratory Evaluation of Field Specimens 15
2.3.1 Appearance, coating thickness and coating breaks 15
2.3.2 Backside appearance 15
2.3.3 Coating adhesion 15
2.3.4 Chloride concentration profiles 16
2.3.5 Aggregate characterization 16
2.3.6 Dry/wet concrete resistivity and weight changes. 16
2.3.7 Evidence of fly ash 17

3. METHODOLOGY - MECHANISTIC INVESTIGATIONS 18
3.1 Mechanism of coating disbondment 18
3.1.2 Experiments with model solutions 18
3.1.3 Tests in concrete 19
3.2 Crevice corrosion and corrosion protection.....19
3.2.1 Pitting initiation potentials 19
3.2.2 Cathodic protection.....21
3.3 Mechanical effects of corrosion.....21
3.3.1 Laboratory time to cracking determinations, coated versus black bar. 21
3.3.2 Computational stress intensity determinations 22
4. RESULTS - FIELD INVESTIGATIONS 24
4.1 Inventory of sites tested 24
4.2 Rebar cover 24
4.3 Concrete resistivity.....24
4.4 Concrete chloride content 25
4.5 Other concrete characteristics.....27
4.6 Rebar continuity and mutual resistance 27
4.7 Half cell potentials 27
4.8 Macrocell current 28
4.9 Polarization resistance 28
4.10 Rebar coating adhesion.....28
4.11 Rebar surface condition 29
4.12 Coating thickness.....31
4.13 Metal and coating backside condition.....31
5. RESULTS - MECHANISTIC INVESTIGATIONS 32
5.1 Mechanism of coating disbondment 32
5.1.1 Disbondment in model solutions 32
5.1.2 Disbondment in concrete 33
5.2 Crevice corrosion and corrosion protection.....34
5.2.1 Pitting initiation potentials 34
5.2.2 Cathodic protection.....34

5.3 Mechanical effects of corrosion.....35
5.3.1 Time to cracking experiments.....35
5.3.2 Computation of stress intensity.....36
6. DISCUSSION OF RESULTS.....38
6.1 Mechanism of corrosion.....38
6.1.1 Introduction. 38
6.1.2 Two key factors. 38
6.1.3 Importance of coating breaks 39
6.1.4 Extent of coating breaks. 39
6.1.5 Importance and extent of coating disbondment 40
6.1.6 Development of disbondment.....40
6.1.7 Electrolyte in disbonded regions 41
6.1.8 Crevice corrosion.....41
6.1.9 Corrosion rate estimation.....42
6.1.10 Performance improvements.....43
6.1.11 Corrosion development - a proposed sequence.....44
6.2 Present condition of bridges in Florida.....45
6.3 Prognosis of future corrosion performance.....47
6.3.1 Objective 47
6.3.2 Approach.....47
6.3.3 Initiation period 48
6.3.4 Propagation period.....51
6.3.5 Prognosis.....52
6.4 Future directions.....56
6.4.1 Use of ECR.....56
6.4.2 Corrosion Protection Alternatives - New Design.....58
6.4.3 Corrosion Protection - Present Structures 60
7. CONCLUSIONS.....62
8. REFERENCES.....65
9. TABLES T1
10. FIGURES F1
11. APPENDIX 1 .....A1

EXECUTIVE SUMMARY

This investigation was aimed at determining the present condition of Florida bridges built with Epoxy-Coated Rebar (ECR), and establishing a prognosis for the future corrosion-related durability of these structures. There are at present over 300 bridges built with ECR in Florida, and the observation of severe corrosion at five major bridges using ECR in the Florida Keys created concern about the condition of the rest and their expected durability.

About 30 large bridges were selected for detailed examination, including a few plain rebar structures for comparison. Portions of the substructure of the selected bridges were examined in detail in the field. The tests included coring for concrete samples, extraction of rebar specimens, and detailed electrochemical characterization of the substructure element to assess the potential for corrosion development. Additional tests were conducted in the laboratory to determine chloride ion penetration rates, concrete characteristics, and the condition of the rebars and their epoxy coating.

Additional laboratory tests were conducted using reinforced concrete specimens and liquids representing the concrete moisture chemistry. These tests were aimed to determine the susceptibility of the coated metal for corrosion development between a partially disbonded coating and the metal, and to establish whether the low mechanical adhesion between ECR and concrete could lead to early crack development compared with similar corrosion in plain rebar.

The field examinations revealed that, except for the five ECR structures already showing corrosion, none of the other ECR structures examined had indications of severe corrosion in progress. In many of the structures examined the extent of chloride penetration was still too small to have caused corrosion initiation.

Virtually all the ECR structures examined showed dramatic reduction of the adhesion bond between the epoxy coating and the underlying rebar metal. This reduction was

observed for all structures five years or older at the time of the examination, whether chloride contamination had taken place or not. The laboratory tests confirmed that the chemical makeup of the concrete pore solution and the electrochemical service conditions of the rebar in the service environment are conducive to extensive loss of adhesion.

Previous and present laboratory tests also revealed that corrosion propensity is significantly aggravated by the presence of disbondment crevices between the metal and the coating. It was concluded that the disbondment is the first step in the ECR degradation leading to eventual corrosion of the steel upon chloride contamination of the concrete.

The laboratory tests indicated also that both ECR and plain rebar would tend to create concrete spalls after essentially the same amount of corrosion products was generated.

Based on the above observations, and on the chloride penetration measurements, a computational model was applied to predict the time to development of corrosion spalls in the structures examined in this study. The model assumed that there is a corrosion initiation period (while the chloride content at the rebar builds up to a threshold value) followed by a corrosion propagation period which ends with spalling of the concrete cover.

The length of the initiation period is determined by the diffusivity of chloride ions in the concrete, which is obtained by analysis of the field-extracted cores. The diffusivity values measured spanned a large range (a factor of one hundred from best to worst). The bridges with the lowest diffusivity tended to be built with modern concrete formulations approaching that of the current FDOT 346 concrete with fly ash cement replacement. For those bridges the model predicted times to spall that can be on the order of 50 to 100 years or more if adequate rebar cover exists. The bridges with the highest diffusivity included those in the Florida Keys. The model predicted for those bridges times to spall on the order of a few years, which was in agreement with the observed events.

The prognosis of corrosion performance indicated therefore that bridges such as the Sunshine Skyway and about one third of the structures examined can be expected to experience service spans approaching or exceeding the current 75-year design goal before extensive corrosion-related repairs are needed. Another third includes bridges that might begin to show signs of corrosion distress within the next decade. Bridges in the remaining third (some of which are already showing damage) should be monitored frequently for possibility of immediate repair needs.

The extended life of the best performing group is ascribed primarily to the concrete quality and concrete cover depth used, and not to the presence of ECR. The experience in the Florida Keys suggests that in cases of highly permeable concrete the use of ECR did not provide significant additional protection.

The investigation results also indicated that materials guidelines emphasizing the use of low permeability concrete (such as FDOT Section 345 Class V designation), and construction design guidelines specifying ample rebar cover, are the most practical approach to attain long term durability in Florida marine substructure service.

The ECR structures presently undergoing corrosion will necessitate continuing attention. Newly acquired results continue to support the use of sacrificial sprayed zinc anodes as a cost-effective alternative to simple gunite repairs of the presently corroding ECR structures.

1. INTRODUCTION

1.1 Background

The Florida DOT commenced using Epoxy-Coated Rebar (ECR) in the late 1970's. Over 300 FDOT bridges were built with ECR. ECR was incorporated as a corrosion protection measure for service in environments that fell within the extremely aggressive category in the FDOT design manual. The use of ECR reflected guidelines established by the FHWA. Those guidelines resulted in part from extensive laboratory investigations on the performance of ECR, which provided indication that the use of ECR would dramatically improve the resistance to chloride-induced corrosion [1.1-1.5].

Among the first FDOT structures built using ECR were several major segmental bridges along U.S. 1 in the Florida Keys. The substructure of these bridges is subject to severe chloride ion accumulation as a result of cyclic seawater splash/spray and evaporation. Previous FDOT experience with substructure in aggressive corrosive environments suggested that, on the average, the service time before development of conspicuous evidence of corrosion was on the order of 12 years for structures built using conventional plain rebar. However, routine examination of the substructure of the Long Key Bridge (built between 1979 and 1983) revealed a corrosion-related spall. Numerous additional spalls developed in other parts of the bridge substructure during subsequent years [1.6,1.7]. In addition, corrosion spalls began to appear also in the substructure of other Keys bridges built with ECR at about the same time as the Long Key bridge. These incidents included observations at the Seven Mile and the Niles Channel bridges in 1987, at the Indian Key Bridge in 1990, and in the Channel Five bridge in 1993 [1.8,1.9].

Several investigations were commissioned by the FDOT to address the causes of the unexpected development of corrosion in the Florida Keys bridges. The results of those investigations have been reported in detail elsewhere [1.10-1.19] and are summarized in Section 6.1 of the present report. It was concluded that ECR (in the form available and

used at the time of construction of the Florida Keys bridges, as well as through the present) cannot be used as the primary means of corrosion protection for marine substructure applications in Florida. The FDOT suspended temporarily the use of ECR in 1988 for marine substructure service, and then permanently for all applications in 1992.

Partly as a result of the Florida experience, a number of other investigations of performance of ECR were initiated. In 1988 the Concrete Reinforcing Steel Institute (CRSI) commissioned an investigation by Ken Clear Co. (KCC) on the effect of service and production variables on the corrosion of ECR [1.20-1.21]. KCC also performed an investigation of ECR performance for the Canadian Strategic Highway Research Program (CSHRP) starting in 1989 [1.22]. Both studies, in addition to other work by KCC resulted in publication in 1991 of the conclusion that ECR, as presently implemented, cannot be relied upon as the main strategy for corrosion protection of steel in chloride-contaminated concrete [1.23]. This conclusion was disputed by the CRSI [1.24], which in turn commissioned additional work to investigate the matter. One of the resulting investigations [1.25] concluded that coating breaks were a key factor in the corrosion performance of ECR. Examinations of ECR performance in the field have also been recently conducted in Pennsylvania [1.26] and Canada [1.27]. Chloride ion buildup to date at the rebar depth in those service environments has not reached severe levels in enough locations to permit sufficient assessment of the rebar performance under very adverse conditions. NCHRP-sponsored work is currently under way to obtain additional assessment of rebar performance in the field and to examine alternative protective coating approaches [1.28]. Investigations are also being conducted focusing on the development of coatings less susceptible to disbondment from the metal substrate and to determine the effect of coating breaks on performance [1.29].

1.2 Information needs critical to FDOT

Since the use of ECR for new FDOT projects has been discontinued, the main research emphasis has shifted to assessment of the condition of the FDOT inventory of

bridges already built using ECR, and to develop a prognosis of future performance. A secondary emphasis is on determining the best way of dealing with the corrosion already developed, and to develop alternative corrosion control methods for new structures.

1.3 Objectives of the project.

The following objectives of the present investigation were developed according to the needs stated above:

1. Assess the corrosion condition of the bridges in Florida that were built using ECR.

2. Develop a means of predicting the future performance of the structures built with ECR, to reveal those bridges where maintenance may be needed in the near future, and to identify structures where long term durability can be expected.

3. Obtain information to decide on the best materials alternatives to ECR construction to be incorporated in future design guidelines.

4. Evaluate ways of dealing with the corrosion in the structures already affected.

1.4 Approach.

The investigation focused its effort primarily on the first and second objectives indicated in 1.3. This emphasis reflects the presence of other FDOT studies which have already addressed materials alternatives [1.30]. A separate FDOT/USF/SHRP investigation has examined the use of galvanic protection anodes for marine substructure in detail. This approach has met with apparent success in field tests at the Long Key, Niles Channel and Seven Mile bridges. As a result, objectives 3 and 4 were treated only inasmuch as they involved details not addressed elsewhere [1.31-1.34].

The first objective (present condition assessment) was addressed by selecting nearly 30 large bridges in the state, mostly built using ECR but also including a few plain rebar bridges for comparison. The structures were examined with a variety of field assessment and laboratory testing techniques. A multidimensional description of the corrosion condition of the structures was thus obtained.

For the second objective (future performance prediction), the results from the field survey were further analyzed and laboratory experiments dealing with the mechanism of corrosion of ECR were conducted. Emphasis was placed on determining the progression of chloride penetration in Florida bridges, the extent of contamination needed to trigger corrosion in both plain rebar and ECR, the relative extent of corrosion required to create concrete spalls in plain bar and ECR structures, and the susceptibility of ECR for disbondment in concrete service. The results of those activities were considered together with those of the previous investigations to propose a damage model of bridges with ECR in Florida. The model was finally used to provide quantitative durability estimates for each of the structures examined.

The third and fourth objectives were addressed by specific tasks on unresolved issues of feasibility of cathodic protection and on the use of the newly acquired information to refine materials selection design guidelines.

The methodology, results and conclusions of this investigation are given in the following sections.

2. METHODOLOGY - FIELD INVESTIGATIONS

2.1 Test site selection.

Test sites were selected by first examining the State records for all structures built with ECR. Of the roughly 300 structures identified, about 25 were selected because of location in highly aggressive environments and substructure containing footers and/or columns (as opposed to simple trestle construction). Table 2.1 lists those structures. The selection did not include ECR-construction bridges that had already been examined in the past (Long Key, Seven Mile, Niles Channel, Indian Key and Channel 5). The Seven Mile bridge was nevertheless added to the list of structures to be investigated, for purposes of comparison. Chloride ion penetration data obtained earlier for the Long Key and Niles Channel bridges were also used for comparative evaluation purposes. Figure 2.1 shows the locations of the structures on the State map.

2.2 Site activities.

2.2.1 Visual examination and soundings

Each substructure was first examined visually in its entirety by boat for evidence of concrete spalls, surface rust and concrete cracks. Suspect regions were further examined by hammer sounding and detailed visual inspection. After the visual inspection a minimum of two substructure members (a footer with column and the adjacent strut portion, if any) were selected for detailed examination as indicated in the following paragraphs.

2.2.2 Rebar cover

Initial determinations of rebar cover were made with Pachometer readings. The actual measurements of record were made directly on extracted cores, using the distance between the concrete surface and the closest flat section of the rebar impression in the core.

2.2.3 Concrete resistivity

Concrete resistivity measurements were made with a C.N.S. RM MKII 4-point Wenner array probe with a 5 cm interpoint spacing and electronic driver/analyzer. The probe operated at a controlled current and frequency of about 20 uA and 13 Hz respectively. The contact points were 3 mm diameter wetted wooden tips. The probe was placed in contact with the column and footer surface at elevations ranging from 0 to 8 ft above the footer level. All measurements were taken in triplicate. No surface preparation was used, except for local removal of surface paint or treatment material at the contact points.

2.2.4 Coring

Concrete cores, with a diameter of 2 in were drilled using a hollow bit cooled with fresh water. Typically, two cores were drilled at each of two elevations (about 12 in and about 72 in) above the footer. Additional cores were extracted from the footer.
The coring bit was positioned to intersect at least one segment from the horizontal rebar hoops at each of the column levels. The position of each core was recorded as elevation above the high tide mark and catalogued.

2.2.5 Rebar sample extraction

The coring bit was advanced until the desired rebar segment was completely cut by the bit. Usually, the core broke at the rebar. The core was pulled out and the rebar segment then extracted. There was virtually no adhesion between the ECR segment and the surrounding concrete. Each rebar segment was catalogued and referenced to its core location.

2.2.6 Field coating adhesion determination

Adhesion between the coating and the base steel was determined in the field by a knife test. In this test, a sharp knife was used to cut a thin slit in the coating, reaching the base metal. The tip of the knife was then used to attempt separating the coating from the metal. The coating was considered disbonded if adhesive coating-metal failure was achieved. The test was performed immediately following extraction of the rebar segment.

2.2.7 Half-cell potentials

The coring procedure exposed bare metal on each side of the bore hole, exposing the cut ends of the rebar hoop from which the rebar segments was extracted. Bare metal was also exposed in the core hole at portions of rebar hoops that were partially cut by the bit, and also at partially cut vertical bars. Each individual metal piece exposed was identified and labeled.

Half-cell potentials of each metal piece were measured with respect to a copper-copper sulfate (CSE) reference electrode placed touching the side of the core hole where the rebar was exposed. In addition, the potential differences between each pair of metal pieces exposed in the column were measured for all possible combinations and recorded in the form of a numerical matrix.

2.2.8 Macrocell current measurements.

Electrical contact through a low-resistance ammeter was made between one metal piece exposed at a high elevation core hole and another at a low elevation core hole of the same column. The pieces were selected such that the potential measurements revealed no electrical continuity between them. The current flowing after 10 minutes of interconnection was recorded as the macrocell current. The ammeter resistance / range was typically 10 ohm / 0-20 mA. If the current was too small to be readable (less than 0.01

mA), the ammeter sensitivity was increased to the next range. Potential drop across the ammeter was typically less than 10 mV.

2.2.9 Mutual resistance measurements

Resistance measurements between each pair of metal pieces exposed in the column were made for all possible combinations and recorded in the form of a numerical matrix. The measurements were made with a Nilsson Model 400 soil resistivity meter (A.C. square wave excitation, 97 Hz) configured as a two-terminal device.

2.2.10 Polarization resistance

An indication of the polarizability of exposed rebar segments was made by means of a simplified polarization resistance test. The selected rebar piece was connected as a working electrode to a potentiostat. Normally the reference electrode was a CSE electrode held in contact with the concrete near the corresponding core hole, and the counter electrode was a conductive rubber pad approximately 6 in by 8 in , in contact with the concrete around the reference electrode. The impressed potential was varied from the corrosion potential in the cathodic direction, by an amount of 12 mV. Both a forward and a return scan were performed, at an average rate of 1 mV/min. The nominal polarization resistance (Rp) was evaluated from the impressed current and the instant-off potential readings in the forward and return scans. Because the length of the tested rebar piece was not known, area-corrected values of the polarization resistance could not be obtained. Only a nominal corrosion current (Inom) was therefore evaluated, by application of the Stearn-Geary relationship

$$Inom = B/Rp$$

where B was estimated to be 0.026 V [2.1].

2.3 Laboratory Evaluation of Field Specimens

2.3.1 Appearance, coating thickness and coating breaks.

The field-retrieved ECR specimens were examined visually for macroscopic coating breaks which were not obviously caused by the extraction process. The amount of the lateral surface of the specimen showing base metal was visually estimated and a percentage bare area was calculated based on the specimen dimensions. Presence or absence of corrosion at the external surface or below delaminated coating was also recorded. The thickness of the coating was determined at 4 points away from deformation ribs by means of a magnetic thickness gage.

2.3.2 Backside appearance

Small portions of the coating were removed by cutting a slit and prying the coating off. The backside was examined visually and with the aid of a 50 X microscope. The presence of contamination and approximate percentage of the surface showing contamination was also recorded.

2.3.3 Coating adhesion

Coating adhesion was determined in the desiccator-stored specimens by means of a knife test similar to that performed in the field. In addition, the coating-metal adhesion was determined in selected specimens by a mechanical pulloff device. The procedure used a metal dolly with a diameter of 0.25 in, contoured to fit the side surface (between deformation ribs) of the ECR specimen. Smaller dolly sizes (down to 3/16 in) were used for specimens with small inter-rib spacing. The dolly was attached by means of a cyanoacrylate adhesive; the ECR surface was previously locally prepared by lightly sandpapering and degreasing with acetone. After setting of the adhesive, the epoxy coating on the perimeter of the dolly was removed with a rotating dental drill bit. The dolly

was then pulled using a universal joint fixture that minimized off-center loading. The pull load was increased slowly to achieve pulloff typically one minute following the beginning of load application. The pulloff force was recorded and divided by the dolly area to obtain a pulloff strength. The epoxy coating was not always removed from the entire area of contact with the dolly. The fraction of the dolly contact surface that corresponded to actual coating removal was recorded; the rest corresponded to failure of the epoxy-cyanoacrylate-metal bond.

2.3.4 Chloride concentration profiles

Chloride concentration profiles were determined by cutting the core into 1 inch slices, starting from the external concrete surface. Each slice was divided into two portions which were pulverized. Analysis of the powders for chloride content was made by an acid solution procedure detailed in the FDOT Research Report 203 [2.2]. Appendix 1 provides additional information on the processing of the chloride profile data.

2.3.5 Aggregate characterization

The coarse aggregate in the cores was examined visually for size distribution and type (limestone or river rock).

2.3.6 Dry/wet concrete resistivity and weight changes.

Concrete cores from each bridge, typically 6 in long or longer were selected for electric resistivity measurements. The cores were allowed to stabilize to laboratory room conditions (typical average temperature 21 ^{o}C and 65% relative humidity) for a period of several weeks. The cores were then fitted with narrow conductive rubber straps at the perimeter of each end and also at two positions separated by 5 cm near the center of the core. The resistance of the 5 cm portion of the core was measured using a Nilsson model 400 resistivity meter in the 4-point connection configuration. The resistivity was computed then by multiplying the resistance by the cross sectional area of the cylinder and dividing by

the 5 cm portion length. Separate calculations showed that systematic non uniformity of current flow within the test portion was negligible for the strap separation values used in the test.

After the dry condition resistivity was evaluated, the cores were placed in a closed test chamber. The chamber contained air at 100% relative humidity, and the specimens were also periodically sprayed with a fine distilled water mist. The weight of the cores was monitored daily until a constant weight was detected. The dry-to-wet weight change was recorded. The resistivity in the wet condition was then measured using a similar technique as that for the dry condition.

2.3.7 Evidence of Fly Ash.

Indirect evidence [4.1] of the use of fly ash was obtained by placing all concrete cores that contained no embedded rebar across the magnetic detection heads of a rebar detector James Instruments Inc., "R-Meter" Model C-4956. Most cores caused no variation of the meter reading above background fluctuations of " 0.5 unit in the fine scale of the instrument. Some of the cores caused distinct positive readings of 1 to 6 units. Positive meter indications were obtained for all cores from bridges for which concrete mix design records were available and the records documented fly ash addition. With one exception (Bridge No. 860467, "ITB"), negative meter indications were obtained for all bridges with records available documenting the use of concrete with no specified fly ash addition. Additional examination of selected cores was performed by acid digestion of ground core samples. The digest was examined microscopically for presence of cenospheres. The digest was also ignited and the ignition residue examined for presence of black particles (usually 0.1 mm to 1 mm in size) that could be attracted with a magnet. Observation of cenospheres and magnetic particles in the examined cores coincided with positive R-Meter test indications.

3. METHODOLOGY - MECHANISTIC INVESTIGATIONS

3.1 Mechanism of coating disbondment

3.1.2 Experiments with model solutions

Specimens to determine the tendency for coating-metal disbondment in model liquid solutions were prepared from #7 rebar samples. The specimen dimensions, test cells and methodology were the same as used in previous investigations, as detailed in References [1.12,1.14]. Small amounts of surface damage (typically 0.5%) were introduced as described in the early reference. The specimens were obtained from regular production runs of a major FDOT ECR supplier. Two sets of specimens were made when the coating plant was using coating powder obtained from one particular manufacturer. The other set was obtained after the coating plant had switch to another powder manufacturer.

The disbondment tests were conducted with simulated concrete pore solutions (SPS). These solutions contained Ca, K and Na ions in proportions representative of those encountered in liquids expressed from mortar and concrete samples [2.3,2.4]. The composition of the test solutions is shown in Table 3.1. Tests were conducted with SPS without chloride addition, and with two different levels of chloride ion addition. All chloride additions were in the form of NaCl. The total amounts of Na in the pore solutions, given in Table 3, reflect the salt addition. Specimens were tested in the open circuit potential condition, and at three different levels of potentiostatically-controlled polarization. The levels were -400, -500 and -750 mV vs SCE. The tests were conducted for a period of 30 days, after which the specimens were removed from the test solution and immediately tested for evidence of disbondment. The disbondment was measured by using a sharp knife and determining the size of the region around the intentionally-induced coating defects in which adhesive failure of the coating could be induced. A disbondment distance was then calculated as the equivalent radius of the disbonded region, as detailed in Reference [1.12].

3.1.3 Tests in concrete

Selected rebar specimens from similar origin as those addressed in the previous section were used to prepare concrete specimens for determining the tendency for disbondment in chloride-free concrete. The reinforced concrete specimens were cylinders (6 in high, 4 in diameter) in which the rebar was axially placed, leaving a cover distance of 1.5 in from the bottom of the rebar segment to the bottom of the cylinder. The bottom rebar end was covered with a plug of metallographic epoxide compound. The other end of the rebar exited at the upper end of the cylinder. The sides of the rebar were subject to the same amount of controlled surface damage as that used for the SPS tests. The concrete mix design is shown in Table 3.2; specimens were cured for 28 days prior to beginning the test. The concrete cylinders were placed in 5 in of tap water. The specimens were tested in duplicate and subject to two different test conditions: open circuit potential and potentiostatically polarized at -500 mV. The specimens were exposed for a period of nearly two years. During the exposure, selected specimens were subject to periodic electrochemical impedance spectroscopy (EIS) testing . The EIS tests in the polarized specimens were performed near the end of temporary 24 hour disconnection periods. Those specimens were repolarized after each EIS test. Selected specimens were demolished after nearly two years of exposure and tested for coating disbondment as described in the previous section. Pulloff measurements (using the technique described in Section 2.3.3) were also performed in selected ECR specimens after demolition.

3.2 Crevice corrosion and corrosion protection

3.2.1 Pitting initiation potentials

These experiments were conducted with specimens machined out of regular #6 rebar stock meeting ASTM A 615 specifications. The bar was sliced and machined into a prism 5 by 10 by 10 mm. The narrow face of the specimens, which faced the test solution, was perpendicular to the rolling direction of the bar. The specimen was mounted in an

epoxide metallographic mount with an electrical connection on the side opposite to the face in contact with the liquid. The active face of the specimen was metallographically ground and polished to a 1 ìm finish, degreased with acetone and immersed in the test solution. The specimen face was in a vertical plane to avoid gravity accumulation effects. The test solutions consisted of either saturated calcium hydroxide (pH=12.4) or an SPS with the same formulation as that indicated in Table 3.1. Controlled amounts of Na Cl were also added to the test solutions to achieve molar Cl^- concentrations of 0.1 to 1.0. A glass test cell per ASTM G5 (except for the specimen configuration indicated above) was used, with graphite counter electrodes and a Luggin capillary probe with a tip placed typically at 1 to 3 mm from the specimen surface.

Potentiodynamic polarization scans were conducted starting toward nobler potentials from -1300 mV or -1200 mV (SCE), at a scan rate of 0.1 mV/sec. The scans continued until the average anodic current density exceeded 100 uA/cm^2, indicating that pitting had been initiated. The sudden increase in current was normally accompanied by visual observation of corrosion products on the specimen surface.

A second series of tests was conducted using specimens identical to those described above, but having a plexiglas sheet lightly touching the lower half of the exposed metal face, so as to create a thin crevice. The pitting/crevice initiation potentials were measured using the same method as before.

To minimize possible experimental artifacts, experiments were also conducted with a simpler arrangement that consisted of placing machined steel specimens with the large flat face resting horizontally on a microscope slide. The slide was then placed in a glass beaker containing the test solution with and without chlorides. The specimen was observed visually from underneath the beaker, and the potential was monitored periodically by brief contact with a sharp steel probe. Times for corrosion initiation based on potential changes and visual observation were thus determined.

3.2.2 Cathodic protection

Exploratory experiments on the feasibility of cathodically protecting ECR were conducted using plain rebar specimens machined as described in 3.2.1, placed in a crevice corrosion test cell so that one narrow face was in contact with lightly touching plexiglass, and an adjacent narrow face was in direct contact with the test solution. The entire assembly was submerged in the test solution, and the potential of the fully exposed face was monitored with a nearby Luggin capillary probe tip. The test cell has been described in detail in Ref.[2.5]. The experiments consisted of determining the time necessary for manifestation of corrosion initiation with and without an applied protecting potential of -1000 mV (SCE).

3.3 Mechanical effects of corrosion

3.3.1 Laboratory time to cracking determinations, coated versus black bar.

Cylindrical reinforced concrete specimens (4 in diameter, 16 in long) were prepared with axially placed segments of # 4 rebar extending the full specimen length. The cylinders were cast with a Type II cement concrete with mix design as shown in Table 3.3. The concrete in the central 8 in of the cylinder contained an additional 20 pounds per cubic yard (pcy) Cl^- added at the time of mixing in the form of NaCl. Vertical casting permitted the sequential introduction of the first 4 in of chloride free concrete, the central 8 in of Cl^--containing mix, and the remaining chloride-free end. The axial rebar was either as-received plain rebar stock, or ECR obtained from normal production runs of a regular FDOT supplier. The surface of the ECR contained also 1% of surface damage in the form of evenly-spaced file marks (typically 2 mm by 2 mm).

After 28 days moist cure the cylinders were fitted with three 6-in long strain gages partially overlapping so as to gird the central perimeter of the specimen. Conductive rubber

belt electrodes, 2 in wide, were placed on each side of the strain gage belt to provide a 4-in long current delivery element surrounding the central portion of the specimen. The specimens were then fitted with power delivery and signal carrying wires, and placed in a 100% humidity chamber.

The central belt electrodes were used to deliver a controlled amount of anodic current to the central rebar, to induce a nominally known amount of corrosion product formation. The current delivery concept is schematically illustrated in Figure 2.2. Electronically controlled currents of 1 and 2.5 mA were delivered to triplicate sets of specimens of plain rebar and ECR.

The strain gage indications were monitored as a function of exposure time, to reflect changes in the cylinder diameter indicative of corrosion product accumulation [2.6]. A sudden increase in the extension of one or more gauges was indicative of the development of a crack at the concrete surface. The time for the strain-gage indication of crack development was recorded. The surface of the specimens was also examined for visual indications of crack development; the exposure time at which cracks were first visually detected was also recorded. Selected specimens were autopsied at the end of the test.

3.3.2 Computational stress intensity determinations.

A plane-strain model of a cylindrical rebar placed axially in a reinforced concrete cylinder was developed using the ANSYS finite element code. The model simulation used a 0.5 in diameter bar in a 4 in diameter cylinder. The model assumed that cracks of length a existed on each side of the rebar cross section. The rebar and concrete materials properties assumed for the calculations are listed in Table 3.4. Two possible conditions were evaluated. The first assumed that complete adhesion existed between the bar perimeter and the immediately surrounding concrete. This condition approximates plain rebar for which good adhesion is considered to exist between the rebar surface and the contacting hardened concrete. The second condition assumed free tangential sliding

between the bar surface and the concrete, simulating the behavior of ECR where only limited adhesion to the concrete exists. In either case, because only bar expansion is considered, the effect of rebar deformation ribs was ignored on first approximation. An example of the finite element grid used is shown in Figure 2.3.

The effect of corrosion product development was simulated by using the thermal expansion module of the ANSYS code, and accounting for lengthwise deformation complications by adequate manipulation of the Poisson modulus parameter of both materials. The resulting stress intensity at the crack tip was computed for both model conditions as a function of crack length.

4. RESULTS - FIELD INVESTIGATIONS

4.1 Inventory of site results.

Table 4.1 (A and B) summarizes the main quantitative results from the field site examinations. The results are keyed by bridge number (following approximately the chronological order of examination), and pier/column number (4.1B only). Magnitudes measured on individual cores (such as chloride diffusivity) are averaged by column and by bridge. Magnitudes determined on the columns (such as rebar continuity) are listed by columns and averaged by bridge.

4.2 Rebar cover.

Table 4.1B lists also minimum rebar covers determined for all the columns examined. In general, rebar cover was found to meet or exceed the design guidelines present at the time of construction. Figure 4.1 displays the distribution of rebar cover from all cores examined in this investigation.

4.3 Concrete resistivity.

The concrete resistivity was at a minimum at points close to the high tide level, and increased at higher levels. Maximum and minimum field resistivity values measured for each substructure column are given are listed in Table 4.1 (A and B).

The core laboratory resistivity measurements averaged for each bridge/column in the wet condition, as well as the corresponding relative weight change, are also listed in Table 4.1 (A and B). Figure 4.2 compares the lowest values measured in the field for each column, with the corresponding average wet core resistivities. The results clustered around the line for an ideal 1:1 relationship.

Figure 4.3 shows that the weight change during wetting of the cores was generally greatest for those cores showing the lowest wet resistivity.

4.4 Concrete chloride content.

Table 4.2 lists the chloride concentration measurements obtained for each of the cores examined. Figure A.1 (Appendix 1) shows an example of a chloride concentration profile. Figures 4.4 to 4.8 summarize information on the amount of chloride present at various depths for different groups of structures. For each group, the corresponding Figure shows the percentage of available cores for which the chloride concentration exceeds either 1.2, 2.4 or 3.6 pcy at the indicated depth. These values are representative of a plausible range of chloride concentration thresholds for active corrosion initiation (see Section 6).

Figure 4.4 is for Group1, consisting of the bridges in the study for which corrosion of ECR was earlier documented (Long Key, Niles Channel, Seven Mile). The figure shows that at, a depth of 3-4 in, 87% of the extracted cores had more than 1.2 pcy; 63% had more than 2.4 pcy, and 56% had more than 3.6 pcy. Figure 4.5 is for Group 2, the bridges in the study that were built with plain rebar. Figure 4.6 (Group 3) includes all bridges not in groups 1 and 2. Figure 4.7 (Group 4) is for all the bridges in Monroe County (Florida Keys). Figure 4.8 (Group 5) is for the Sunshine Skyway Bridge only.

The results indicate that for the largest group investigated (Group 3, Figure 4.6) significant chloride contamination at typical rebar depths (see Figure 4.1) was not prevalent. In contrast, the structures in Monroe Co. show high chloride contamination levels at typical rebar depths.

Figure A.2 shows the computational fitting procedure used to evaluate the apparent, effective chloride diffusion coefficient (D) as well as the calculated chloride surface concentration. The results from those computations are listed in Table 4.2. Values of the

effective diffusion coefficient, averaged per bridge column and per bridge are listed in Table 4.1 (the bridge and column averages include data only for cases in which the calculated chloride surface concentration was 1 pcy or greater).

Figure 4.9 shows the cumulative distribution of calculated chloride surface concentrations. Figures 4.10 and 4.11 show the average chloride concentration of the first one-inch core slice, and the calculated chloride surface concentration, respectively, for all cores tested, as a function of height above the high tide line. As expected, the calculated surface chloride concentration is larger than the first-slice average but otherwise both magnitudes span large ranges of values. The maximum values for a given elevation show a general decreasing trend with elevation, reflecting the greater distance from the seawater level. Within a given structure this correlation with height may be better, as exemplified in Figure 4.12 for the Sunshine Skyway bridge. The same figure shows that the computed apparent diffusion coefficients tended to remain within the same order of magnitude regardless of height of the core over the high tide line. Figure 4.13 shows the distribution of effective chloride diffusivities averaged for each bridge and ranked by increasing order. Results from cores extracted earlier in bridges not addressed in the present study, but of importance because of observation of ECR corrosion (Long Key, Niles Channel) have been also included in Figure 4.13. Only D values for cores showing a calculated surface concentration of 1 pcy or more were considered for this ranking. The results show that the effective chloride diffusivities varied widely from structure to structure, spanning over two orders of magnitude.

The wet concrete resistivity measured in the laboratory was in general greatest for the group of specimens with the lowest effective chloride diffusivities. A similar correlation was observed between the minimum field resistivity and the corresponding average D values for individual bridges. As shown in Figure 4.3, these correlations extend to the weight changes experienced by the cores during drying in the laboratory.

4.5 Other concrete characteristics.

Figure 4.14 shows two extremes of coarse aggregate morphology visually observed in the extracted cores. The amount of coarse aggregate fines was visually evaluated and listed in Table 4.1A (HI, MED, LO). The cores were also visually examined for coarse aggregate type. With the exception of Bridge 570082 (CHO, Table 4.1A), which had river rock aggregate, the remaining structures used limestone as the coarse aggregate. Indirect evidence of fly ash addition from rebar position meter indication of magnetic activity [4.1], is listed (YES-NO) in Table 4.1A. It should be noted that most of the bridges showing indication of fly ash addition are also placed within the upper third of the ranking in Figure 4.13, corresponding to the lowest chloride diffusivities.

4.6 Rebar continuity and mutual resistance.

Figure 4.15 shows the distribution of degree of continuity measured for structures that contained ECR. Each datum corresponds to a different substructure member (footer + column) investigated. The median degree of continuity observed was 30%. See also Table 4.1 (A and B).

Figure 4.16 shows the maximum mutual resistance observed between elements at each substructure member, using the degree of continuity as a descriptive parameter. As expected, there is significant scatter but a general decreasing trend is evident as the degree of continuity increases. See also Table 4.1B.

4.7 Half cell potentials.

Table 4.1B shows the highest and lowest half cell potentials recorded for each structural member examined. These parameters show no discernible trend as a function of the other magnitudes examined in this investigation.

4.8 Macrocell current.

Macrocell currents for individual structural members are shown in Figure 4.17 using the degree of continuity as a descriptive parameter. There is a general increase in the level of macrocell current as the degree of continuity increases. This is to be expected, since a greater level of interconnection would provide access to a larger electrochemically active area. See also Table 4.1 (A and B).

4.9 Polarization Resistance / Nominal corrosion current.

The nominal corrosion current values obtained for each structural element and corresponding bridge averages are listed in Table 4.1 (A and B). The values for structural elements are shown in Figure 4.18 using the degree of continuity as a parameter. The nominal currents tend to increase with the degree of rebar continuity, which is to be expected as indicated in the previous subsection. Figure 4.19 compares the highest and lowest nominal corrosion current values for the bridges with ECR to the values obtained in the plain rebar bridges. Because of inherent limitation of the polarization technique [4.2], it is not possible with the present data set to determine actual corrosion rates or to differentiate between Faradaic (corrosion) processes and non-Faradaic (interfacial capacitance) effects. Extended measurements with a larger number of plain rebar structures for comparison, and careful selection of corrosion condition (for example, cases where corrosion initiation has clearly taken place in both types of structures) would be necessary to refine a polarization method for useful assessment of corrosion condition in ECR structures. This was not feasible within the scope of the present project.

4.10 Rebar coating adhesion.

Field results.

The results of knife adhesion tests performed in the field, immediately upon rebar extraction, are listed in Table 4.1A (YES: fully disbonded; NO: no disbondment; P: partial

disbondment). Lack of adhesion was widespread and affected virtually all the structures tested that were older than 4 years.

Laboratory results.

Knife tests were performed on selected field-extracted specimens after drying in desiccators for periods ranging from one month to over two years. Loss of adhesion was manifested in most of the specimens thus examined.

Coating pulloff tests were performed with selected field-extracted rebar specimens, after placement in desiccators for a minimum of one month. The specimen drying was intended to allow time for possible recovery from wet adhesion loss, and to detect any irreversible disbondment. Tests were also performed with control ECR specimens that were stored in the laboratory in the as-produced condition and had never been in service. The results are displayed as a cumulative distribution graph in Figure 4.20. While the pulloff test is limited by the effectiveness of adhesion between the test dolly and the epoxy, the results nevertheless show a clear reduction in adhesion for the field-exposed rebar group versus the unexposed controls. The adhesion strength between the epoxy and the rebar metal in the control group was always greater than that between the test dolly and the epoxy (as evidenced by the consistent failure of the test dolly - epoxy joint in that group). Thus, the effect of field exposure on reducing adhesion is likely to be even greater than the difference apparent in Figure 4.20. See also Table 4.1 (A and B).

4.11 Rebar surface condition.

Rebar type.

The type of rebar extracted from the structures investigated is indicated in Table 4.1A (E: ECR or P: plain "black" bar).

Corrosion.

Table 4.1A lists the presence (YES) or absence (NO) of corrosion (either at exposed metal spots or underneath the coating) in the rebar specimens extracted in the field. Very few of the specimens (mostly from the Seven Mile bridge) examined in the bridges selected for this investigation showed any conspicuous signs of corrosion. While not newly examined in the present study, Long Key bridge and Niles Channel bridge are also represented in the listing since ECR corrosion was observed at these bridges earlier. The corrosion observed in Seven Mile, Long Key and Niles Channel has been described in detail elsewhere [1.6-1.8]. There was minor undercoating corrosion in one of the specimens extracted from one of the Vaca Cut bridges in the Florida Keys. While corrosion was not observed in the rebar segments extracted from one of the Indian River bridges (700174, IR2), there was evidence of a corrosion-induced spall elsewhere in the same structure (which was constructed with plain rebar). This observation was included in Table 4.1.

Coating Breaks.

The extent of coating breaks (bare areas) in the field-extracted ECR specimens was determined visually (unaided eye). The results for all ECR specimens examined are represented as a cumulative graph in Figure 4.21. The median extent of visual coating breaks affected about 0.4% of the specimen surface. During the examinations damage clearly produced during rebar extraction was disregarded, but the reported measurements should be considered nevertheless as an upper limit of the amount of visually observable surface damage actually present at the time of concreting. Conversely, coating breaks not detectable by the unaided eye (sizes . 0.1 mm) are not reflected in the listing. Figure 4.22 shows that the data field presently available cannot identify a significant correlation between construction date and the degree of measured coating breaks. Figure 4.23 presents a ranking of the bridges investigated by the average percent bare area (see also Table 4.1A), revealing no clearly identifiable correlation with structure type or location . Figure 4.24 shows that the substructure elements with the lowest average values of rebar percent bare area were within the lowest rebar continuity group. This agrees with the

expectation that good coating integrity will result in a smaller degree of rebar interconnection.

4.12 Coating thickness.

The results of magnetic thickness testing of the field-extracted specimens are displayed as a cumulative graph in Figure 4.25. The results show a median thickness of about 0.009 inch, with 90% of the values falling in the interval of .007 inch to .013 inch. These values generally agree with the thickness values expected from the materials specifications at the time of construction of the structures examined. See also Table 4.1A.

4.13 Metal and coating backside condition.

Most specimens showed an undercoating metal condition ranging from nearly bright to slightly darkened, with few exceptions. The condition of the coating backside was examined in detail for selected specimens that had shown pronounced knife test disbondment both in the field and in laboratory pulloff tests performed after extended desiccator storage. Specimens that actually showed corrosion products were excluded to avoid uncertainty in separating corrosion products from contamination initially present. Figure 4.26 shows a typical backside appearance. Aside from contamination spots which affected only a small percentage (less than 10%) of the coating surface, the coating backside was essentially clean. Qualitative examination of the steel surface appearance did not reveal conspicuous deviation from normally blasted surfaces

5. RESULTS - MECHANISTIC INVESTIGATIONS

5.1 Mechanism of coating disbondment.

5.1.1 Disbondment in model solutions.

The objective of these tests was to establish whether solutions containing Ca^{++}, K^{+} and Na^{+} ions (at concentrations representative of those expected in concrete pore solutions) could cause significant coating disbondment, at steel potentials typical of actual service conditions. Figure 5.1 shows the results of the disbondment tests performed with chloride-free solutions. The results confirmed that significant coating disbondment can take place under moderate cathodic polarization conditions (-400 to -750 mV vs SCE) with present-day coated rebar produced by a representative provider to the FDOT, using powder from two different sources and actual run products (intended for normal shipments and not specially made for these tests).

Figures 5.2 and 5.3 show the results of similar testing conducted with two different levels of chloride addition. Table 5.1 shows the open circuit potentials for each of the three test conditions. At the lower level of chloride addition (0.06 M) there was no indication of corrosion deterioration underneath the coating, and both materials showed essentially similar levels of disbondment as in the chloride-free test. The content of chloride ion introduced corresponded roughly to 0.3 pcy of concrete (assuming porosity on the order of 10%).

At the high level of chloride contamination (0.45 M, roughly equivalent to a Cl^{-} concentration of 2 pcy of concrete) and at the more negative potentials (-500 to -750 mV vs SCE) there was about the same level of disbondment as that observed in the chloride free and low chloride content solutions. However, at -400 mV the disbondment was significantly larger than in the other conditions. Also in contrast with the other conditions, the impressed currents needed to maintain -400 mV vs SCE were anodic (Table 5.1), showing that

significant corrosion was underway. This was confirmed by direct observation of crevice corrosion in the open circuit and anodically polarized specimens.

5.1.2 Disbondment in concrete.

These tests examined the effect of long term service in chloride-free concrete on coating adhesion. If the loss of adhesion were a form of cathodic disbondment, the effect could be expected to depend on the potential that the rebar develops during service (stronger effect for more negative potentials). The conditions selected for the test were open circuit service in chloride-free concrete (about -200 mV vs. SCE) and artificially maintained -500 mV vs SCE. The selected test potentials are well within those encountered in actual service. Table 4.1 shows that potentials even lower than -500 mV vs SCE (taking into account the Copper/Sulfate to SCE conversion) were observed in some of the structures inspected, even in the absence of indications of extensive chloride contamination.

Figure 5.4 compares typical EIS spectra for specimens exposed at the open-circuit potential and under a constant polarization of -500 mV. The -500 mV specimens showed a distinctly lower value of the impedance limit at low frequencies. The effect remained even after several days of interrupting the polarization current. The results are compatible with the development of a large disbonded area underneath the crevice, manifested as an increase in the effective interfacial capacitance and corresponding development of a transmission-line configuration.

Selected specimens, both in the open circuit condition and depolarized, were demolished after approximately 500 days of exposure. Knife tests immediately after demolition revealed significant disbondment of both types of specimens, but more pronounced in the specimens polarized at -500 mV. The results were confirmed by pulloff tests (see Table 5.2) The specimens were placed in desiccators for one to two weeks and tested again. Knife tests revealed residual disbondment in the polarized specimens, and to

a much lesser extent in the open circuit specimens. The results of the tests suggest that cathodic disbondment plays a role in the loss of adhesion observed in the field.

5.2 Crevice corrosion and corrosion protection.

5.2.1 Pitting initiation potentials.

Figures 5.5 and 5.6 illustrate typical results of experiments to determine the pitting initiation potential Ep in laboratory solutions. Table 5.3 summarizes the results of the entire test sequence. Figure 5.7 shows the dependence of Ep on the extent of chloride addition for specimens with and without built-in crevices. The open surface results for the $Ca(OH)_2$ solutions are in general agreement with previous reports [4.3], showing a decrease in Ep as chloride content is increased. In the open-surface SPS solution tests, higher values of Ep were observed together with virtually no effect of chloride addition, as expected from the higher pH of the SPS solution. The presence of crevices resulted in a dramatic reduction of Ep in both the $Ca(OH)_2$ and SPS tests. The Ep values obtained in the latter were close to those obtained in the open-surface $Ca(OH)_2$ tests.

5.2.2 Cathodic Protection

Duplicate experiments (a and b) were conducted in a nominal SPS + 0.45M NaCl solution (Table 3.1). In each case, no crevice attack was observed during 7 days of cathodic protection at -1000 mV vs. SCE. The cathodic protection was removed after the 7th day, but the crevice cell was left undisturbed. Depolarization potentials were monitored as a function of time.

In experiment (a) corrosion was observed inside the crevice after approximately 19 hours of discontinuing cathodic protection. The external, free metal surface showed no evidence of attack. The crevice wall attack was not uniform, but instead exhibited three distinct morphological regions. The first region was near the crevice mouth (opening) and

exhibited little or no attack and remained in its shiny, as polished state similar to that of the external metal surface. This first region extended approximately 1 mm into the crevice. The second region, just next to the first, contained a large buildup of brownish-black corrosion products which extended for about 0.5 to 1 mm along the crevice. The third region, extending through the remaining length of the crevice, had undergone an apparent uniform corrosion reaction, as determined through ex-situ metallography.

Experiment (b) also did not result in any active corrosion during the course of seven days under cathodic protection. Similar to experiment (a), after discontinuing the cathodic protection, active corrosion initiated while the metal outside the crevice remained unattacked. Morphological observations of the crevice wall were similar to that of experiment (a). The time for corrosion initiation following interruption of cathodic protection in experiment (b) was however only about 100 minutes.

The results described above are from experiments that were only exploratory in nature. The experiments showed evidence that corrosion development inside the crevice can be delayed by application of an external potential. The appearance of corrosion soon after interruption of external CP, together with the findings from the previous section, underscore the propensity for corrosion development in tight crevices when the external environment represents chloride-contaminated concrete pore solutions.

5.3 Mechanical effects of corrosion.

5.3.1 Time to cracking experiments.

Figures 5.8 and 5.9 show examples of the strain readings as a function of test time for the 1 mA tests, for black rebar and ECR. The voltage trend is indicative of the overall circuit resistance; current was kept constant by the circuitry. The time between first voltage application and the first strain excursion is the time to cracking per strain gage determination. Visual crack detection was obtained usually some time afterward. Figure

5.10 shows that there is general correlation between both methods of crack time determination.

The time for cracking strongly depends on the amount of current applied (Figure 5.10). However, regardless of the amount of current the time for cracking for both types of bar was of similar magnitude. Figure 5.11 shows that under the same level of corrosion product generation the specimens with ECR may tend to crack at a time about 50% longer than that for the black bar specimens. The difference, however, may not be statistically significant.

The results suggest that, at least with the test conditions used, the mechanical effects of equal amounts of corrosion are similar for both types of bar. If this conclusion were to be valid for other configurations, this would aid in predicting lifetime of ECR structures (with proper scaling) based on the experience with plain bar.

5.3.2 Computation of stress intensity.

Figure 5.12 shows the results of exploratory calculations of the stress intensity at the tip of a crack for full interfacial friction versus frictionless conditions, for the property parameters listed in Table 3.4 and crack lengths ranging from 0.25 in to 1 in. The stress intensity is about 30% greater for the frictionless case. For the same amount of corrosion in plain bars and ECR, the analysis would suggest that ECR would tend to crack somewhat earlier than plain bars. The results in Figure 5.11 indicate an equally moderate effect, but in the opposite direction. While the experimental and computational results are conflicting as to the direction of any possible effect of lower friction in ECR versus plain bar, both agree in that the effect is not likely to be dramatic, at least with the test geometry chosen.

The computational approach assumed concrete as an elastic, isotropic, homogeneous material thus neglecting the effects of micro-cracking, shrinkage, creep, aggregate size effects, etc. Ribs on the reinforcing steel and the deformation properties of

the epoxy coating were also neglected. A more refined analysis plus extension to other reinforced concrete geometries (such as a two-dimensional assembly of bars) may provide more valuable insights in future investigations.

6. DISCUSSION OF RESULTS

6.1 Mechanism of corrosion.

6.1.1 Introduction.

The results of the present and prior investigations confirm that epoxy-coated rebar, as supplied and used in the structures of interest in Florida, is susceptible to severe corrosion. The corrosion was severe enough to result in widespread deterioration of the substructure of major bridges in the State after service times of less than one decade. The observed corrosion represented a failure of the corrosion protection scheme in those substructures. Since the use of ECR was the principal component of that scheme, the observed deterioration came as a surprise in light of the optimistic expectations of the performance of ECR which existed at the time of construction and for several years thereafter.

6.1.2 Two key factors.

The present field and laboratory investigation has identified two factors that appear to be critical to the development of severe corrosion in ECR. The first factor is the presence of breaks in the coating that expose some of the metal surface to direct contact with the surrounding electrolyte. Coating breaks relevant to corrosion initiation can range from holidays invisible to the naked eye, produced at the time of manufacturing, to narrow cracks in the coating produced during fabrication bending of the rebar, to macroscopic abrasion, gashes and cuts caused during transportation, field handling and vibration while concreting. The second factor is the development of extensive loss of adhesion between the coating and the base metal after relatively short service times in concrete, even in the absence of chloride ion contamination.

6.1.3 Importance of coating breaks.

Coating breaks permit electrolytic contact between different portions of the rebar system, and allow for the transport from the concrete to the metal surface of species active in the corrosion process. While transport of water, oxygen and chloride ions directly through the epoxy cover is possible, the process rates observed in this and other investigations can often be explained simply by transport and conduction at coating breaks, without the need for invoking epoxy permeation processes. In instances where coating breaks were carefully avoided, the onset of corrosion was significantly extended and electrochemical process rates were found to be very slow. This was also manifested in at least one bng-term (9 years) field test where corrosion-free performance was achieved under highly aggressive conditions [6.1]. Post-test evaluation in that test revealed a virtually flaw-free rebar surface. Microscopic examination of the coating showed also extensive foaming, which is often associated with curing temperatures higher than usual. While the foaming might have impaired the coating ability to pass the bend acceptance test, high curing temperatures could have improved the coating adhesion in those rebars, with consequent better corrosion resistance.

6.1.4 Extent of coating breaks.

Coating breaks were observed in the majority of the specimens extracted from the field. Semiquantitative evaluation of the extent of uncovered metal in the field samples has been presented in Figure 4.21, showing a median of about 0.4% unrepaired exposed metal surface (a 2% maximum allowable was specified at the time of construction of the structures examined). Laboratory investigations showed that significant amounts of corrosion macrocell current (arguably sufficient to cause concrete cracks after about 15 years) can flow in ECR systems when 2% surface damage is introduced and substructure corrosion conditions are prevalent [1.15]. Results from recent investigations have been interpreted as indicative that severe corrosion can develop in ECR when surface damage exceeds a fraction of 1% [1.25].

6.1.5 Importance and extent of coating disbondment.

Loss of adhesion between the coating and the steel, by itself, is not the sole cause for corrosion. However, the loss of adhesion can be viewed as a symptom of the accumulation of fluids between the coating and the steel, which is a necessary condition for the development of electrochemical reactions at the metal surface at a significant rate. Virtually every ECR specimen extracted from the field showed disbondment as determined by a knife test immediately upon extraction. As shown in Figure 4.20, the loss of adhesion was confirmed by a less subjective mechanical pulloff test. The pulloff tests also showed that the loss of adhesion was still observable in a majority of specimens after being stored in desiccators for extended periods of time. This suggested irreversible loss of adhesion, such as could be expected from a mechanism involving dissolution at the rebar surface of the metal oxide layer to which the coating was initially attached [1.14].

6.1.6 Development of disbondment.

Laboratory experiments published previously [1.12] have shown that disbondment in regular production ECR can take place around coating breaks under freely corroding conditions in sodium chloride solutions. The disbondment radius increases roughly proportional to the exposure time. Tests have also shown that the loss of adhesion in ECR has the general characteristics of cathodic disbondment [1.14]. The disbondment in ECR proceeds at a significant rate even at what would be considered relatively mild cathodic polarization conditions [1.12]. Previous investigations have also shown that ECR disbondment can take place under cathodic polarization in Na(OH) solutions, without the need of chloride ions being present [1.12]. The present work has shown that simulated pore solutions containing representative concentrations of K and Na ions can also promote coating disbondment (around coating breaks) under mild cathodic polarization conditions, such as those encountered in concrete service. The present tests in actual concrete specimens have shown that service in chloride-free concrete under both moderate cathodic

polarization and open circuit conditions can lead to significant disbondment after only 500 days. Extensive disbondment has been observed also in a previous investigation [1.12] in chloride-free concrete at rebar specimens containing 2% surface damage and placed at the cathodic end of extended corrosion macrocells. While experiments have shown wide variation between the rates of disbondment of ECR as provided by different suppliers, there is no clear evidence that surface contamination at the time of coating is particularly responsible for the phenomenon. Most specimens extracted from the field and showing extensive, irreversible disbondment had very clean underside surfaces (per naked eye inspection). Upon microscopic examination, only a small percentage of the surface (typically less than 10%) could be identified as having possible traces of contamination.

6.1.7 Electrolyte in disbonded regions.

The field and laboratory evidence strongly indicates that ECR, as produced and utilized in the structures considered here, will have experienced massive disbondment between the epoxy and the base metal after few (less than five) years of placement in service. While there is no direct evidence of fluid accumulation in the resulting crevice, EIS measurements in this and a previous investigation [1.16] showed indications of transmission-line behavior that can be explained by the presence of electrolytic conduction paths between the coating breaks and a surrounding crevice area. This can also be interpreted from the results of cyclic large-signal polarization tests performed with disbonded ECR samples, which showed a pronounced cathodic polarization loop upon reversal of the polarization scan direction (a much smaller loop was observed in surface-damaged but not disbonded specimens).

6.1.8 Crevice corrosion.

The presence of extended, electrolyte-filled openings at the coating-metal interface sets the stage for the development of severe crevice corrosion at that region if the appropriate species are present. The pitting initiation potential experiments showed that

corrosion can develop at crevices, at typical rebar potentials, with relatively low chloride to hydroxide ion ratios in the bulk solution. The experiments with rebar specimens in simulated pore solutions showed that crevice corrosion could be maintained with external (that is, at the crevice opening or break in the coating) potentials as low as -500 mV (SCE). Based on the laboratory tests with model solutions, the chloride concentration threshold for maintaining active corrosion within the crevice appeared to be at least as low as that required for plain rebar in concrete [4.5]. Figure 5.7 suggests that the chloride concentration threshold for corrosion initiation in disbonded ECR with coating breaks might be even lower than for plain steel bars.

6.1.9 Corrosion rate estimation

The overall rate of corrosion in chloride-contaminated concrete of ECR which contains surface breaks and disbonded crevice areas is difficult to quantify. Typically, both corrosion macrocell current measurements and polarization tests show nominal corrosion currents for ECR that are about one order of magnitude lower than for plain bar under similar chloride-contamination circumstances [4.6]. However, the macrocell corrosion current can only reveal a part of the overall corrosion rate, leading to inherent underestimation of the overall rate of metal dissolution. As shown in Ref. [4.7], polarization measurements, including EIS and simple polarization resistance tests can also significantly underestimate the rate of metal dissolution if most of it takes place inside the crevice. Because of these limitations, the corrosion rate (averaged over the nominal external surface of the ECR) can be only approximately estimated for the cases relevant to this study.

The results presented in Refs [1.12, 1.15] showed that 2% surface damage (and the concurrent disbondment) can create significant macrocell currents for ECR in marine substructure conditions. Mathematical modeling in those studies suggested that the corrosion macrocell current alone acting on the ECR could cause observable cracking within 15 years of service. The added effect of local cell corrosion could be expected to

shorten the time to cracking to below that estimate. It has been suggested that in realistic field conditions, with significant surface damage and disbondment, use of ECR would only add a few years to the time necessary for development of cracking [1.23]. Perhaps the most useful piece of evidence as to the corrosion rate of ECR in the conditions of interest is given by the observation of cracking in the Florida Keys bridges after only 6 to 10 years of service. As it will be shown in Section 6.3.3, consideration of the time needed for corrosion initiation leads to the conclusion that the propagation period for ECR in the Keys bridges was on the same order (about 3.5 years) as that which is commonly experienced with plain bar in other field situations [4.8]. This conclusion is in agreement with the above arguments from laboratory tests, and will be used as a working assumption to estimate the lifetime of structures where the ECR has encountered initial surface damage levels on the order of 1% to 2%.

6.1.10 Performance improvements

The effective corrosion rate of ECR with levels of surface damage lower than 1% to 2% cannot be estimated with the information available to date. Preliminary results from theoretical analysis of the corrosion configuration of the system [4.9] suggest that the rate of deterioration is more sensitive to the extent of disbondment than to the dimension of the coating breaks. Recently reported analysis of laboratory experiments [1.25] suggests that a pronounced reduction in the number of coating breaks (for example, down to a fraction of 1%) is essential to achieve a meaningful reduction in the overall rate. This reduction, coupled with a lowering of the tendency of the coating for disbondment in concrete service, might result in corrosion protection performance of a magnitude consistent with early expectations in the application of ECR. The practical difficulties to be overcome to consistently achieve very low coating breaks in actual finished structures (and to achieve a demonstrable disbondment-free coating performance over many decades of service in concrete) represent challenges that are beyond the scope of this report.

6.1.11 Corrosion development - a proposed sequence.

The following sequence of events leading to the observed deterioration in the bridges in Monroe County can be proposed. The sequence expands the concepts originally proposed in a previous report [1.12], and incorporates the present findings. Figure 6.1 shows schematically the main stages of the corrosion development process.

Pre-service history: ECR is produced according to the specifications existing at the time of the construction projects (Figure 6.1, A). The bars contain a small number of initial coating imperfections, as permitted by the acceptance criteria. The bars are then shipped and fabricated as required. Shipping introduces additional surface damage; fabrication creates disbondment by mechanical means (B). The bars are exposed to the construction yard environment for a time that may range from a few days to over a year. Salt water exposure at the yard creates additional disbondment; further deterioration might result from heating/cooling cycles, ultraviolet exposure and additional mechanical damage during handling (C). Rebar cage assembly procedures, positioning in concrete forms, as well as concrete pouring and vibration, create additional surface damage.

Service-in-concrete history: The ECR is exposed to a low-chloride concrete environment for a period that may range from several months to several years, depending on position with respect to the water level and concrete permeability (see Section 6.3). During that time the concrete pore solution interacts with the rebar coating and penetrates between coating and metal in regions where disbondment had taken place during pre-service. Exposure to the low or moderate chloride content concrete aggravates coating delamination (D). Upon arrival of the chloride front corrosion begins at the exposed metal at imperfections and in the crevices below the disbonded coating. Corrosion macrocells develop with cathodic regions where there is good oxygen availability. The cathodes take place not only at metal exposed by imperfections but also to some extent in the surrounding disbonded crevices. Low concrete resistivity and a measure of electrical continuity of the rebar cage promote macrocell action over significant distances, making for

an unfavorable anode-to-cathode ratio. The resulting intense action at the anodic portion causes additional disbondment and corrosion at the crevices (E). Eventually, the corrosion morphology consists of extensive coating delamination, accumulation of corrosion products and low pH liquid below the coating, and metal consumption manifested by spots of severe pitting on a background of more general wastage. Then externally observable corrosion develops in a relatively short time, comparable to that experienced by plain rebar in a similar concrete environment.

In summary, the corrosion may be viewed as resulting from the presence of normal production imperfections which were then aggravated by fabrication, handling, and a severe construction yard environment. This is followed by placing the rebars in moist, warm, eventually high chloride-level substructure service which is conducive to severe corrosion, aggravated by extended macrocell formation.

6.2 Present condition of ECR-bridges in Florida

The corrosion condition of four major structures in Monroe County (Long Key , Niles Channel, Seven Mile and Indian Key bridges) which showed early ECR deterioration has been documented elsewhere [1.6-1.8]. A fifth bridge (Channel Five) has shown signs of extensive ECR corrosion-induced deterioration, as revealed by continuing inspections. As part of the present investigation, of all the above structures only the Seven Mile bridge was revisited for reference purposes. Previous (1988) chloride content data from the Long Key and Niles Channel bridges were also included in this report.

The present investigation did not reveal severe corrosion in any of the structures examined outside the group mentioned above. A minor amount of corrosion was observed in one of the specimens extracted from the Vaca Cut bridges, which are in the Florida Keys. Outside the Keys, chloride concentrations at typical ECR rebar depths were generally low (Table 4.2, Figures 4.4-4.8). In about 15% and 6% of the cores examined in the bridges outside the Keys the chloride concentration exceeded 1.2 and 3.6 pcy respectively at

typical rebar depths. The sample population is not large enough to permit a meaningful estimate of the effective threshold for corrosion initiation of ECR in the field. However, the complete lack of observations of corrosion in ECR specimens in this group suggests that the effective chloride concentration threshold for corrosion initiation was not far below 1.2 pcy, at least at the present age of the bridges. Future monitoring of these structures will be needed to establish whether the threshold values become smaller after long service times, per the discussion in Section 6.1.8. The plain rebar bridges did show an instance of corrosion spalling (700184, IR2, Table 4.1), when chloride contamination was pronounced.

The most important finding of ECR deterioration in this study was the observation of coating-metal disbondment at almost all of the structures examined. As indicated in the previous section, coating disbondment is considered to be a key step in the corrosion development. The ECR in all these structures appears therefore to be already susceptible to the development of severe crevice corrosion if the chloride concentration reaches the value for corrosion initiation.

The measurements of the extent of electrical continuity of rebar assemblies (Figure 4.15) and of the levels of macrocell current attainable (Figure 4.17) suggest that other conditions are present in many of the ECR structures examined that can aggravate the corrosion process [1.12, 1.15].

ECR coating thickness measurements (Figure 4.25.) fell within expected values and no particular problem is foreseen from that circumstance. The measurement of the extent of coating breaks (Figure 4.21) could only be made approximately. Nevertheless, the median level of surface damage recorded (0.4%) was significantly below the limit of 2% unrepaired spots prevalent as a specification guideline at the time of construction of many of the structures examined. There was no evidence of gross backside contamination of the coatings. These observations suggest therefore that surface condition of the rebars generally satisfied the requirements in place at the time of construction.

With the exception of the affected structures in Monroe County, the present condition of bridges containing ECR in Florida is generally free of corrosion. The findings elsewhere in this report suggest that this condition is the result of very low levels of chloride contamination at the rebar depth. The low chloride level can be related to one or more favorable factors of a given bridge, such as early age, low concrete permeability, relatively mild environmental conditions, and effective concrete surface coatings. There is no indication that the absence of corrosion is related to the presence of the epoxy coating on the rebar. On the other hand, the presence of widespread coating-metal disbondment and the observation of some extent of coating breaks suggest that severe deterioration might occur later in the life of these structures.

6.3 Prognosis of Future Corrosion Performance.

6.3.1 Objective.

The main objective of this section is to provide an estimate of the length of service time Tc, for the substructure of bridges built with ECR in Florida before external signs of corrosion deterioration develop. External signs of corrosion deterioration include the appearance of detectable corrosion-induced cracks, rust stains, or evidence of delamination from hollow hammer impact soundings. It is desired to obtain an estimate of Tc for each bridge, based on field/laboratory characterization, service parameters and construction records.

6.3.2 Approach.

The estimates are based on a two-step deterioration model that includes an incubation period T1 where the reinforcing steel is experiencing negligible corrosion, and a subsequent propagation period T2 in which corrosion is proceeding at a finite rate. This approach has been used often to model the corrosion of uncoated rebar [4.8,4.10]. For that case, it is commonly assumed that during the initial period the concentration of chloride

ions at the rebar surface has not yet exceeded the threshold necessary to initiate active corrosion, and that therefore the corrosion rate is very small. After the threshold chloride concentration is reached (at t = T1) corrosion is assumed to proceed at a much higher rate than during the initial period. In this type model the length of the initial period is determined by the transport process of chloride ions through concrete, while the length of the second period depends on how fast the steel corrosion deteriorates the concrete and results in observable symptoms.

The two-step model has been assumed to apply also to the case of structures constructed using ECR. The application of the model is formal, in that it is not assumed that the steel surface beneath the coating is necessarily in the passive state during the incubation period. It is nevertheless proposed that the rate of corrosion is very small in chloride-free concrete, and that the rate increases significantly after a critical chloride content is reached in the concrete surrounding the epoxy-coated rebar. The rate is assumed to be the average metal loss taking place per unit time over a macroscopic length of epoxy coated rebar. It is recognized that appreciable disparities in local rate of metal dissolution may be present between steel surfaces immediately below breaks in the coating, underneath disbonded coating, and in regions where good coating adhesion is still present.

The following sections address the application of the model to the case of ECR.

6.3.3 Initiation Period.

Transport of Chloride Ions to the Rebar Surface.

In the marine substructure environment the concrete surface is exposed to seawater continuously. The concentration of chloride ions tends to be greatest in the surface of the splash-evaporation zone, about two to six feet above the high tide line. Chloride ions migrate to the interior of the concrete by several possible processes. It is expected that capillary convection of seawater is important in the first few millimeters below the surface.

Further into the concrete bulk, diffusion is a likely mechanism of transport. Since the chloride ions must move across a typical distance of several inches before reaching the rebar, it is common to assume that transport is exclusively diffusional. Another simplification often used is to treat the concrete as a homogeneous medium, since the characteristic dimension of the larger heterogeneities (coarse aggregate, typically 3/4 in) is several times smaller than the typical transport distances. Further simplification consists of considering that the effective diffusion coefficient D of chloride in concrete is constant in the region being examined. Under those assumptions, the chloride ion concentration C follows Fick's second law:

$$DL^2C = MC/Mt \qquad (1)$$

Equation (1) (in which t is the time) has a simple solution for the case when diffusion is one-dimensional, and the concentration of chloride ions at the concrete surface Cs does not vary with time:

$$C(x,t) = Cs - (Cs - Co)\ \mathrm{erf}\ (x / 2\%(D\ t)) \qquad (2)$$

where Co is the initial chloride content of the concrete, x is the distance from the concrete surface, and t is the time of exposure.

One-dimensional diffusion can be reasonably assumed for the surface of large diameter columns or the flat faces of square or rectangular members. The concentration of chloride at the surface of the concrete changes with time, from the value Co at the beginning to higher values as exposure to the seawater environment continues. The increase is expected to be rapid during the early service times, with the rate of increase decreasing with time. Work by Uji et al [4.11] suggests that the chloride surface concentration in marine substructure increases with the square root of the time of exposure, but their experimental evidence is not conclusive. As shown later, the surface

concentrations in the splash-evaporation zone estimated from the present field results approach the value expected from concrete containing saturated salt solutions, but do not follow an identifiable pattern with exposure time. As a simplification, it will be assumed that at each site an individual, relatively constant steady state surface concentration of chloride ions is reached after a short time of exposure. Equation (2) will then be applied assuming this and all the previously mentioned simplifications.

Values of the effective diffusion coefficient D and the calculated surface concentration Cs were obtained by fitting Eq.(2) to the chloride profiles determined for field cores. The procedure followed is described in Appendix I. The results of the computations are shown in Table 4.2. Average values of D were obtained for each bridge, using only data for cores that had a calculated value of Cs greater that 1 pcy. Figure 4.13 shows the average D ranked by value for each of the bridges examined. As indicated in Section 4.4, the effective diffusivity ranking is roughly matched by rankings based on low field resistivity, wet lab resistivity, and laboratory weight change of the cores during drying. All these variables are indirectly related to the permeability of the concrete [6.2] and show reasonably consistent results.

Eq. (2) can then be used to predict the chloride distribution profile into the concrete as a function of exposure time and D. Knowledge of the effective values of D, Cs and Co for a bridge substructure member allows estimation of the length of time needed to reach a given critical chloride concentration value at a given depth below the concrete surface.

As shown in the previous sections, the critical chloride concentration value Ct for triggering the onset of the propagation period in ECR is not precisely known. However, the evidence discussed above suggests that Ct for ECR is at best of the same order as that for plain steel bars. The value of Ct for plain steel is generally recognized to correspond to the condition whereby the concentration of chloride ions in the concrete pore solution is on the order of 0.3 to 0.6 that of hydroxyl ions. The pH of the pore solution can vary appreciably depending on the cement characteristics and the type of admixtures used; for example,

concrete made using fly ash addition could have a pH as much as one unit lower than that of a plain cement concrete [4.12]. Additional complication stems from the type of units used to measure concrete chloride content. The units used commonly in analysis (mass per concrete volume) relate only indirectly to the pore solution concentration, through the total concrete porosity which can only be roughly estimated. Because of these uncertainties, the service life estimations have been made using a set of nominal Ct values expressed in pcy. These values range from 1.2 pcy (an empirical amount commonly proposed as a chloride concentration threshold [4.13]) to three times as much. This choice of parameters is consistent with the lack of observation of conspicuous corrosion in the ECR or plain bar specimens extracted from locations where the chloride concentration was within the 1.2 to 3.6 pcy range.

6.3.4 Propagation period

The length of the propagation period is affected by numerous factors including the corrosion rate of the rebar, the extent and rate of accumulation of corrosion products, the locale where the corrosion products reside, the nature of the corrosion products (solid, liquid, mechanical properties, stoichiometry), the mechanical characteristics of the concrete (strength, toughness, creep properties), the size and shape of the concrete cover over the rebar, and the rebar size and assembly configuration.

The experimental information shown in Section 5.3 suggests that there are no dramatic differences in the time to the observation of external cracking between ECR and plain rebar systems, when the same amount of corrosion is artificially created in both. The experiments addressed a very limited set of circumstances, but in the absence of other evidence it will be assumed that ECR structures will show external signs of damage at about the same time as plain rebar systems would if the rates of corrosion were the same. As discussed in Section 6.1.9, the rates of corrosion of both systems in the propagation period can be comparable if coating surface damage of the magnitude often observed in the field is present.

The factors mentioned above preclude an estimate of the absolute length of the propagation period based solely on materials properties and corrosion severity. Instead, an estimate based on empirical observations will be used. A recent survey of corrosion development in bridge decks revealed a typical length of the propagation period that was on the order of 3.5 years [4.8]. Assuming for the moment that 3.5 years is also a representative value for substructure conditions in Florida, the total time until observation of concrete spalls (or similar deterioration indications such as cracks or delamination) can be evaluated by adding the length of the initiation and propagation periods.

6.3.5 Prognosis

The time for the initiation period was calculated by equating the value of C(x,t) in Equation (2) to 1.2, 2.4 and 3.6 pcy, and computing the value of t required to satisfy the equation. These calculations were done for values of D ranging from 0.01 to 10 in^2/y, and for various choices of x, Cs and Co. Figure 6.2 illustrates the results of the calculations (plus the proposed 3.5 years for propagation) for the case of the concrete cover x = 4 in, Cs = 20 pcy and Co = 0 pcy, conditions roughly approaching those encountered in the structures of interest.

The model results predict that for situations of very rapid chloride penetration (D roughly 1 in^2/y or higher) the time to spall is determined mainly by the length of the propagation period, and is not strongly dependent on the value of the chloride concentration threshold. In other words, the chloride transport to the rebars is so fast that the rebars begin to corrode shortly after being placed in service. For example, for D = 1 in^2/y the initiation period is only 4.5 years for Ct = 3.6 pcy, and 2.5 years for Ct = 1.2 pcy. Correspondingly shorter initiation times are to be expected if the rebar cover is smaller: 1.5 and 0.8 years respectively for the conditions just discussed and a cover of only 2 in. Times to spall for the 2 in cover case are shown in Figure 6.3.

The bridges of Monroe county showing severe ECR corrosion had rebar covers intermediate between those assumed in Figures 6.2 and 6.3 [1.6-1.8], and measured values of D in the approximate range 1 - 2 in^2/y. Those bridges had experienced delamination/spalls starting from about 6 to 10 years after construction, values which approach well the model predictions made with the assumed nominal propagation period length of 3.5 years. The model predictions are consistent also with typical past observations for the time to spall in FDOT piling reinforced with plain steel (about 12 years for 2 in covers) if one assumes a value for D equal to the median of the values in Figure 4.13 (0.1 in^2/y). Based on these observations and on the evidence discussed in Section 6.1.9, the value of 3.5 years will be retained as an approximate indication of the expected length of the propagation period, pending the development of more precise information in the future.

For structures with thick cover and low diffusion coefficients, the projected time to spall is long and dominated by the initiation period. Structures with modern concrete mix designs resulting in diffusion coefficients of 0.05 in^2/y or less and with concrete cover consistently exceeding 4 in, have projected times to spall on the order of 50 to 100 years or more. However, because of the long projected times it is important to emphasize the limitations of the data set and of the model used to arrive at the estimates.

The data set used to evaluate effective diffusion coefficients (Table 4.2) includes profiles with substantial deviations (both random and systematic) from ideal diffusional behavior, as expected from any field investigation. The chloride concentration profiles of the cores with the lowest values of D were steep, with most of the chloride penetration in the near-surface region where Fickian transport is only a poor approximation (as indicated in Section 6.3.3). The calculated values of Cs in those cases can only be considered as nominal. Sample-to-sample variability of calculated D values within individual bridges was also significant, as illustrated in Figure 4.12. Therefore the values of D assigned to individual bridges should be viewed as approximate estimates. No special distinction

should be made between structures unless their respective D values differ by a sizable amount (for example a factor of two or more). It should also be kept in mind that the value of D for a given structure is likely to change with time, usually toward smaller values as the concrete experiences long-term curing [6.3]. In that case, the time for corrosion initiation could be significantly longer than estimated above.

Other model limitations are due to lack of provision for factors such as complicated chloride diffusion geometry (corner effects, small diameter components) and variability in rebar cover within a structure. These limitations can be addressed by refinements in input parameters and other customization of the model. The main conclusions concerning ECR are not expected to be dramatically changed by those refinements (although future durability assessments merit detailed investigation). Other factors to which the model prediction could be potentially more sensitive are listed below.

The long-term model durability predictions may be overly pessimistic for ECR if the more recently built structures eventually develop a propagation stage much longer than the 3.5 years assumed in the calculations. This extension in the propagation stage could result from possible improvements in the overall corrosion protection ability of the ECR used during the mid 1980's, compared with those ECR produced a few years earlier. Improvement might have resulted from changes in the coating materials or processing, and also from improvements in the handling of the products (for example, bare tie wires were no longer used in the most recent projects). It is also possible that since the projected chloride concentration increase at the rebar level is slower at low D values than at high D values, the propagation period would take place in the presence of much lower average chloride contamination at the rebar depth. This in turn might activate fewer of the possible corrosion sites at the coated rebar surface with subsequent reduction in the overall corrosion rate. A similar argument could be made concerning a possible extension of the length of the initiation period. Unfortunately, these possible scenarios are speculative and awaiting the development of long term field demonstration data. The scale of the projected service times creates also a severe demand in the performance of the coated material if a

significant improvement over plain rebar is to be effected. For example, even if a tenfold improvement in propagation time over black bar were to be achieved with ECR, that would correspond to an increase in the time to spall of only about 30% for a bridge with 4 in cover, Ct = 1.2 pcy, and a value of D = 0.02 in^2/y (within the expectations of current construction). The uncertainties inherent to long term projections would make questionable the benefit realized with the associated expense and possible negative effects of using ECR. Some of those effects are discussed in the next paragraph.

Factors that might make the model projections too optimistic for ECR should also be considered. Of foremost importance is the condition of the coating-metal interface in cases where the chloride contamination front may take several decades to reach the rebar. Additional deterioration could develop in that extended time frame, beyond the simple loss of adhesion which has been observed in the specimens examined here (aged 5 to 12 years). This long time deterioration could take the form of sizable electrolyte accumulation at the epoxy-metal gap. In such case, the results summarized in Figure 5.7 suggest that corrosion could develop in the presence of much smaller chloride concentrations than those required at earlier stages. The conditions could be further aggravated in modern concretes with significant amounts of pozzolanic additions. The pozzolanic reaction of Type F fly ash, commonly used now in FDOT construction, is known to progress over long-time intervals at the expense of the calcium and alkali hydroxides in the cement paste [4.14,4.15]. The pH of the pore solution is consequently reduced, sometimes by as much as a full unit [4.12]. This effect could partly counteract the otherwise highly beneficial effect of the presence of fly ash and other pozzolans like silica fume, namely the pronounced reaction in concrete permeability which translates usually in very low values of D. As shown in Figure 5.7, the susceptibility for localized corrosion for a given chloride content is much greater in the 12.4 pH solution than in the 13.3 pH SPS medium. While pH reduction could affect the value of Ct for both ECR and plain rebar, Figure 5.7 shows that the effect was more pronounced for creviced configurations. A serious reduction in the value of Ct would reduce the length of the initiation period. This effect would be most noticeable in structures with low values of D, which otherwise have the highest projected durability.

The post-spall history, although not considered in the durability model, is potentially of great importance. In the case of plain rebar, cathodic protection is a demonstrated option to extend (corrosion-related) structure life indefinitely beyond spall development. That option is not easy to implement in ECR substructure because of the need to effect numerous individual electrical contacts to the bars to be protected. Partial assembly connections are discussed in Section 6.4.3. The total cost penalty for lack of available straightforward CP in bridges using ECR could result in severe limitation of overall service life compared with the case of a plain rebar system.

Keeping in mind the positive and negative qualifications mentioned above, the simplified model predictions suggest that the bridges in the upper third of the ranking in Figure 4.13 have a reasonable chance of experiencing from several decades to over one hundred years of service without extensive corrosion damage (however, because there is indication that most of the structures in that group were built using concrete with fly ash, caution is in order per the discussion above on chloride concentration thresholds). Structures in the lower third of the ranking are either already experiencing manifestations of corrosion damage or expected to do so during the next few years. Structures in the middle third should be further evaluated paying special attention to the specific distribution of concrete cover, presence of surface treatments, exposure conditions and possible weak points to refine their prognosis.

6.4 Future Directions.

6.4.1 Use of ECR.

The results on present condition and prognosis of Florida bridges built with ECR show that a significant fraction of the substructures (all located in Monroe Co.) are experiencing severe corrosion damage. Immediate deterioration is not expected in most of the remaining structures investigated. The field observations did reveal widespread

development of coating-metal disbondment. This disbondment was identified in the mechanistic investigations as a key step in the corrosion process, and it is expected that corrosion will eventually occur in most of the structures investigated. The results indicate that ECR failed to provide significant protection in those cases where very aggressive corrosion conditions existed. The time intervals to develop visible corrosion damage are projected to be determined in large part by the characteristics of the concrete cover, with the coating providing comparatively little additional protection. Another important negative factor of ECR is the difficulty foreseen in providing reliable long term cathodic protection when it becomes eventually needed.

The factors mentioned above argue strongly against the use of ECR, as presently available, for future FDOT substructure projects. New developments in coating materials, coating application and ECR utilization are being tested by industry and government organizations. It is conceivable that these efforts will result in a product with performance superior to that experienced in Florida to date. Unfortunately, the experience in the Florida Keys was a dramatic example of how preliminary testing by itself, while desirable for screening and optimization tests, was not enough to predict actual field performance in the real service environment. Realistic field demonstration is essential to confirm the performance expectations for any product or practice modification. It is also possible that long-term performance in some of the substructures already built with ECR in the State will exceed the present prognosis. However, field evidence to confirm any of those possibilities is not yet available. Because of the nature of the corrosion process in concrete, and of the performance to date, convincing field evidence of adequate performance of existing or new ECR implementations is likely to require decades to develop.

As a result of the above considerations, it is concluded that the use of ECR as implemented today is not a demonstrated corrosion protection option for marine substructure service in the State. This conclusion supports decisions by the FDOT [4.16] to discontinue the use of ECR.

6.4.2 Corrosion Protection Alternatives - New Design

New substructure construction can use various alternatives to ECR for corrosion protection. These alternatives include the use of denser concrete, the use of corrosion inhibitors, the use of galvanized rebar, and combinations thereof. An analysis of the relative merits of these alternatives is contained in Reference [1.30] and a recent update (also[1.30]).

The most promising alternative combination presently considered by the FDOT for extremely aggressive conditions consists of the use of plain rebar with a concrete cover of 4 in. The concrete mix design in this alternative conforms to FDOT Section 346 Class V designation, including pozzolanic addition for low permeability. The specific amount and type of pozzolanic addition depends on desired performance and resulting economic benefit. The concrete used in the substructure of the Sunshine Skyway bridge approached the 346 specification and used relatively inexpensive Type F fly ash as a pozzolanic admixture. As shown earlier, this structure had very low chloride diffusivities, which are projected to result in times to corrosion initiation in the 100 years range for the conditions assumed in the calculations for Figure 6.2. It appears therefore that extended corrosion-free service lives could be achieved with existing concrete technology and plain rebar. Proposed variations of concrete cover and mix design for different sections of the bridge substructure are listed in Chapter 7 of the FDOT Structures Design Manual. Caution should be exercised concerning possible reductions in the chloride concentration threshold (Ct) at high pozzolanic addition values, as indicated earlier.

The service life following onset of corrosion in plain rebar substructure can be addressed in practice either by application of cathodic protection or by conventional repairs, depending on the cost effectiveness of each approach. For cases where cathodic protection is determined to be economically advantageous, the structural design can be planned from the start to facilitate placement of anodes later in the life of the structure.

Using conservative values for the effective chloride diffusion coefficient, the update in Ref. [1.30] has concluded that the lowest life-cycle cost for a 75 year design life can be achieved with fly ash as the only pozzolanic addition plus (if necessary) sacrificial zinc cathodic protection during the last 15 years. Condensed silica fume as an alternative pozzolanic addition was not found by the analysis to be cost effective.

Other alternatives such as the use of galvanized rebar and wider application of corrosion inhibitors are being investigated at present by the FDOT. In the meantime and based on the most recent economic studies [1.30], the FDOT design philosophy incorporates the use of plain rebar, dense and thick concrete cover, and consideration of cathodic protection installation as a later backup measure. This approach offers a conservative combination of long projected service life with a well established backup corrosion control method.

It may be argued that using ECR, instead of plain rebar, with the present guidelines would provide a so-called "belt and suspenders" design approach for added corrosion protection. The findings of this investigation indicate against that idea. As discussed in Section 6.3.3, the placement of ECR instead of plain rebar would create possible risk of early corrosion initiation at coating-metal crevices, and also negate the straightforward implementation of cathodic protection after corrosion initiation. The possible positive effects of using ECR (increased initiation period, significantly reduced rate of corrosion during propagation) are not sufficiently supported by the present findings. The use of ECR assemblies with complete electric continuity to permit easy application of cathodic protection has been proposed elsewhere [1.23]. However, such proposal poses unanswered questions as to the degree to which unwanted macrocell currents would be promoted, and as to the cost and practical feasibility of implementing 100 % continuity without creating undue additional coating damage. In the absence of supporting field demonstration with adequate long term performance that approach remains unproven.

6.4.3 Corrosion Protection - Present Structures.

The exploratory laboratory findings described in Section 5.2.2, together with field experience with galvanic anodes (see below) suggest that cathodic protection, if actually reaching the rebar, can be effective in controlling ECR corrosion. However, the presently corroding bridge substructures in Monroe County present a challenge for implementing conventional cathodic protection, since connections to each individual rebar segment cannot be practically achieved. In addition, conventional impressed current cathodic protection systems are costly to implement in marine substructure applications.

Sacrificial, sprayed zinc sacrificial anodes that make connection only to those rebars exposed by a spall have been examined as a less costly alternative to impressed current, fully connected systems. Sprayed anodes have been applied to selected bents at the Niles Channel, Seven Mile and Long Key bridges. The oldest of these installations has been in place over 4.5 years and it is still delivering typical current densities on the order of 0.5 mA/ft^2. This value is representative of the current densities that provide effective protection in the case of old/damaged coating in pipeline applications. Conventional patching of spalls at the Niles Channel and Long Key bridges has lasted typically two years before additional repair was needed. In contrast, repair experience has shown that new spalls are much fewer in the bents with applied sacrificial anodes since the anodes were placed. Reports on the field performance of these anodes have been prepared elsewhere as part of a parallel USF-FDOT investigation supported by the Strategic Highway Research Program [1.32]. While it is recognized that not all the rebars in the affected substructure are protected by the anode, the approach appears to be promising as a cost effective alternative to frequent patching. The anode life before a new application is needed is estimated to exceed 5 years.

Physical intervention of the corroding substructure assemblies to create electrical continuity, and subsequent application of conventional cathodic protection, is not

considered at present to be a justifiable expense. If galvanic anode protection proves not to be effective in the Monroe County structures, the physical and economic feasibility of conventional cathodic protection will need to be evaluated. Complete replacement of substructure bent elements is considered at this time as an option for portions of the Long Key bridge, which suffers from additional unrelated structural deterioration.

As indicated in the Prognosis section, most of the bridges investigated that are not already corroding are not expected to show signs of ECR corrosion in the immediate future. Future corrosion control in those structures should be considered based on the experience that is presently being developed in the Monroe County bridges.

7. CONCLUSIONS

1. Severe corrosion of ECR is presently (early 1994) limited to the substructure of five major bridges in the Florida Keys. One smaller bridge (Vaca Cut 2, also in the Florida Keys) showed early indication of ECR corrosion. Twenty-four other structures examined for this study in salt water environments in the State showed no indication of ECR corrosion.

2. Epoxy coating disbondment from the steel substrate, confirmed by instrumented laboratory tests, was observed in virtually all of the structures examined. The disbondment was present even in the absence of chloride ion contamination, and it was observed in specimens that were desiccator dried over long periods of time.

3. The observed coating disbondment was not associated with any conspicuous undercoating contamination.

4. The coating thickness and total extent of coating breaks were generally within the production and use guidelines that were in effect at the time of construction of the bridges investigated..

5. ECR rebar assemblies showed a median value of 30% electrical continuity. Significant amounts of electric macrocell currents were recorded upon interconnection of separate elements.

6. The structures showing corrosion tended to exhibit much higher chloride diffusivities and lower concrete resistivities than those constructed with modern concrete formulations.

7. Laboratory experiments confirmed that significant coating disbondment can take place under moderate levels of cathodic polarization in liquid solutions representative of concrete pore solution.

8. Long term laboratory tests with ECR in concrete showed tendency for coating disbondment at the open circuit potential, and aggravated tendency for disbondment at -500 mV vs SCE.

9. Laboratory polarization measurements of pitting and crevicing potentials showed that the tendency for chloride-induced corrosion in alkaline solutions representative of concrete pore liquids is significantly aggravated by the presence of crevices. The polarization experiments suggest that the threshold chloride content for corrosion initiation under delaminated coatings is smaller than for uncoated steel. Initial results suggest that cathodic protection of the creviced area is feasible in conditions representative of concrete service.

10. Laboratory experiments with reinforced concrete specimens indicate that the time for development of corrosion-induced cracks is comparable for both plain rebar and ECR, when the same amount of corrosion products is being generated. Finite element computations suggest that the ECR has a somewhat greater susceptibility for crack propagation when equal amounts of corrosion product exist. In any event, the differences in mechanical behavior for corrosion-induced crack development in both types of systems do not appear to be dramatic.

11. Based on analysis of the results with an initiation-propagation corrosion model, the time-to-spall in the Florida Keys structures was dominated by the propagation stage. This in turn suggests that the corrosion propagation times were comparable to those normally experienced by plain rebar.

12. Corrosion-related durability of the remaining structures built with modern concrete formulations and thick cover is expected to be dominated primarily by the characteristics of the concrete

.

13. Of the structures examined in this investigation, about one-third have a service prognosis of at least several decades before showing extensive corrosion damage. Another third includes bridges that might begin to show signs of corrosion distress within the next decade. Bridges in the remaining third (some of which are already showing damage) should be monitored frequently for possibility of immediate repair needs.

14. The field evidence from chloride concentration profiles suggests that concrete formulations approaching the current 346 design with Type II cement and fly ash have a very good chance of providing significant durability. This approach has also been found to be the most cost-effective in recent economic analyses. Concrete cover meeting a 4 inch minimum (when permitted by structural considerations) is a key parameter in achieving long term durability.

15. Sprayed zinc sacrificial anodes represent a cost-attractive alternative to simple spall repair of presently corroding ECR structures.

8. REFERENCES

1.1 Virmani, Y., Clear, K. and Pasko, T., Time to Corrosion of Reinforcing Steel in Concrete Slabs, Vol.5:Calcium Nitrite Admixture and Epoxy-Coated Reinforcing Bars as Corrosion Protection Systems, Report No. FHWA/RD-83/012, National Technical Information Service, Springfield, Virginia, 1983.

1.2. Clear, K. and Virmani, Y., Corrosion of Nonspecification Epoxy-Coated Rebars in Salty Concrete, Public Roads, 1983 (June), Vol 47, 1.

1.3 Pike, R., Hay, R., Clifton, J., Beeghly. H and Mathey, R.,Public Roads, Vol.37, p.185, 1973.

1.4 Satake, J., Kamakura, M., Shirakawa, K., Mimaki, N., and Swamy, N., Long Term Corrosion Resistance of Epoxy-Coated Reinforcing Bars. In Corrosion of Reinforcement in Concrete Construction, ed.A.P. Crane, Ellis Horwood Publishers, Chichester, 1983, p.357.

1.5 Williams, J., "Solving the Rebar Corrosion Problem with Epoxy Coatings", Paper No. 107, Corrosion/79, National Association of Corrosion Engineers, Houston, 1979.

1.6. Kessler, R. and Powers, R. Interim Report, Corrosion Evaluation of Substructure, Long Key Bridge, Corrosion Report No. 87-9A, Materials Office, Florida Department of Transportation, Gainesville, 1987.

1.7 Powers, R. Corrosion of Epoxy Coated Rebar, Keys Segmental Bridges, Corrosion Report No. 88-8A, Florida Dept. of Transportation, Gainesville, Florida, 1987.

1.8 Florida D.O.T. Corrosion Task Force, Minutes, September 25, 1990 Mtg.

1.9 R.G. Powers, personal communication.

1.10 Sagüés, A. and Zayed, A., Corrosion of Epoxy-Coated Reinforcing Steel (Phase I),Final Report to Florida Department of Transportation, State Proj. No. 99700-7425, WPI 0510419, FL/DOT/SMO/89-419, University of South Florida, December, 1989.

1.11 Sagüés, A. and Zayed, A., Corrosion of Epoxy-Coated Reinforcing Steel (Phase II), Final Report to Florida Department of Transportation, State Proj. No. 99700-7494, University of South Florida, December, 1989.

1.12 Sagüés, A., "Mechanism of Corrosion of Epoxy-Coated Reinforcing Steel in Concrete", Final Report No. FL/DOT/RMC/0543-3296, National Technical Information Service, Springfield, VA 22161, April 1991.

1.13 Zayed, A., Sagüés, A. and Powers, R. Corrosion of Epoxy Coated Reinforcing Steel in Concrete, Paper No. 379, Corrosion/89, National Association of Corrosion Engineers, Houston, 1989.

1.14 Sagüés, A. and Powers, R. Effect of Concrete Environment on the Corrosion Performance of Epoxy-Coated Reinforcing Steel, Paper No. 311, Corrosion/90, National Association of Corrosion Engineers, Houston, 1990.

1.15 Sagüés, A. , Perez-Duran. H. and Powers, R., Corrosion, Vol 47, p.884, 1991.

1.16 Sagüés, A. and Zayed, A., Corrosion, Vol. 47, p.852, 1991.

1.17 Zayed, A. and Sagüés, A., Corrosion Science Vol.30, p.1025, 1990.

1.18 Sagüés, A., Powers, R., Zayed, A., "Marine Environment Corrosion of Epoxy-Coated Reinforcing Steel", in Corrosion of Reinforcement in Concrete, C. Page, K.Treadaway and P. Bamforth, Eds., pp.539-549, Elsevier Appl. Sci., London-New York, 1990.

1.19 Sagüés, A., Powers, R. and Kessler, R., "Corrosion Processes and Field Performance of Epoxy-Coated Reinforcing Steel in Marine Substructures", Paper No. 299, Corrosion/94, National Association of Corrosion Engineers, Houston, 1994.

1.20 Sohanghpurwala, A. and Clear, K., Effectiveness of Epoxy Coatings in Minimizing Corrosion of Reinforcing Steel in Concrete, Transportation Rsch. Board , 69th Annual Meeting, Paper Preprint No. 89-0432, Washington, January 7-11, 1990.

1.21 Concrete Reinforcing Steel Institute "CRSI Performance Research: Epoxy Coated Reinforcing Steel", Interim Report-January 1992, Part I prepared by Kenneth C.Clear, Inc. and Part II prepared by Wiss, Janney, Elstner Associates, Inc., CRSI, 1992.

1.22 Kenneth C. Clear, Inc., "Effectiveness of Epoxy-Coated Reinforcing Steel". Final Report, March 1992, submitted to the Canadian Strategic Highway Research Program, 1992.

1.23 Clear, K.C., "Effectiveness of Epoxy-Coated Reinforcing Steel", Concrete International, p. 58, Vol. 14, May 1992.

1.24 Concrete Reinforcing Steel Institute, Concrete International, Vol. 14, No.5, p.59, 1992.

1.25 Pfeifer, D., Landgreen, J. and Krauss, P., "Investigation for CRSI on CRSI-Sponsored Corrosion Studies at Kenneth C. Clear Inc.", CRSI Performance Research: Epoxy Coated Reinforcing Steel, Final Report, Schaumburg, Illinois, U.S.A. June, 1992.

1.26 Malasheskie, G., Maurer, D., Mellot, D., and Arellano, J., "Bridge Deck Protective Systems", Report FHWA-PA-88-001+85-17, (prepared by Pennsylvania Dept. of Transportation), July 1988, available from National Tech. Info. Center, Springfield, VA.

1.27 Hededahl, P., and Manning, D., "Field Investigation of Epoxy-Coated Reinforcing Steel" Report MAT-89-02, Ontario Ministry of Transportation, December, 1989.

1.28 In Preparation: Final Report for National Cooperative Highway Research Program (NCHRP), Project 10-37, "Performance of Epoxy-Coated Reinforcing Steel in Highway Bridges", Transportation Research Board, National Research Council, Washington, D.C.

1.29 U.S. Federal Highway Administration, Solicitation DTFH61-92-R-00127 "Corrosion Resistant Reinforcement for Concrete Components", 1992.

1.30 Hartt, W. and Stronge, W., "Feasibility and Economics of Bridge Corrosion Protection Alternatives", Report Fl/DOT/SMO/89-360, November, 1989 (Final Report for FDOT contract 99700-7466-010). See also by Hartt, W., "Feasibility and Economics of Bridge Corrosion Protection Alternatives - An Addendum Study (WPI No. 0510691), Florida Atlantic University, Boca Raton, Florida, March 23, 1994.

1.31 R. Powers, A. Sagüés and T. Murase, "Sprayed-Zinc Galvanic Anodes for the Cathodic Protection of Reinforcing Steel in Concrete", p. 732 in "Materials,: Performance and Prevention of Deficiencies and Failures", Proc. of the Materials Engineering Congress, Mat. Eng. Div., ASCE, T.D. White, Ed., American Soc. of Civil Engineers, New York, 1992.

1.32 Sagüés, A. and Powers, R., "Low-Cost Sprayed Zinc Galvanic Anode for Control of Corrosion of Reinforcing Steel in Marine Bridge Substructures", Final Report, Contract No. SHRP-88-ID024, Strategic Highway Research Program, Washington, 1993.

1.33 Research Contract "Performance of Alternative Material Rebars in Marine Service" A.Sagüés, P.I., Florida Department of Transportation, 1/1/93-6/30/94

1.34 Research Contract "Performance of Galvanized Rebar in Marine Substructure Service", A. Sagüés, P.I., International Lead Zinc research Organization, 4/1/93-3/31/94

2.1 Andrade, C. and Gonzalez, J., Werkstoffe und Korrosion, Vol. 29, p.515, 1978.

2.2 Kessler, J., Arrebola, V., Lingerfelt, R. and Brown, R., "Determination of Low-Levels of Chloride in Concrete and Raw Materials", Report Florida 203, Florida Dept. of Transportation, Gainesville, 1978.

2.3 Andersson, K., Allard, B., Bengtsson, M. and Magnusson, B., Cement and Concrete Rsch., Vol. 19, p. 327, 1989.

2.4 Diamond, S., Cement and Concrete Research, Vol.11, p.383, 1981.

2.5 Pickering, H., Corrosion Sci., Vol. 29, p.325, 1989.

2.6 Pickering, H., Corrosion, Vol.42, p.125, 1986.

4.1 Andrade, C., Lozano, J., Segui, V., Vicens, E,. and Hernandez, E., "Identification of High Alumina Cement in Concrete by the Use of the Pachometer", Informes de la Construccion, Vol. 44, No. 419, p.65, May-June 1992.

4.2 A. Sagüés, "Corrosion Measurement Techniques for Steel in Concrete", Paper No. 353, 22 pp., Corrosion/93, National Assoc. of Corrosion Engineers, Houston, 1993.

4.3 Berke, N., "The Use of Anodic Polarization to Determine the Effectiveness of Calcium Nitrite as an Anodic Inhibitor", p.78 in Corrosion Effects of Stray Currents and the Techniques for Evaluating Corrosion of Rebars in Concrete", ASTM STP 906, V. Chaker, Ed., ASTM, Philadelphia, 1986.

4.4 Brown, R., Poore, T., Edgell, T and Riemenschneider, J., "Corrosion Monitoring of Reinforced Concrete Piles at Matanzas Inlet", FDOT Interim Report 82/255, Unpublished notes, 3M Company, January, 1989.

4.5 Tuutti, K., Corrosion of Steel in Concrete, Swedish Cement and Concrete Research Institute, Stockholm, 1982.

4.6 Andrade, C., Cruz Alonso, M. and Gonzalez, J., "An Initial Effort to Use the Corrosion Rate Measurements for Estimating Rebar Durability", p.29 in Corrosion Rates of Steel in Concrete, ASTM STP 1065, N. Berke, V. Chaker and D. Whiting, Eds., ASTM, Philadelphia, 1990.

4.7 Kranc, S.C. and Sagüés, A.A., "Computation of Corrosion Macrocell Current Distribution and Electrochemical Impedance of Reinforcing Steel in Concrete", in Computer Modeling in Corrosion, ASTM STP 1154, R.S. Munn, Ed., American Society for Testing and Materials, Philadelphia, p.95, 1992.

4.8 Weyers, R.E. et al, "Concrete Bridge Protection, Repair and Rehabilitation Relative to Reinforcement Corrosion, a Methods Application Manual", Strategic Highway Research Program, National Research Council, Washington, D.C., 1993.

4.9 Cottis, R, "The Influence of Coating Disbondment on the Corrosion of Coated Reinforcement", to be published, 1993.

4.10 Tuutti, K., "Effect of Cement Type and Different Additions on Service Life", p.1285, in Concrete 2000, R.K. Dhir and M.R. Jones, E&FN Spon, London, 1993.

4.11 K.Uji, Y.Matsuoka and T.Maruya, "Formulation of and Equation for Surface chloride Content of Concrete due to Permeation of Chloride", in Corrosion of Reinforcement in Concrete, C.Page, K.Treadaway and P. Bamforth, Eds., p.258, Elsevier, New York, 1990.

4.12 Rasheeduzzafar, Dakhil, F., Bader, M. and Khan, M., ACI Materials Journal, Vol. 89, p. 439, 1992.

4.13 Slater, J., "Corrosion of Metals in Association with Concrete", ASTM STP 818, ASTM, Philadelphia, 1983.

4.14 Helmuth, R., "Fly Ash in Cement and Concrete", Portland Cement Association, Skokie, 1987.

4.15 K. Wesche, Editor, "Fly Ash in Concrete", RILEM Report 7, E & FN Spon, London, 1991.

4.16 Potter, J., Florida DOT Memorandum to District Structures Design Engineers, "Use of Epoxy Coated Reinforcing Steel", Tallahassee, July 14, 1992.

6.1 Kessler, R.J. and Powers, R.G., "Evaluation of Coated Versus Uncoated Reinforcement in Marine Environment", Report 90-12A, Materials Office, Florida Department of Transportation, Gainesville, Florida, December 1990.

6.2 Berke, N.S. and Hicks, M.C., "Estimating the Life Cycle of Reinforced Concrete Decks and Marine Piles Using Laboratory Diffusion and Corrosion Data", p.207 in "Corrosion Forms and Control for Infrastructure", ASTM STP 1137, Victor Chacker, Ed., American Society for Testing and Materials, Philadelphia, 1992.

6.2 Bamforth, P.B., "Concrete Classifications For R.C. Structures Exposed to Marine and Other Salt-Laden Environments", 11 pp., Paper presented at "Structural Faults and Repair", Edinburgh, 29 June-1 July 1993.

TABLE 2.1

Epoxy Coated Rebar Investigation - List of Bridges and Locations

Bridge name	Abbr.	County	Location	Bridge Number	Rebar Type
Green	GRN	Manatee	Bus. US 41 over Manatee River	130132	ECR
I-75 SB	75S	Manatee	I-75 Southbound over Manatee River	130103	ECR
I-75 NB	75N	Manatee	I-75 Northbound over Manatee River	130104	ECR
Halifax	HAL	Volusia	SR 40 over Halifax River	790132	ECR
Indian River 1	IR1	Brevard	US 192, Melbourne Causeway (Channel)	700181	ECR
Indian River 2	IR2	Brevard	US 192, Melbourne Causeway (Channel	700174	Plain
New River	NWR	Broward	SR 811 over New River, Ft. Lauderdale	860319	ECR
Vaca Cut 2	*VA1*[a]	Monroe	US 1 over Vaca Cut, Marathon	900126	ECR
Vaca Cut 1	*VA2*[a]	Monroe	US 1 over Vaca Cut, Marathon	900124	ECR
Alafia River 1	AL1	Hillsborough	I-75 over Alafia River	100358	Plain
Alafia River 2	AL2	Hillsborough	I-75 over Alafia River	100359	Plain
Snake Creek	SNK	Monroe	US 1 over Snake Creek, Florida Keys	900077	ECR
ICWW-A	ITA	Broward	SR 838 over Intracoastal Waterway	860466	ECR
ICWW-B	ITB	Broward	SR 838 over Intracoastal Waterway	860467	ECR
Matanzas	MAT	Lee	SR 865 over Mantanzas Pass, Ft. Myers	120088	ECR
Perdido	PER	Escambia	US 98 over Perdido Bay	480140	ECR
Choctawatchee	CHO	Okaloosa	SR 30 over East Pass, Destin	570082	ECR
Peace River 1	*PC1*[a]	Charlotte	US 41 Northbound over Peace River	010092	ECR
Peace River 2	*PC2*[a]	Charlotte	I-75 over Peace River	*010058*[a]	ECR
Peace River 3	*PC3*[a]	Charlotte	I-75 over Peace River	*010057*[a]	ECR
Apalachicola	APA	Franklin	US 98 over Apalachicola River	490031	ECR
ICWW-2	IT2	Dade	SR 852 over Intracoastal Waterway	870607	ECR
ICWW-3	IT3	Dade	SR 852 over Intracoastal Waterway	870606	ECR
New Pass	NWP	Sarasota	SR 789 over New Pass, Longboat Key	170158	ECR
ICWW-4	IT4	Palm Beach	SR 786 over Intracoastal Waterway	930349	Plain
Hobe Sound	HOB	Martin	SR 707 over Hobe Sound	890107	ECR
Miami River 1	MI1	Dade	Miami Ave. over Miami River	874663	ECR
Miami River 2	MI2	Dade	Miami Ave. over Miami River	874664	ECR
Skyway	SSK	Pinellas	I-275 over Tampa Bay	150189	ECR

Additional Bridges

Long Key	LKY	Monroe	US 1, Florida Keys	900094	ECR
Niles Channel	NIL	Monroe	US 1, Florida Keys	900117	ECR
Seven Mile	7MI	Monroe	US 1, Florida Keys	900026	ECR

a) Modified 03/01/02 to correct erratum in original printed version

Table 3.1

Composition of Test Solutions, Liquid Disbondment Tests (g/liter)

Solution	NaOH	KOH	NaCl	$Ca(OH)_2$ *	pH
Simulated Pore Solution (SPS)	8.33	23.3	---	10	13.45
Low Chloride (0.06 M)	8.37	23.4	3.63	10	13.45
High Chloride (0.45 M)	8.57	24.0	28.2	10	13.45

***Saturated**

Table 3.2

Concrete Mix Design, Tests of Coating Disbondment in Chloride-Free Concrete

w/c:	**0.41**
Cement Type:	**II**
Coarse Aggregate:	**1745 pcy**
Fine Aggregate:	**1167 pcy**
Cement:	**537 pcy**
Unit Weight:	**3835 lb**

Table 3.3

Concrete Mix Design,

Tests for Cracking with ECR and Plain Rebar

w/c:	**0.45**
Cement Type:	**II**
Coarse Aggregate:	**1812 pcy**
Fine Aggregate:	**1140 pcy**
Cement:	**582 pcy**
Unit Weight:	**3796 lb**

The center portions of the specimens received an additional 20 pcy chloride introduced as NaCl at the time of casting.

Table 3.4

Materials Properties Used

in Stress Intensity Computations

E steel =	**30×10^6 psi**
E concrete =	**4.4×10^6 psi**
v steel =	**0.3**
v concrete =	**0.175**

TABLE 4.1A FIELD INVESTIGATION-BRIDGE SUMMARY

BRIDGE NO.	BRIDGE NAME	MACROCELL CURRENT (uA)	CORR CURRENT (uA)	FLY ASH	AMOUNT OF FINES	WEIGHT CHANGE (%)	WET RES (Kohm-cm)	MAXIMUM FIELD RES (Kohm-cm)	MINIMUM FIELD RES (Kohm-cm)	D (sq in/yr)	EPOXY OR PLAIN	KNIFE DISBOND	PULLOUT STRENGTH (PSI)	PULLOUT PERCENT (%)	REBAR SURFACE CORR	DEGREE OF CONT (%)	BARE AREA (%)	COATING THICKNESS [mils]
130132	GRN	1.0E-01	1.4E+00	YES	MED	2.93	24	168	66	0.032	E	YES	1804	85	NO	10	0.22	10.7
900026	7MI	3.1E+01	4.2E+01	NO	HI	4.15	7.8	24	5.0	0.96	E	YES	949	100	YES	31	2.7	16.6
130103	75S	1.2E+00	9.8E-01	YES	LO	3.10	21	82	36	0.014	E	YES	772	0	NO	18	0.80	14.1
130104	75N	3.0E-02	5.9E-02	YES	LO	3.22	25	105	26	0.037	E	YES	1384	100	NO	7	0.05	26.6
790132	HAL	5.7E+03	2.6E+01	NO	LO	2.99	8.3	28	6.1	0.31	E	YES	599	50	NO	63	1.9	9.6
700181	IR1	6.5E+01	1.5E+01	NO	MED	4.01	6.2	27	4.0	0.27	E	YES	545	100	NO	39	0.76	7.2
700174	IR2	*	1.8E+04	NO	MED	3.20	13	32	8.4	1.2	P	*	*	*	YES	*	*	*
860319	NWR	5.0E+00	1.6E+04	NO	HI	3.76	7.5	132	3.3	0.069	E	YES	315	100	NO	81	0.90	8.5
900126	VA1	4.0E+00	1.5E+01	NO	MED	4.93	4.5	33	2.5	1.2	E	YES	513	90	NO	30	0.43	8.9
900124	VA2	7.1E+00	3.6E+04	NO	MED	5.36	4.8	53	2.2	0.87	E	YES	1373	100	YES	20	0.74	7.7
100358	AL1	*	9.0E+04	NO	LO	3.09	7.3	114	14	0.080	P	*	*	*	NO	*	*	*
100359	AL2	*	1.7E+07	NO	LO	3.05	8.6	69	19	0.11	P	*	*	*	NO	*	*	*
900077	SNK	4.0E-01	5.4E+00	NO	HI	4.93	3.4	14	6.5	0.40	E	YES	1890	0	NO	20	5.0	8.0
860466	ITA	2.9E+02	5.8E-01	NO	HI	4.05	5.2	9.0	5.6	0.17	E	YES	854	2	NO	30	0.03	7.7
860467	ITB	0.0E+00	4.5E+01	YES	HI	3.87	26	171	4.1	0.025	E	NO	1797	85	NO	4	0.55	10.8
120088	MAT	2.5E+02	6.6E-01	YES	LO	2.76	52	192	53	0.019	E	YES	*	*	NO	16	0.99	20.7
010092	PC1	4.0E+02	2.3E+02	YES	LO	2.95	21	198	23	0.046	E	P	1512	0	NO	91	3.8	10.1
010058	PC2	2.6E+03	5.1E+00	YES	LO	3.02	19	193	22	0.018	E	P	599	10	NO	67	1.0	9.6
010057	PC3	3.0E-01	1.5E+02	YES	LO	2.15	35	182	29	0.018	E	P	471	100	NO	40	2.4	11.4
570082	CHO	3.8E+00	3.1E+02	NO	LO	2.11	8.2	40	13	0.71	E	YES	*	*	NO	77	1.0	16.3
480140	PER	1.8E+00	1.3E+02	YES	LO	1.59	28	342	41	0.011	E	YES	*	*	NO	84	2.3	7.6
490031	APA	1.5E-01	5.0E+01	NO	LO	1.76	18	134	18	0.062	E	NO	*	*	NO	6	0.03	10.7
870607	IT2	3.0E+01	1.7E+02	NO	HI	3.07	4.6	37	5.9	0.25	E	YES	1112	21	NO	86	0.31	7.9
870606	IT3	2.9E+01	1.7E+01	NO	HI	3.32	3.7	22	5.0	0.17	E	YES	428	97	NO	64	1.2	7.2
170158	NWP	2.1E+00	4.4E-01	NO	LO	2.46	30	322	33	0.065	E	YES	984	0	NO	6	5.0	10.5
930349	IT4	*	5.4E+02	NO	MED	3.18	2.8	18	4.9	0.34	P	*	*	*	NO	75	*	*
890107	HOB	7.2E+01	1.7E+02	NO	HI	4.14	3.0	74	2.5	0.27	E	YES	684	100	NO	25	0.01	11.3
874663	MI1	2.7E+01	1.2E+03	NO	HI	3.48	4.1	42	6.0	0.024	E	YES	513	100	NO	20	0.24	10.2
874664	MI2	9.8E+01	7.6E+02	NO	HI	3.42	4.2	286	8.4	0.065	E	YES	685	100	NO	34	0.05	11.3
150189	SSK	1.1E+01	8.6E+00	YES	LO	2.18	32	314	24	0.020	E	YES	827	20	NO	13	0.57	11.8
900117	NIL	*	*	NO	*	*	*	*	*	0.97	E	YES	*	*	YES	*	*	*
900094	LKY	*	*	NO	*	*	*	*	*	2.9	E	YES	*	*	YES	*	*	*

RES = RESISTIVITY

CORR = CORROSION

D = EFFECTIVE DIFFUSION COEFFICIENT

CONT = CONTINUITY

* = NO DATA

KNIFE DISBOND = DISBONDMENT PER KNIFE TEST: YES = FULLY DISBONDED

NO = NO DISBONDMENT

P = PARTIAL DISBONDMENT

NOTES:

MAGNITUDES ARE AVERAGE FOR THE BRIDGE EXCEPT WHERE INDICATED

MACROCELL CURRENT VALUES ARE ABSOLUTE VALUES

TABLE 4.1B FIELD INVESTIGATION-COLUMN SUMMARY (pg 1of 3)

BRIDGE NO.	BRIDGE NAME	CONST DATE	TEST YEAR	AGE@ TEST (YR)	PIER NO.	COL	HALF CELL LO (mv)	HALF CELL HI (mv)	MACROCELL CURRENT (uA)	CORR CURRENT (uA)	MAX MUT RESIST (ohm)	WEIGHT CHANGE (%)	WET RES (Kohm-cm)	MAXIMUM FIELD RES (Kohm-cm)	MINIMUM FIELD RES (Kohm-cm)	D (sq in/yr)	PULLOUT STRENGTH (psi)	PULLOUT PERCENT (%)	DEGREE OF CONT (%)	REBAR COVER (in)
130132	GRN	1985	1991	6	9	B	-154	47	*	*	*	2.93	24	113	78	0.03	1468	70	*	2.8
130132		1985	1991	6	24	A	-108	-6	1.0E-01	1.4E+00	17000	*	*	223	54	0.05	2140	100	10	3.1
900026	7MI	1982	1991	9	59	A	-493	-293	1.2E+01	4.2E+01	1000	4.15	7.8	14	3.3	1.25	949	100	33	*
900026		1982	1991	9	196	B	-208	-130	5.0E+01	*	220	*	*	17	5.9	***0.75***[a)]	*	*	29	4.7
900026		1982	1991	9	196	A	*	*	*	*	*	*	*	20	1.5	*	*	*	*	*
900026		1982	1991	9	158	A	*	*	*	*	*	*	*	45	9.3	*	*	*	*	*
900026		1982	1988	6	20	*	*	*	*	*	*	*	*	*	*	0.98	*	*	*	*
900026		1982	1988	6	63	*	*	*	*	*	*	*	*	*	*	1.70	*	*	*	*
130103	75S	1980	1991	11	27	C	-325	-14	1.9E+00	1.2E+00	8.7	2.98	23	75	43	0.01	772	0	28	5.5
130103		1980	1991	11	18	C	-141	91	4.0E-01	7.9E-01	42000	3.23	19	82	36	0.02	*	*	8.7	5.0
130104	75N	1980	1991	11	27	A	-224	112	1.0E-01	0.0E+00	1000000	3.22	25	105	38	0.05	1384	100	4.4	3.8
130104		1980	1991	11	18	A	-102	138	1.0E-02	5.9E-02	27000	*	*	140	26	0.03	*	*	8.8	4.0
790132	HAL	1986	1991	5	17	C	-275	-68	1.0E+04	1.2E+01	73	3.13	9.5	18	6.1	*	599	50	60	4.0
790132		1986	1991	5	5	A	-324	-69	*	4.0E+01	0	2.91	8.2	23	10	*	*	*	100	4.3
790132		1986	1991	5	13	A	-602	-204	1.3E+03	1.2E+02	15	2.88	6.3	28	7.9	0.31	*	*	30	4.4
700181	IR1	1985	1991	6	20	A	-302	-138	1.0E+01	2.0E+01	75	4.37	5.8	15	4.0	*	*	*	60	4.1
700181		1985	1991	6	5	B	-277	-100	1.2E+02	1.1E+01	220	3.65	6.6	16	7.6	0.27	545	100	17	3.0
700181		1985	1991	6	24	B	*	*	*	*	*	*	*	27	6.3	*	*	*	*	*
700174	IR2	1985	1991	6	19	A	-276	-123	*	1.8E+04	2.0	3.20	13	25	8.4	1.18	*	*	*	4.8
700174		1985	1991	6	24	A	*	*	*	*	*	*	*	32	8.9	*	*	*	*	*
860319	NWR	1981	1991	10	7	A	-469	-101	5.0E+00	3.3E+04	16	*	*	36	4.2	*	315	100	62	3.6
860319		1981	1991	10	7	B	-273	-204	*	1.6E+02	1.6	3.76	7.5	132	3.3	0.07	*	*	100	4.4
900126	VA1	1982	1991	9	2	A	-483	-120	1.0E+00	1.5E+01	3700	4.69	5.2	33	2.5	1.42	513	90	40	5.5
900126		1982	1991	9	4	A	-417	-158	7.0E+00	*	240	5.17	3.9	23	3.4	1.00	*	*	20	6.7
900124	VA2	1982	1991	9	2	B	-530	-211	1.0E-01	0.0E+00	630	5.18	5.4	53	3.7	0.87	1226	100	0	5.8
900124		1982	1991	9	4	B	-574	-214	1.4E+01	7.2E+04	480	5.54	4.2	16	2.2	*	1520	100	40	6.1

CONST = CONSTRUCTION
COL = COLUMN
CORR = CORROSION
MUT RESIST = MUTUAL RESISTANCE
RES = RESISTIVITY
D = EFFECTIVE DIFFUSION COEFFICIENT
CONT = CONTINUITY
* = NO DATA

a) Modified 03/01/02 to correct erratum in original printed version

TABLE 4.1B FIELD INVESTIGATION-COLUMN SUMMARY (pg 2 of 3)

BRIDGE NO.	BRIDGE NAME	CONST DATE	TEST YEAR	AGE@ TEST (YR)	PIER NO.	COL	HALF CELL LO (mv)	HALF CELL HI (mv)	MACROCELL CURRENT (uA)	CORR CURRENT (uA)	MAX MUT RESIST (ohm)	WEIGHT CHANGE (%)	WET RES (Kohm-cm)	MAXIMUM FIELD RES (Kohm-cm)	MINIMUM FIELD RES (Kohm-cm)	D (sq in/yr)	PULLOUT STRENGTH (psi)	PULLOUT PERCENT (%)	DEGREE OF CONT (%)	REBAR COVER (in)
100358	AL1	1981	1991	10	8	A	-137	66	*	9.0E+04	*	*	*	76	14	0.08	*	*	*	4.8
100358		1981	1991	10	6	C	-27	108	*	*	*	3.09	7.3	114	21	*	*	*	*	4.0
100359	AL2	1981	1991	10	6	C	-156	98	*	*	*	2.91	8.0	63	19	0.11	*	*	*	4.9
100359		1981	1991	10	8	C	-100	82	*	1.7E+07	*	3.26	9.5	69	23	*	*	*	*	4.3
900077	SNK	1981	1992	11	8	B	-644	-251	4.0E-01	5.4E+00	39000	4.36	4.4	14	6.5	0.39	1890	0	20	6.4
900077		1981	1992	11	5	B	-432	-394	*	*	*	5.51	2.3	13	8.2	0.41	*	*	*	6.8
860466	ITA	1989	1992	3	B	B	-479	-161	2.9E+02	5.8E-01	470	4.05	5.2	9	5.6	0.12	854	2	30	4.7
860467	ITB	1989	1992	3	B	B	-168	-55	0.0E+00	4.5E+01	31000	3.87	26	171	4.1	0.03	1797	85	3.6	4.8
120088	MAT	1980	1992	12	13	A	-249	310	2.0E+00	2.9E-01	12000	*	*	192	53	0.02	*	*	13.3	4.3
120088		1980	1992	12	13	B	-686	-66	5.0E+02	1.0E+00	66000	2.76	52	168	78	0.02	*	*	19.1	4.3
010092	PC1	1983	1992	9	24	1	-301	-95	0.0E+00	3.8E+02	3.6	*	*	198	23	0.05	1512	0	100	3.7
010092		1983	1992	9	32	2	-390	-129	8.0E+02	6.8E+01	5400	2.95	21	196	23	0.04	*	*	82	4.5
010058	PC2	1980	1992	12	54	1	-186	-36	7.0E-01	2.2E+00	430	2.81	22	192	53	0.02	599	10	67	4.4
010058		1980	1992	12	37	1	-127	44	5.1E+03	8.0E+00	840	3.24	16	193	22	0.01	*	*	67	3.9
010057	PC3	1980	1992	12	54	2	-187	-9	3.0E-01	1.5E+02	4300	2.15	35	182	29	0.02	471	100	40	3.6
570082	CHO	1979	1992	13	33	1	-329	-157	3.8E+00	3.1E+02	890	2.11	8.2	40	13	0.71	*	*	77	3.9
480140	PER	1981	1992	11	27	1	-196	90	*	1.3E+02	3.9	*	*	342	41	0.01	*	*	100	4.3
480140		1981	1992	11	37	1	20	94	1.8E+00	1.3E+02	910	1.59	28	194	64	0.01	*	*	67	4.2
490031	APA	1988	1992	4	16	1	-102	-68	1.0E-01	2.1E-01	82000	1.79	16	106	18	*	*	*	0	2.0
490031		1988	1992	4	31	1	-96	-44	2.0E-01	1.0E+02	18000	1.74	19	134	55	0.06	*	*	11	3.3
870607	IT2	1983	1992	9	12	3	-232	-129	*	3.4E+02	1.7	2.97	5.2	37	9.2	0.06	1112	21	100	4.3
870607		1983	1992	9	13	2	-501	-75	3.0E+01	5.2E+00	85	3.16	4.1	27	5.9	0.34	*	*	71	5.3
870606	IT3	1983	1992	9	12	1	-389	-206	1.8E+01	1.3E+01	93000	3.39	3.4	22	13	0.01	428	97	60	3.1
870606		1983	1992	9	13	3	-428	-76	3.9E+01	2.2E+01	59	3.19	4.4	17	5.0	0.25	*	*	67	3.7

CONST = CONSTRUCTION
COL = COLUMN
CORR = CORROSION
MUT RESIST = MUTUAL RESISTANCE
RES = RESISTIVITY
D = EFFECTIVE DIFFUSION COEFFICIENT
CONT = CONTINUITY
* = NO DATA

TABLE 4.1B FIELD INVESTIGATION-COLUMN SUMMARY (pg 3 of 3)

BRIDGE NO.	BRIDGE NAME	CONST DATE	TEST YEAR	AGE@ TEST (YR)	PIER NO.	COL	HALF CELL LO (mv)	HALF CELL HI (mv)	MACROCELL CURRENT (uA)	CORR CURRENT (uA)	MAX MUT RESIST (ohm)	WEIGHT CHANGE (%)	WET RES (Kohm-cm)	MAXIMUM FIELD RES (Kohm-cm)	MINIMUM FIELD RES (Kohm-cm)	D (sq in/yr)	PULLOUT STRENGTH (psi)	PULLOUT PERCENT (%)	DEGREE OF CONT (%)	REBAR COVER (in)
170158	NWP	1986	1992	6	4	2	-254	25	3.8E+00	4.4E-01	78000	2.15	26	322	33	0.12	984	0	7.1	5.7
170158		1986	1992	6	8	3	-268	69	3.0E-01	4.3E-01	14000	2.76	33	189	90	0.01	*	*	4.8	3.9
930349	IT4	1982	1993	11	4	NC	-465	-374	*	2.9E+02	1.5	3.65	2.3	8.5	4.9	0.34	*	*	83	3.2
930349		1982	1993	11	5	NC	-414	-317	*	7.9E+02	0.72	2.71	3.3	18	6.8	*	*	*	67	3.8
890107	HOB	1987	1993	6	A	NC	-460	-383	6.1E+01	3.3E+02	15	4.31	2.7	20	2.5	0.14	*	*	50	4.0
890107		1987	1993	6	B	NC	-372	-184	8.2E+01	4.0E+00	300	3.79	3.7	10	4.3	0.39	684.4	100	0	4.6
890107		1987	1993	6	3	P8	*	*	*	*	*	*	*	74	10	*	*	*	*	*
890107		1987	1993	6	2	P3	*	*	*	*	*	*	*	46	15	*	*	*	*	*
874663	MI1	1985	1993	8	A	NC	-477	-186	2.7E+01	8.6E+02	770	3.59	4.4	42	0.0	0.02	513.35	100	17	3.0
874663		1985	1993	8	B	NC	-580	-125	2.8E+01	1.5E+03	350	3.38	3.7	27	6.0	0.03	*	*	22	3.9
874664	MI2	1985	1993	8	A	NC	-424	-107	1.5E+01	4.8E+01	370	4.01	4.3	286	18	0.02	684.6	100	17	3.2
874664		1985	1993	8	B	NC	-682	-209	1.8E+02	1.5E+03	160	2.82	4.0	27	8.4	0.11	*	*	50	4.4
150189	SSK	1986	1993	7	1	*	-323	-13	4.0E+01	2.1E+01	49000	2.18	33	217	53	0.03	292	100	47	5.2
150189		1986	1993	7	135	*	-544	-348	3.0E-01	*	*	2.38	22	*	*	0.01	1026.8	0	6.7	3.4
150189		1986	1993	7	136	2	-283	-63	*	*	37000	1.77	35	179	37	0.02	280.2	0	6.7	4.2
150189		1986	1993	7	5	NC	-484	-352	*	1.1E+01	9800	2.16	45	314	47	0.02	855.6	0	20	4.5
150189		1986	1993	7	86	1	-618	-120	1.6E+00	2.3E+00	2700	2.42	24	133	24	0.02	1680	0	0	4.9
150189		1986	1993	7	88	NC	-314	-59	0.0E+00	5.9E-01	32000	2.18	24	165	71	0.02	*	*	0	3.0
900117	NIL	1980	1988	8	7	*	*	*	*	*	*	*	*	*	*	6.08	*	*	*	*
900117		1980	1988	8	16	*	*	*	*	*	*	*	*	*	*	0.27	*	*	*	*
900117		1980	1988	8	16A	*	*	*	*	*	*	*	*	*	*	0.76	*	*	*	*
900117		1980	1988	8	19A	*	*	*	*	*	*	*	*	*	*	0.23	*	*	*	*
900117		1980	1988	8	22A	*	*	*	*	*	*	*	*	*	*	0.33	*	*	*	*
900094	LKY	1980	1988	8	98	*	*	*	*	*	*	*	*	*	*	2.17	*	*	*	*
900094		1980	1988	8	84	*	*	*	*	*	*	*	*	*	*	3.53	*	*	*	*

CONST = CONSTRUCTION
COL = COLUMN
CORR = CORROSION
MUT RESIST = MUTUAL RESISTANCE
RES = RESISTIVITY
D = EFFECTIVE DIFFUSION COEFFICIENT
CONT = CONTINUITY
* = NO DATA

TABLE 4.2 CHLORIDE CONCENTRATION DATA (pg. 1 of 4)

BRIDGE NO.	BRIDGE NAME	PIER NO.	YEAR BUILT	TEST YEAR	AGE @ TEST	PPM Cl	INCH AHT	CHLORIDE CONCENTRATION (pcy) AT THE INDICATED DISTANCES (in) FROM THE SURFACE 0.5	1.5	2.5	3.5	4.5	5.5	6.5	7.5	8.5	D	Cs	Co
130132	GRN	9	1985	1991	6	16501	34	4.97	0.18	0.14	0.11	*	*	*	*	*	0.019	17.0	0.10
130132	GRN	9	1985	1991	6	16501	40	7.12	0.21	0.10	0.09	*	*	*	*	*	0.017	20.0	0.10
130132	GRN	9	1985	1991	6	16501	92	0.66	0.13	0.08	0.07	*	*	*	*	*	0.043	1.20	0.08
130132	GRN	24	1985	1991	6	16501	40	9.14	1.29	0.46	0.44	0.25	0.17	0.17	*	*	0.047	17.0	0.17
900026	7MI	59	1982	1991	9	23000	30	19.6	14.08	13.76	*	*	*	*	*	*	1.25	20.0	2.50
900026	7MI	196	1982	1991	9	23000	42	17.0	12.24	9.69	7.13	6.41	5.86	*	*	*	***0.75*** [a]	***18*** [a]	***2.5*** [a]
900026	7MI	20	1982	1988	6	23000	60	14.7	*	***9.31*** [a]	***6.43*** [a]	***5.34*** [a]	*	*	*	*	0.98	16.5	2.50
900026	7MI	63	1982	1988	6	23000	0	16.0	14.0	13.11	8.76	*	*	*	*	*	1.87	18.0	2.50
900026	7MI	63	1982	1988	6	23000	24	17.0	15.29	13.0	7.89	*	*	*	*	*	1.52	19.0	2.50
900026	7MI	63	1982	1988	6	23000	48	11.9	9.34	6.31	4.12	*	*	*	*	*	0.54	14.0	2.50
900026	7MI	63	1982	1988	6	23000	72	5.30	4.70	3.18	2.29	*	*	*	*	*	0.32	6.30	2.50
900026	7MI	63	1982	1988	6	23000	96	2.85	4.09	2.66	2.18	*	*	*	*	*	**	**	**
900026	7MI	63	1982	1988	6	23000	120	2.43	3.45	2.48	2.18	*	*	*	*	*	**	**	**
130104	75N	27	1980	1991	11	12141	31	11.7	2.65	0.18	0.14	0.19	*	*	*	*	0.045	18.0	0.16
130104	75N	18	1980	1991	11	12141	29	6.44	0.99	0.10	0.24	*	*	*	*	*	0.028	11.5	0.17
130103	75S	27	1980	1991	11	12141	30	6.29	0.24	0.22	0.13	0.09	0.13	0.12	*	*	0.011	16.0	0.11
130103	75S	18	1980	1991	11	12141	40	11.4	0.69	0.20	0.13	0.18	*	*	*	*	0.016	25.0	0.15
790132	HAL	13	1986	1991	5	10493	21	8.93	5.51	0.97	0.26	0.26	0.19	*	*	*	0.31	11.0	0.20
700181	IR1	5	1985	1991	6	22720	24	11.6	5.64	2.76	0.63	0.28	0.26	0.04	0.21	0.20	0.27	14.0	0.16
700174	IR2	19	1985	1991	6	22720	31	10.3	10.27	7.28	4.78	2.10	*	*	*	*	1.18	13.0	0.20
860319	NWR	7	1981	1991	10	8562	38	0.84	0.34	0.21	0.12	0.12	*	*	*	*	0.069	1.20	0.12
860466	ITA	B	1989	1992	3	11876	21	2.17	0.65	0.19	0.16	0.11	0.11	*	*	*	0.17	3.50	0.10
860466	ITA	B	1989	1992	3	11876	81	0.58	0.11	0.12	0.10	0.03	0.10	*	*	*	0.082	1.00	0.10
860467	ITB	B	1989	1992	3	11876	18	2.97	0.03	0.05	0.02	0.03	*	*	*	*	0.023	10.0	0.03
860467	ITB	B	1989	1992	3	11876	70	0.97	0.01	0.03	0.01	0.02	*	*	*	*	0.027	3.00	0.01
900126	VA1	2	1982	1991	9	21442	24	11.9	13.0	11.0	7.014	4.90	*	*	*	*	1.42	15.0	0.40
900126	VA1	4	1982	1991	9	21442	75	2.81	3.04	2.46	2.25	2.23	2.35	2.057	*	*	1.00	3.00	2.00
900124	VA2	2	1982	1991	9	21442	16	26.9	17.34	13.64	9.06	8.25	4.87	*	*	*	0.76	28.0	0.40
900124	VA2	2	1982	1991	9	21442	27	18.2	15.81	10.76	7.85	5.25	5.07	*	*	*	0.98	20.0	0.40

PPM Cl = CHLORIDE CONCENTRATION (ppm) OF THE WATER AT THE SITE

INCH AHT = THE ELEVATION (in) ABOVE THE HIGH TIDE THAT THE CORE WAS EXTRACTED

D = EFFECTIVE DIFFUSION COEFFICIENT (sq in/yr)

Cs = CALCULATED SURFACE CHLORIDE CONCENTRATION (pcy)

Co = BULK CHLORIDE CONCENTRATION (pcy)

* = NO DATA

** = NOT COMPUTED

a) Modified 03/01/02 to correct erratum in original printed version

TABLE 4.2 CHLORIDE CONCENTRATION DATA (pg. 2 of 4)

BRIDGE NO.	BRIDGE NAME	PIER NO.	YEAR BUILT	TEST YEAR	AGE @ TEST	PPM Cl	INCH AHT	CHLORIDE CONCENTRATION (pcy) AT THE INDICATED DISTANCES (in) FROM THE SURFACE									D	Cs	Co
								0.5	1.5	2.5	3.5	4.5	5.5	6.5	7.5	8.5			
100358	AL1	8	1981	1991	10	7232	61	1.12	0.29	0.31	0.25	*	*	*	*	*	0.008	3.00	0.27
100358	AL1	8	1981	1991	10	7232	76	1.34	0.98	0.42	0.26	0.29	0.26	0.32	*	*	0.15	1.70	0.29
100359	AL2	6	1981	1991	10	7232	7	9.51	4.47	1.79	0.70	0.36	*	*	*	*	0.12	12.5	0.30
100359	AL2	6	1981	1991	10	7232	47	1.05	0.70	0.24	0.32	*	*	*	*	*	0.10	1.40	0.27
900077	SNK	5	1981	1992	11	3440	60	3.99	4.66	3.23	2.20	2.05	1.89	1.95	*	*	0.41	5.00	1.80
900077	SNK	8	1981	1992	11	3440	43	4.99	5.75	3.74	2.53	2.18	1.88	1.98	*	*	0.39	6.50	1.80
120088	MAT	13	1980	1992	12	17000	4	37.2	3.03	0.14	0.16	*	*	*	*	*	0.018	76.0	0.16
120088	MAT	13	1980	1992	12	17000	28	17.6	1.25	0.23	0.12	0.11	0.13	*	*	*	0.019	35.0	0.11
120088	MAT	13	1980	1992	12	17000	103	0.64	0.20	0.05	0.01	*	*	*	*	*	0.061	0.90	0.01
010092	PC1	24	1983	1992	9	13840	5	29.7	7.04	0.64	0.26	0.23	0.18	0.26	0.20	*	0.059	45.0	0.20
010092	PC1	24	1983	1992	9	13840	47	13.6	2.32	0.21	0.17	0.20	0.21	0.13	0.15	*	0.041	23.0	0.13
010092	PC1	32	1983	1992	9	13840	104	1.14	0.28	0.19	0.05	*	*	*	*	*	0.037	2.00	0.10
010058	PC2	54	1980	1992	12	17750	-1	17.6	2.83	0.25	0.12	0.12	0.12	0.092	0.081	*	0.031	30.0	0.08
010058	PC2	54	1980	1992	12	17750	48	10.8	0.54	0.15	0.15	0.24	0.16	0.155	0.183	*	0.013	25.0	0.16
010058	PC2	37	1980	1992	12	17750	19	14.6	1.29	0.16	0.14	*	*	*	*	*	0.018	30.0	0.15
010058	PC2	37	1980	1992	12	17750	90	0.98	0.23	0.18	0.20	0.55	*	*	*	*	0.010	2.00	0.30
010057	PC3	54	1980	1992	12	17750	-1	17.9	1.32	0.21	0.23	0.21	0.22	0.137	*	*	0.017	37.0	0.14
010057	PC3	54	1980	1992	12	17750	20	10.2	0.74	0.21	0.16	0.24	0.14	0.137	*	*	0.019	20.0	0.13
570082	CHO	33	1979	1992	13	7374	43	8.78	7.37	6.66	5.36	*	*	*	*	*	1.38	9.40	0.30
570082	CHO	33	1979	1992	13	7374	107	4.23	1.30	0.21	0.29	0.30	*	*	*	*	0.043	6.40	0.20
480140	PER	27	1981	1992	11	6106	4	19.6	0.93	0.21	0.20	0.27	0.14	0.232	*	*	0.015	45.0	0.20
480140	PER	27	1981	1992	11	6106	47	3.24	0.32	0.33	0.19	0.27	0.21	0.433	*	*	0.010	8.20	0.30
480140	PER	37	1981	1992	11	6106	21	7.39	0.46	0.44	0.36	*	*	*	*	*	0.009	20.0	0.36
490031	APA	16	1988	1992	4	13490	41	0.53	0.43	0.39	0.36	0.41	0.45	0.342	*	*	4.53	0.50	0.30
490031	APA	16	1988	1992	4	13490	114	0.50	0.45	0.49	0.37	0.39	0.39	*	*	*	0.96	0.50	0.39
490031	APA	31	1988	1992	4	13490	8	2.48	0.54	0.37	0.36	0.35	0.39	*	*	*	0.062	4.50	0.34
490031	APA	31	1988	1992	4	13490	77	0.40	0.37	0.36	0.35	0.38	0.37	0.387	*	*	20.7	0.50	0.15

PPM Cl = CHLORIDE CONCENTRATION (ppm) OF THE WATER AT THE SITE

INCH AHT = THE ELEVATION (in) ABOVE THE HIGH TIDE THAT THE CORE WAS EXTRACTED

D = EFFECTIVE DIFFUSION COEFFICIENT (sq in/yr)

Cs = CALCULATED SURFACE CHLORIDE CONCENTRATION (pcy)

Co = BULK CHLORIDE CONCENTRATION (pcy)

* = NO DATA

** = NOT COMPUTED

TABLE 4.2 CHLORIDE CONCENTRATION DATA (pg. 3 of 4)

BRIDGE NO.	BRIDGE NAME	PIER NO.	YEAR BUILT	TEST YEAR	AGE @ TEST	PPM Cl	INCH AHT	CHLORIDE CONCENTRATION (pcy) AT THE INDICATED DISTANCES (in) FROM THE SURFACE									D	Cs	Co
								0.5	1.5	2.5	3.5	4.5	5.5	6.5	7.5	8.5			
870607	IT2	12	1983	1992	9	12000	31	2.31	0.79	0.37	0.19	0.24	0.22	0.21	*	*	0.064	3.50	0.20
870607	IT2	13	1983	1992	9	12000	40	2.18	2.31	1.42	0.76	0.78	*	*	*	*	0.64	2.70	0.30
870607	IT2	13	1983	1992	9	12000	118	0.95	0.25	0.27	0.26	0.17	0.09	*	*	*	0.049	1.40	0.15
870606	IT3	12	1983	1992	9	12000	66	0.94	0.26	0.28	*	*	*	*	*	*	0.009	2.40	0.26
870606	IT3	13	1983	1992	9	12000	9	8.67	6.19	4.24	2.02	1.42	1.03	0.68	*	*	0.45	10.0	0.30
870606	IT3	13	1983	1992	9	12000	85	0.88	0.26	0.12	*	*	*	*	*	*	0.045	1.40	0.11
170158	NWP	4	1986	1992	6	20915	8	33.6	11.7	1.58	2.36	0.98	1.31	*	*	*	0.12	49.0	0.30
170158	NWP	4	1986	1992	6	20915	95	0.26	1.33	0.14	0.21	0.19	0.34	*	*	*	0.30	0.70	0.30
170158	NWP	8	1986	1992	6	20915	22	17.6	0.40	0.15	0.15	0.18	0.27	*	*	*	0.014	54.0	0.27
170158	NWP	8	1986	1992	6	20915	81	2.43	0.26	*	*	*	*	*	*	*	0.002	20.0	0.26
890107	HOB	A	1987	1993	6	25915	35	1.14	0.73	0.44	0.38	*	*	*	*	*	0.20	1.40	0.35
890107	HOB	A	1987	1993	6	25915	92	0.76	0.51	0.36	0.37	0.44	0.44	0.43	*	*	0.077	1.00	0.41
890107	HOB	B	1987	1993	6	25915	20	4.37	5.60	2.73	1.43	0.56	0.41	0.44	*	*	0.75	6.00	0.40
890107	HOB	B	1987	1993	6	25915	68	0.91	0.44	0.40	0.41	*	*	*	*	*	0.039	1.40	0.40
930349	IT4	5	1982	1993	11	7100	49	0.52	0.26	0.21	0.34	0.28	0.13	0.10	0.148	*	0.65	0.50	0.15
930349	IT4	5	1982	1993	11	7100	82	0.56	1.13	0.16	0.12	0.14	0.16	0.10	*	*	0.34	0.90	0.10
930349	IT4	4	1982	1993	11	7100	3	10.1	7.66	4.87	2.26	1.25	0.63	0.22	*	*	0.35	12.0	0.22
930349	IT4	4	1982	1993	11	7100	54	0.72	0.88	0.29	*	*	*	*	*	*	0.90	0.70	0.30
874663	MI1	A	1985	1993	8	12000	87	0.51	0.15	0.17	0.15	0.16	0.15	0.14	*	*	0.018	1.00	0.15
874663	MI1	B	1985	1993	8	12000	35	0.80	0.24	0.15	0.16	0.16	0.17	0.15	*	*	0.028	1.50	0.15
874663	MI1	B	1985	1993	8	12000	67	0.41	0.16	0.15	0.16	*	*	*	*	*	0.012	0.90	0.15
874664	MI2	A	1985	1993	8	12000	25	1.66	0.22	0.17	0.16	0.16	0.15	0.16	*	*	0.022	3.50	0.15
874664	MI2	A	1985	1993	8	12000	82	0.89	0.20	0.17	*	*	*	*	*	*	0.022	1.80	0.15
874664	MI2	B	1985	1993	8	12000	44	2.24	1.07	0.35	0.21	*	*	*	*	*	0.12	3.20	0.15
874664	MI2	B	1985	1993	8	12000	91	2.47	1.06	0.25	0.21	0.15	0.15	*	*	*	0.10	3.50	0.15

PPM Cl = CHLORIDE CONCENTRATION (ppm) OF THE WATER AT THE SITE
INCH AHT = THE ELEVATION (in) ABOVE THE HIGH TIDE THAT THE CORE WAS EXTRACTED
D = EFFECTIVE DIFFUSION COEFFICIENT (sq in/yr)
Cs = CALCULATED SURFACE CHLORIDE CONCENTRATION (pcy)
Co = BULK CHLORIDE CONCENTRATION (pcy)

* = NO DATA
** = NOT COMPUTED

TABLE 4.2 CHLORIDE CONCENTRATION DATA (pg. 4 of 4)

BRIDGE NO.	BRIDGE NAME	PIER NO.	YEAR BUILT	TEST YEAR	AGE @ TEST	PPM Cl	INCH AHT	CHLORIDE CONCENTRATION (pcy) AT THE INDICATED DISTANCES (in) FROM THE SURFACE 0.5	1.5	2.5	3.5	4.5	5.5	6.5	7.5	8.5	D	Cs	Co
150189	SSK	1	1986	1993	7	20000	50	8.65	0.52	0.27	0.24	0.24	0.19	*	*	*	0.022	20.0	0.20
150189	SSK	1	1986	1993	7	20000	100	2.13	0.45	0.22	0.22	0.19	*	*	*	*	0.041	3.80	0.20
150189	SSK	1	1986	1993	7	20000	128	8.16	0.60	0.90	0.19	0.17	0.20	*	*	*	0.026	17.5	0.20
150189	SSK	5	1986	1993	7	20000	21	18.1	0.65	0.27	0.26	0.28	*	*	*	*	0.019	45.0	0.25
150189	SSK	5	1986	1993	7	20000	36	14.5	0.51	0.26	0.25	0.23	*	*	*	*	0.015	40.0	0.23
150189	SSK	86	1986	1993	7	20000	40	14.1	0.61	0.32	0.31	0.28	0.30	*	*	*	0.018	36.0	0.30
150189	SSK	86	1986	1993	7	20000	58	15.3	0.60	0.31	0.33	0.34	0.41	*	*	*	0.016	41.0	0.35
150189	SSK	88	1986	1993	7	20000	0	18.0	0.99	0.34	0.37	*	*	*	*	*	0.022	41.8	0.35
150189	SSK	135	1986	1993	7	20000	24	16.2	0.49	0.17	*	*	*	*	*	*	0.019	40.0	0.20
150189	SSK	135	1986	1993	7	20000	48	19.6	0.39	0.28	*	*	*	*	*	*	0.012	60.0	0.25
150189	SSK	135	1986	1993	7	20000	72	14.0	0.29	0.27	0.27	*	*	*	*	*	0.009	50.0	0.25
150189	SSK	135	1986	1993	7	20000	96	5.96	0.18	0.19	0.19	*	*	*	*	*	0.004	30.0	0.25
150189	SSK	136	1986	1993	7	20000	12	34.1	0.64	0.47	*	*	*	*	*	*	0.015	95.0	0.25
150189	SSK	136	1986	1993	7	20000	36	18.5	0.28	0.22	0.20	0.22	*	*	*	*	0.011	60.0	0.25
150189	SSK	136	1986	1993	7	20000	60	16.3	1.29	0.41	0.23	*	*	*	*	*	0.027	35.0	0.25
150189	SSK	136	1986	1993	7	20000	84	13.2	0.27	0.21	0.20	*	*	*	*	*	0.012	40.0	0.25
150189	SSK	136	1986	1993	7	20000	108	12.4	0.43	0.17	0.19	*	*	*	*	*	0.017	32.0	0.18
900017	NIL	7	1983	1988	5	24000	54	9.72	10.3	7.12	*	*	*	*	*	*	6.08	10.0	0.30
900017	NIL	16	1983	1988	5	24000	0	22.8	10.9	9.43	7.78	*	*	*	*	*	0.46	25.0	0.30
900017	NIL	16	1983	1988	5	24000	24	11.5	6.75	4.46	1.81	*	*	*	*	*	0.33	13.5	0.30
900017	NIL	16	1983	1988	5	24000	48	7.60	4.39	3.13	*	*	*	*	*	*	0.34	9.00	0.30
900017	NIL	16	1983	1988	5	24000	72	5.15	2.73	0.94	*	*	*	*	*	*	0.14	7.15	0.30
900017	NIL	16	1983	1988	5	24000	96	3.02	1.06	0.14	0.09	*	*	*	*	*	0.089	4.50	0.01
900017	NIL	16A	1983	1988	5	24000	29	20.4	17.5	11.1	7.71	6.67	*	*	*	*	0.76	25.0	0.30
900017	NIL	19A	1983	1988	5	24000	47	23.1	13.6	6.28	2.69	0.65	*	*	*	*	0.23	30.0	0.30
900017	NIL	22A	1983	1988	5	24000	74	6.13	5.18	2.32	1.08	0.24	0.29	*	*	*	0.33	8.00	0.30
								CHLORIDE CONCENTRATION (pcy) AT THE INDICATED DISTANCES (in) FROM THE SURFACE											
								1.00	3	5	7	9	*	*	*	*			
900094	LKY	84	1982	1988	6	24000	17	25.7	22.6	11.8	11.7	*	*	*	*	*	3.53	29.0	0.30
900094	LKY	98	1982	1988	6	24000	20	28.6	16.5	14.7	*	*	*	*	*	*	2.17	31.6	0.30

PPM Cl = CHLORIDE CONCENTRATION (ppm) OF THE WATER AT THE SITE

INCH AHT = THE ELEVATION (in) ABOVE THE HIGH TIDE THAT THE CORE WAS EXTRACTED

D = EFFECTIVE DIFFUSION COEFFICIENT (sq in/yr)

Cs = CALCULATED SURFACE CHLORIDE CONCENTRATION (pcy)

Co = BULK CHLORIDE CONCENTRATION (pcy)

* = NO DATA

** = NOT COMPUTED

Table 5.1

Open Circuit Potentials

Liquid Disbondment Tests

Solutions	PM1A	PM1B	PM2
SPS	-200	-170	-150
Low Chloride	---	-140	-220
High Chloride	---	-450	-550

Shown are the average potentials (SCE) of each group at the end of the 30 day period.

Table 5.2

Coating Pulloff Tests of Specimens Exposed in Chloride-Free, Water-Saturated Concrete

ECR Supplier	Exposure Time (Days)	Test Condition	Open Circuit		-500 mV	
			Pulloff	Knife Test Adhesion	Pulloff	Knife Test Adhesion
1	600	Immediately After Removal	430 psi, 100%	Poor	1030 psi, 4%	Very Poor
1	600	After 2-1/2 Weeks in Dessicator	1380 psi, 0% 3530 psi, 0%	Good	3440 psi, 0% 3530 psi, 0%	Good
2	570	Immediately After Removal	0 psi, 100% 1980 psi, 0% 950 psi, 0%	Very Poor	250 psi, 100%	Very Poor

Table 5.3

Pitting-Crevice Potentials (mV SCE)

Molar [Cl-]	$Ca(OH)_2$	$Ca(OH)_2$ Creviced	SPS	SPS CREVICED
0	610	700	530	550
0	700	---	600	---
0.1	50	-200	600	-150
0.1	105	---	620	550
0.1	694	---	---	380
0.1	705	---	---	---
0.3	-300	-330	595	-200
0.3	0	---	595	-80
0.5	-200	-400	---	20
1	-330	-450	575	30
1	-40	---	600	336

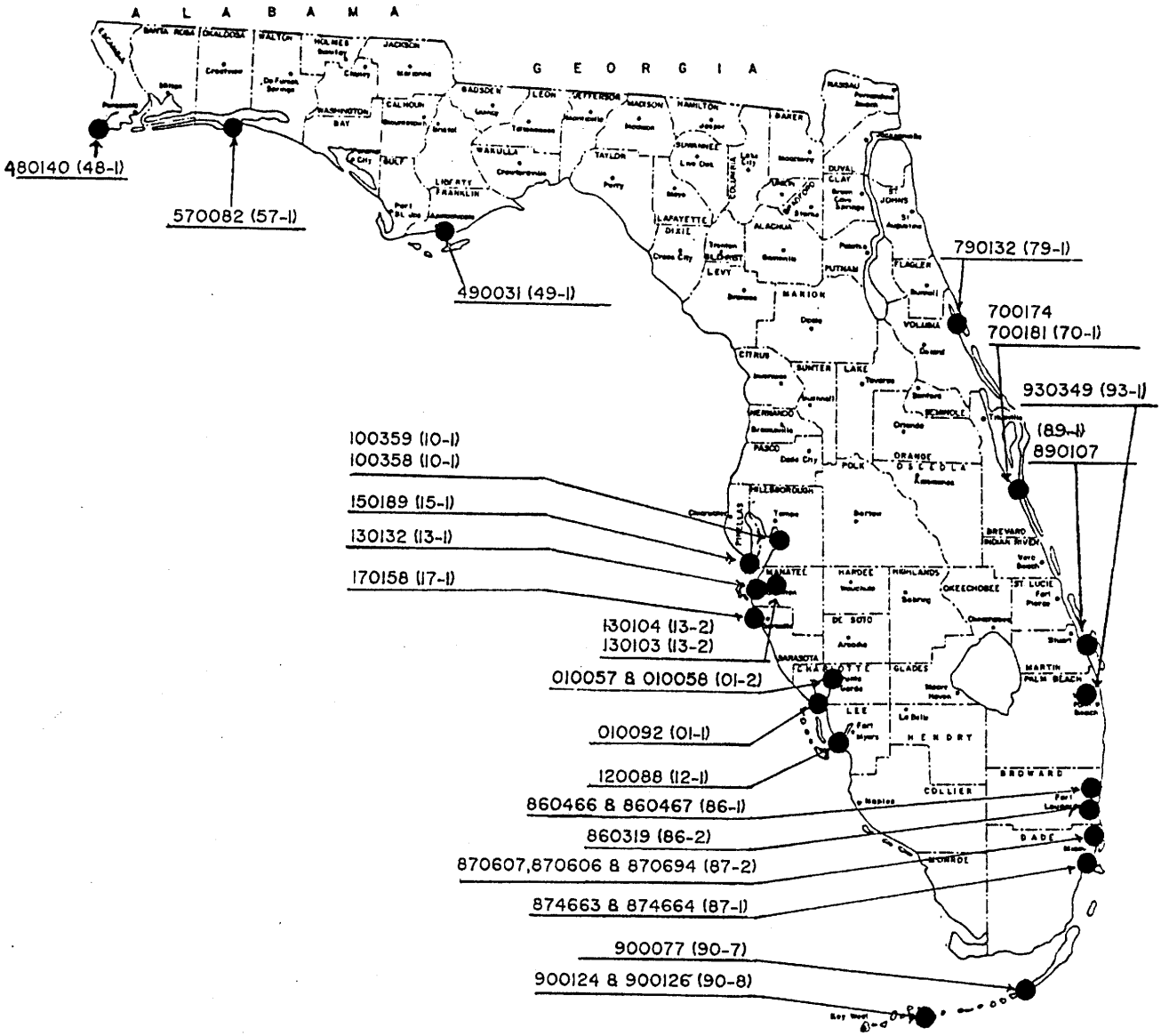

Figure 2.1. Test Site Locations.

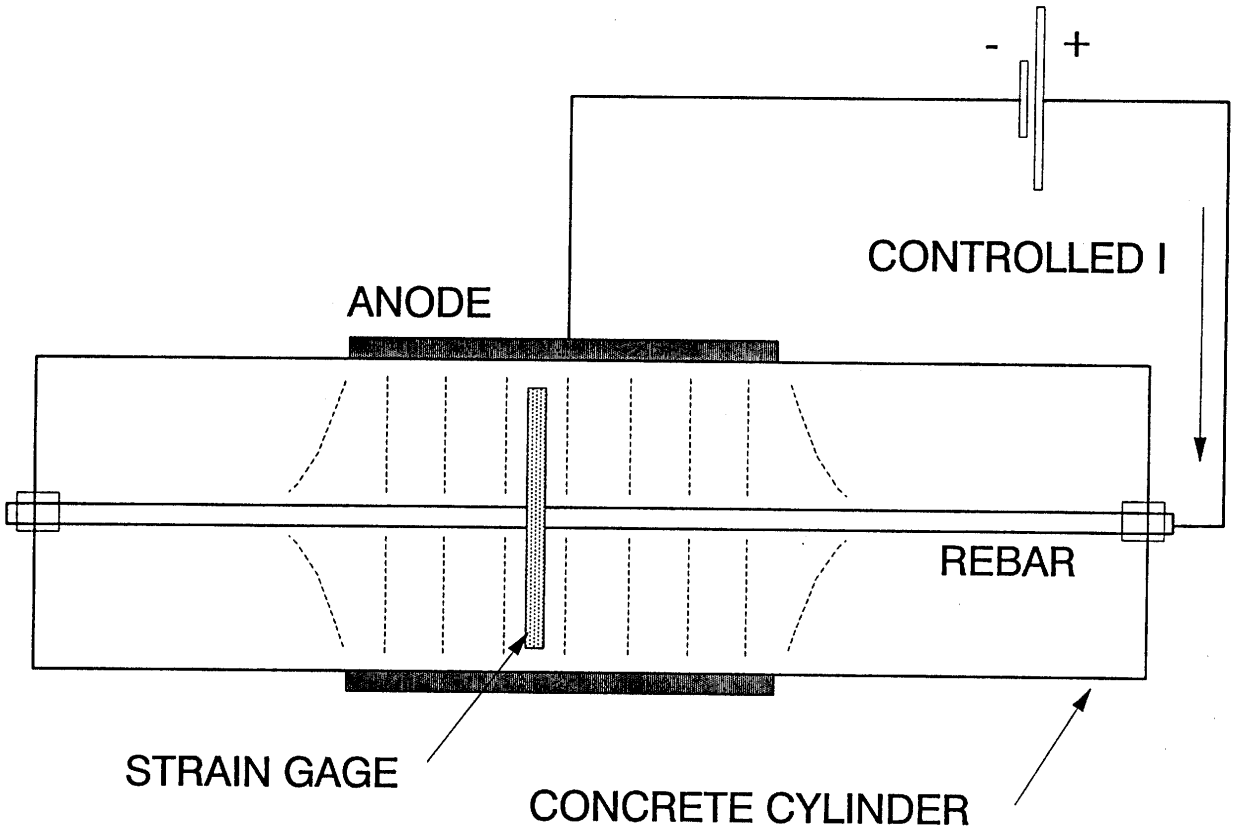

Figure 2.2. Schematic of Current Delivery Arrangement.

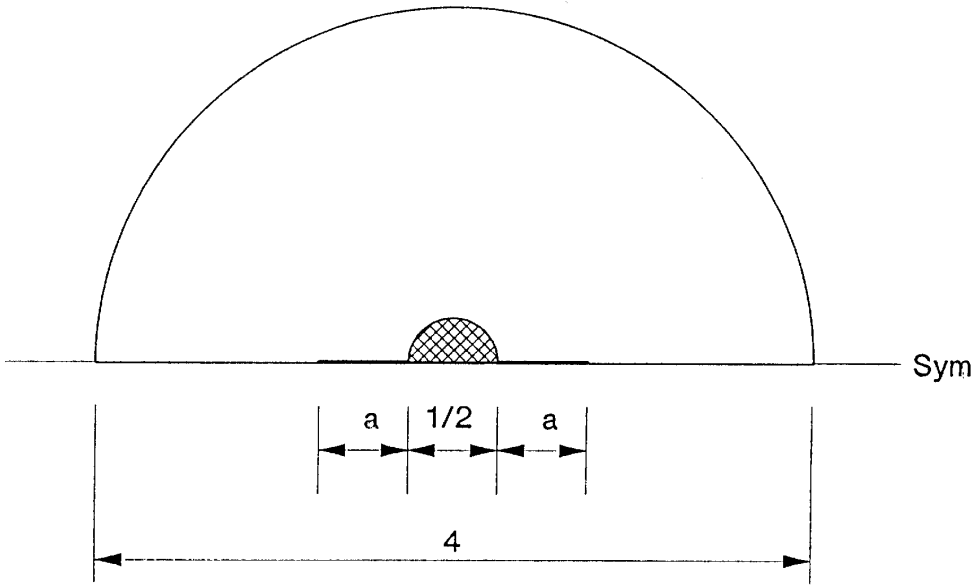

Note: Dimensions in inches

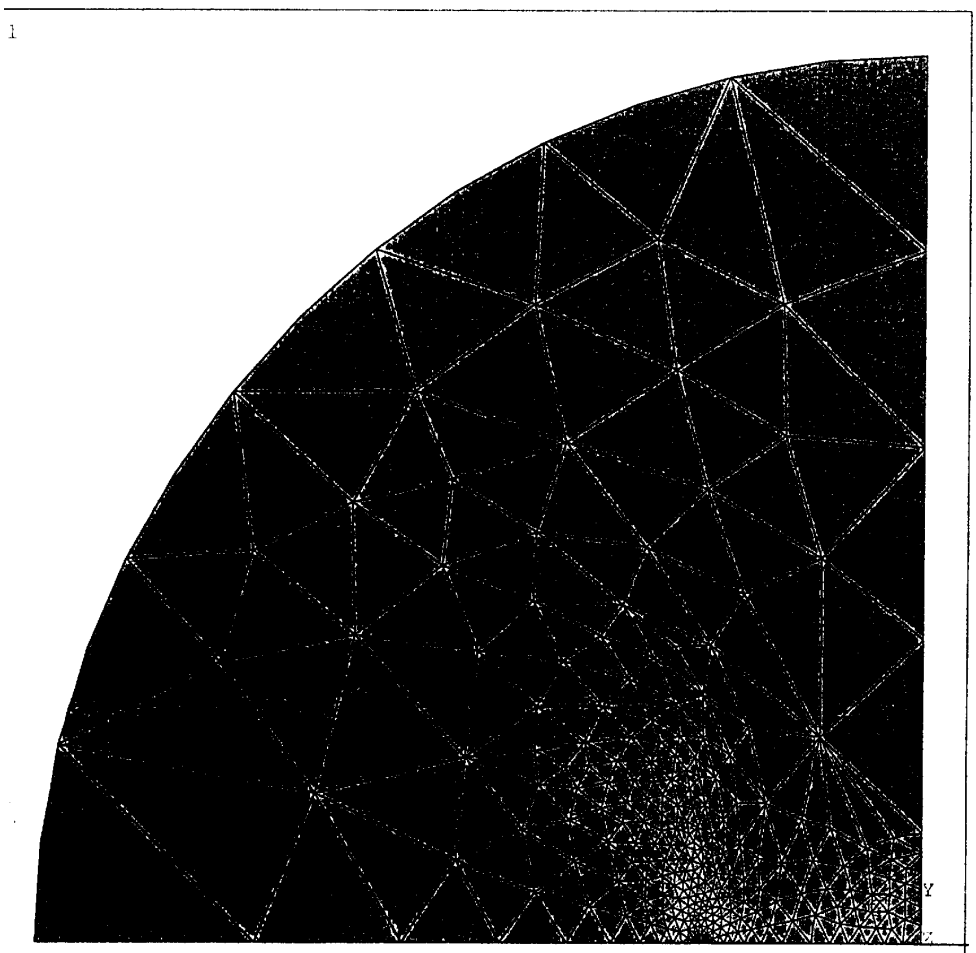

Finite element idealization, a = 0.5 inches

Figure 2.3. Top: Model System (Half Shown). Bottom: Finite Element Grid.

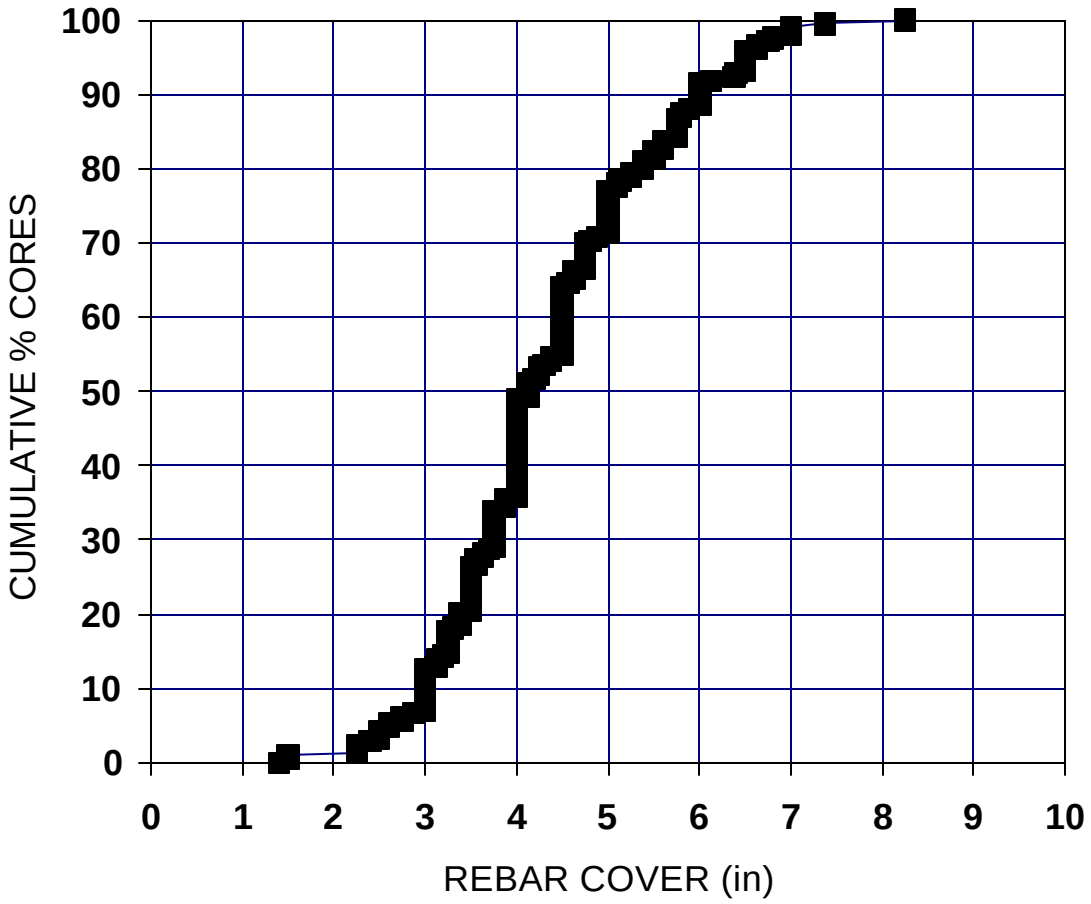

Figure 4.1. Distribution of Rebar Cover Thicknesses.

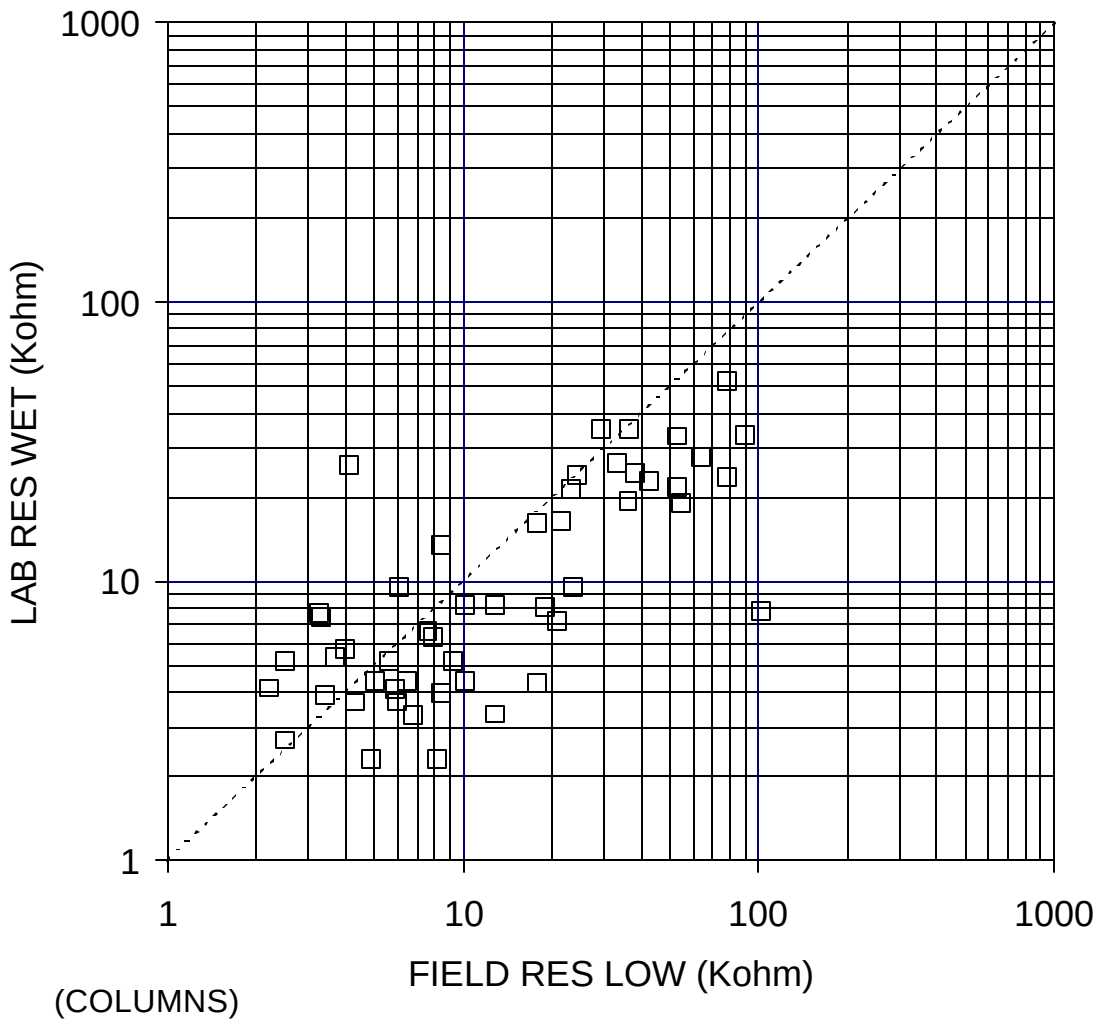

Figure 4.2. Resistivity (wet condition) of Field-extracted Cores vs. Minimum Resistivity Measured at the Field Test Site, Averaged by Column.

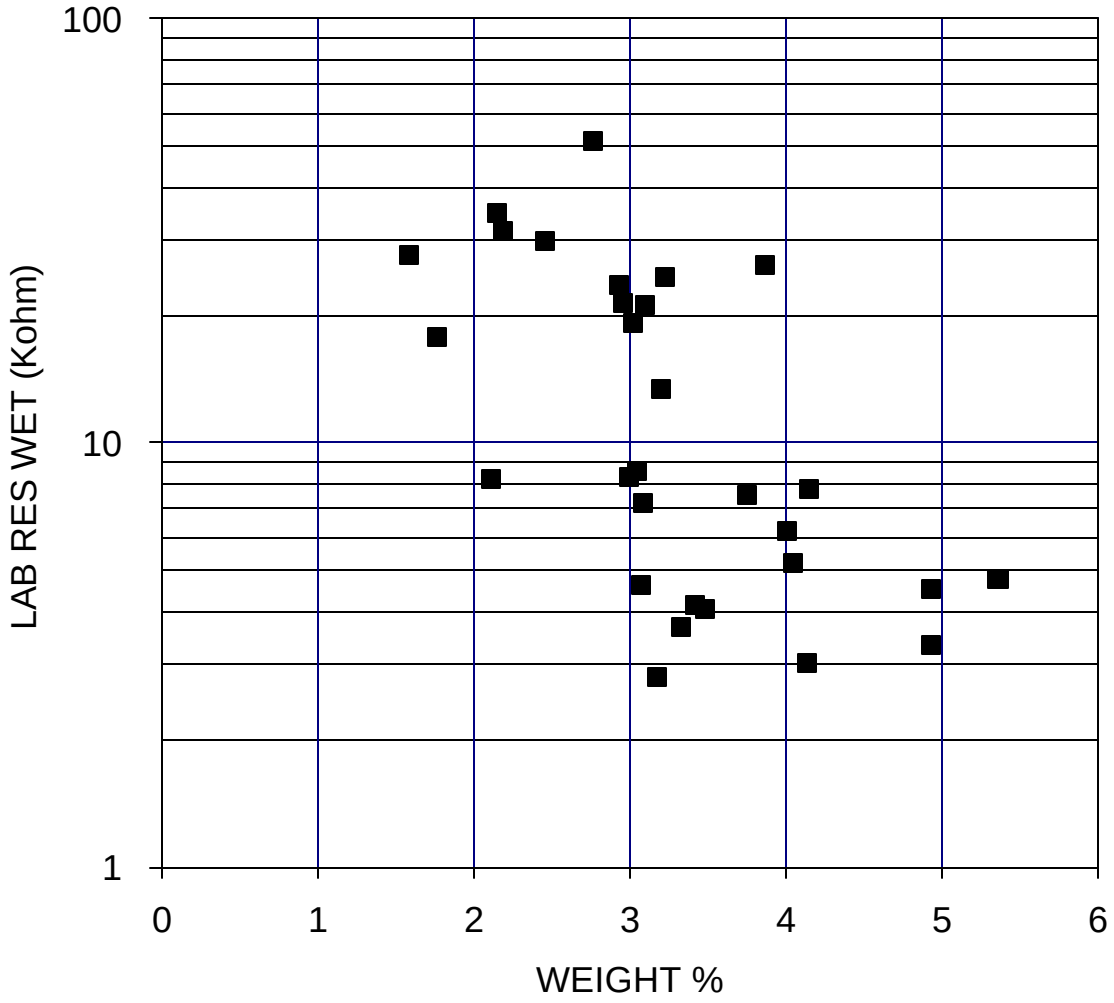

Figure 4.3. Resistivity (wet condition) of Field-extracted Cores vs. Weight Increase (in % of Laboratory-dry Weight) Upon Wetting.

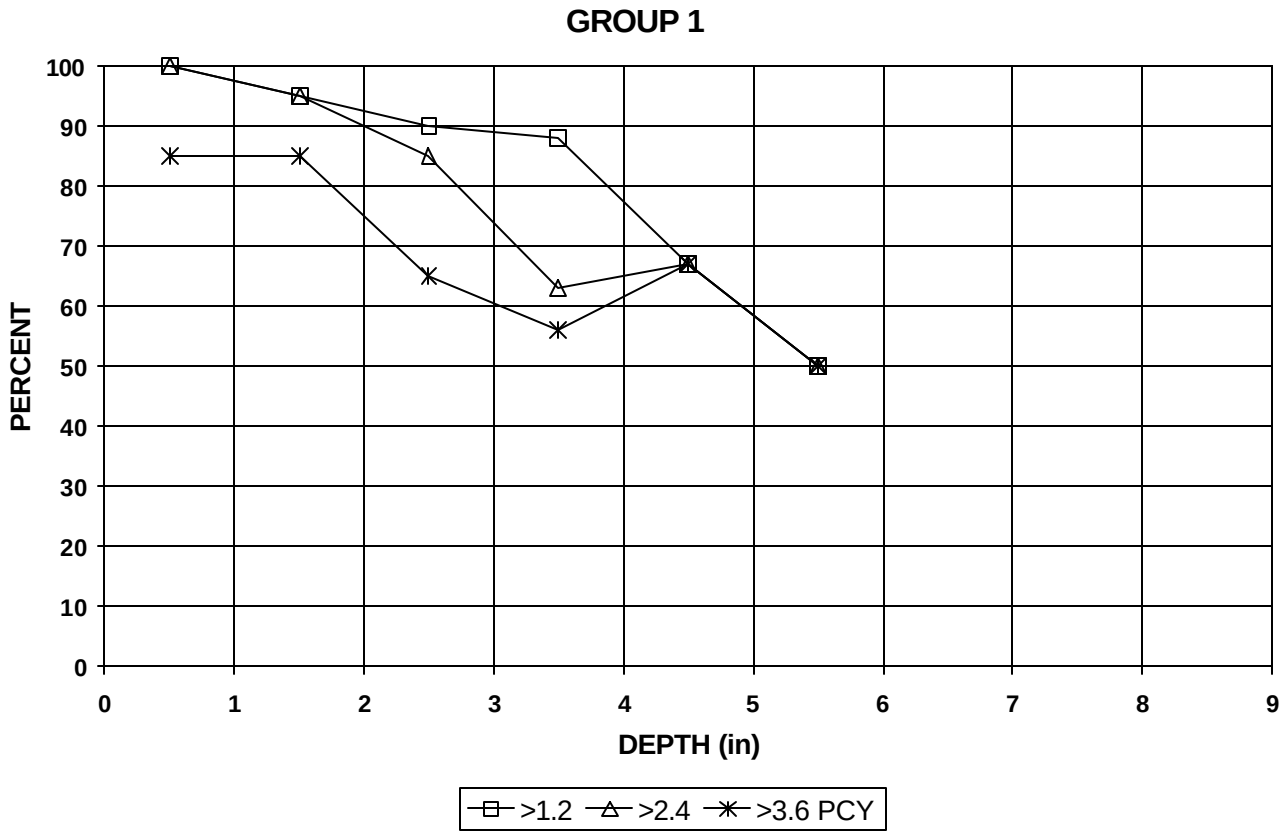

Figure 4.4 Chloride Penetration. Bridges for which Corrosion was Known Previously to Exist. Percentage of Cores for which the Chloride Content at the indicated Depths Exceeded 1.2, 2.4 and 3.6 pcy.

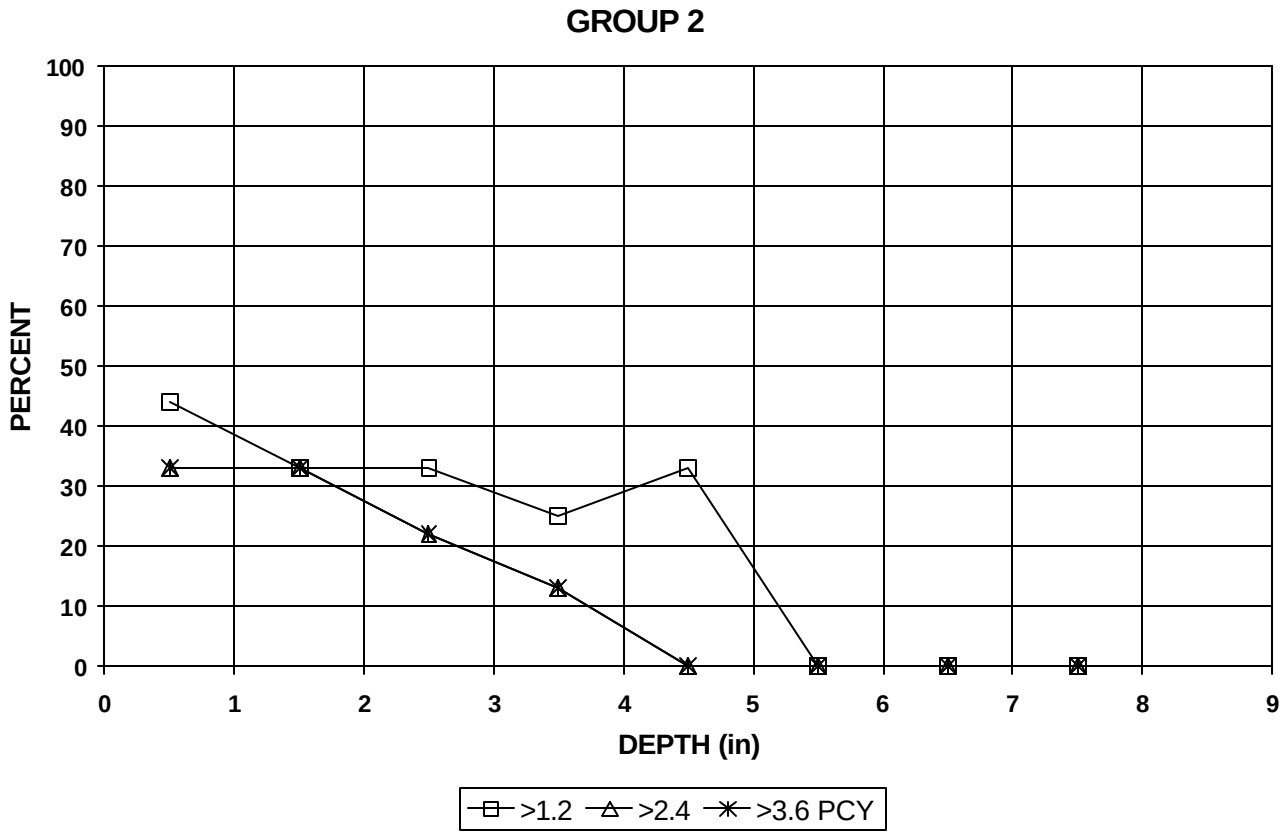

Figure 4.5 Chloride Penetration. Plain Rebar Substructures. Percentage of Cores for which the Chloride Content at the indicated Depths Exceeded 1.2, 2.4 and 3.6 pcy.

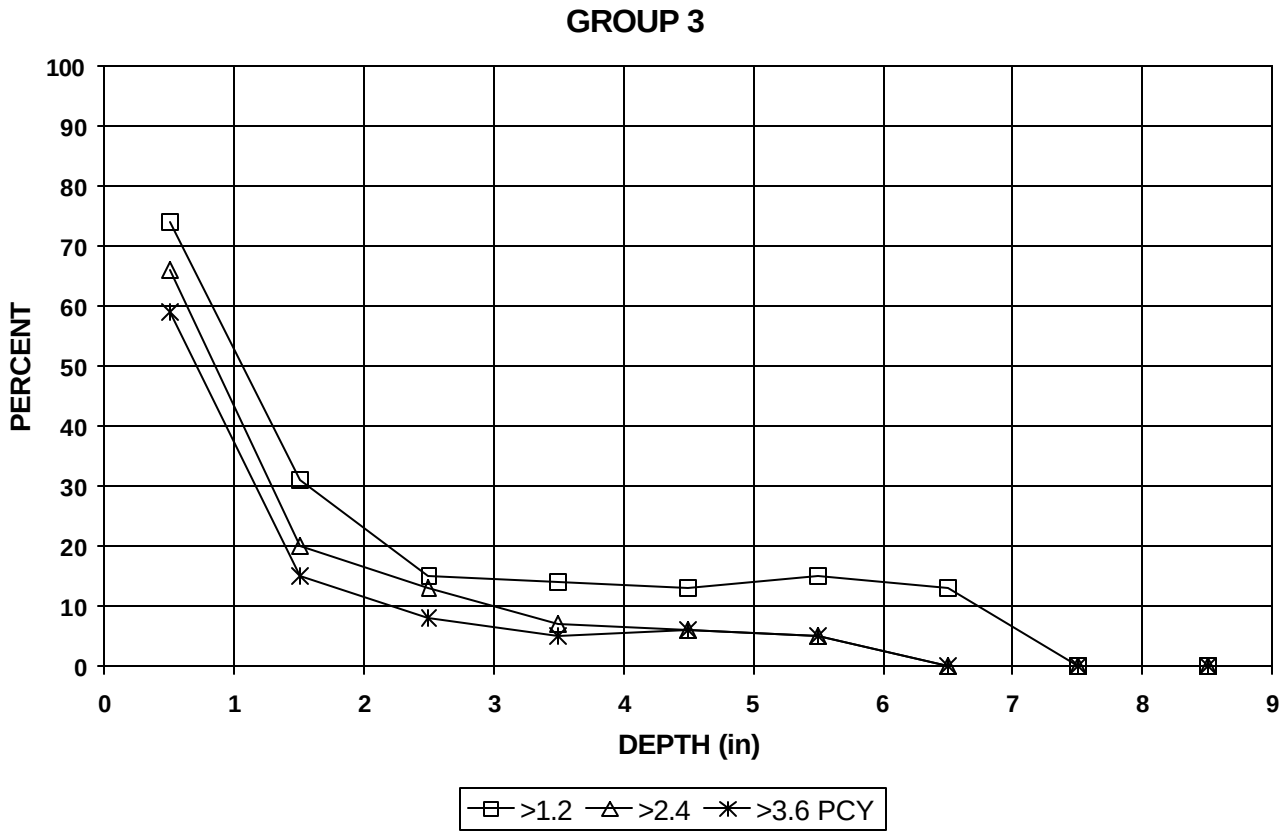

Figure 4.6 Chloride Penetration. Data for Bridges not Addressed in Figures 4.4 or 4.5. Percentage of Cores for which the Chloride Content at the indicated Depths Exceeded 1.2, 2.4 and 3.6 pcy.

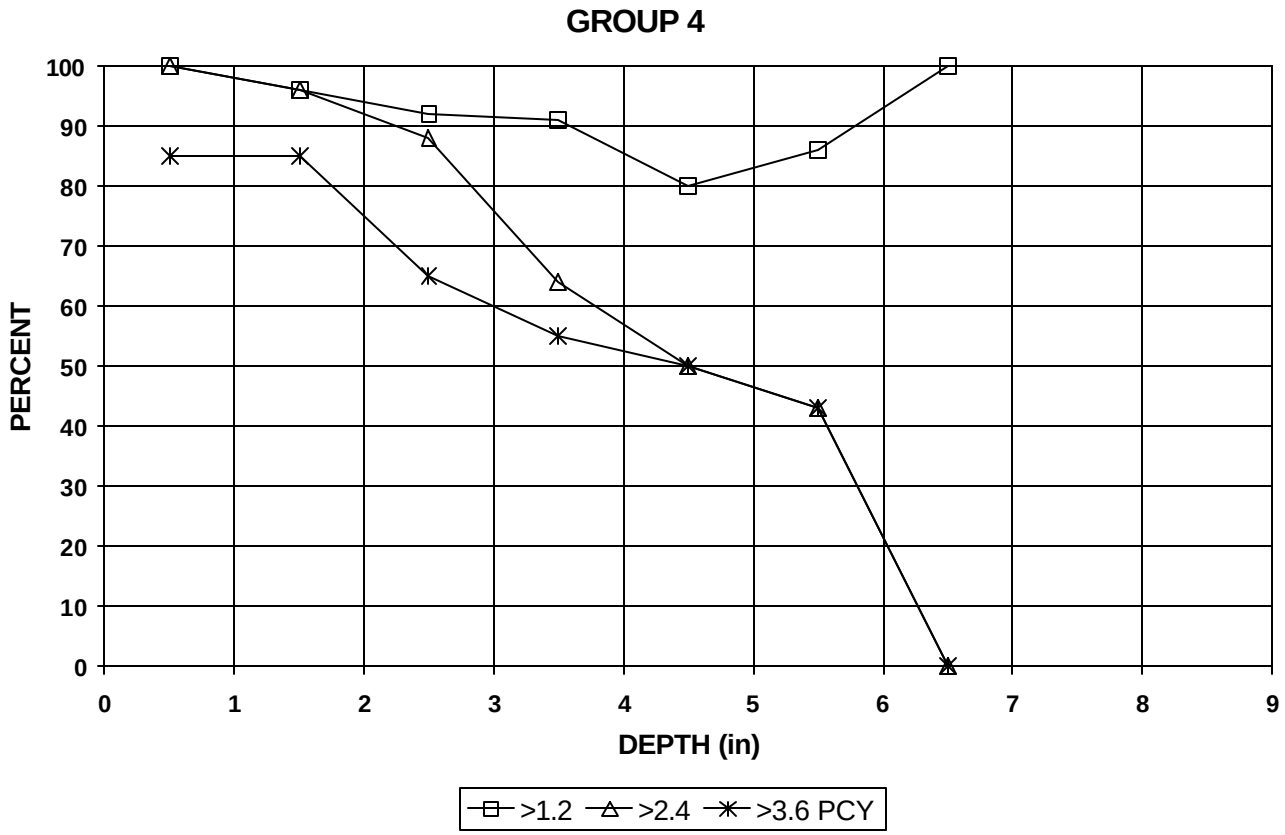

Figure 4.7 Chloride Penetration. Monroe County Bridges. Percentage of Cores for which the Chloride Content at the indicated Depths Exceeded 1.2, 2.4 and 3.6 pcy.

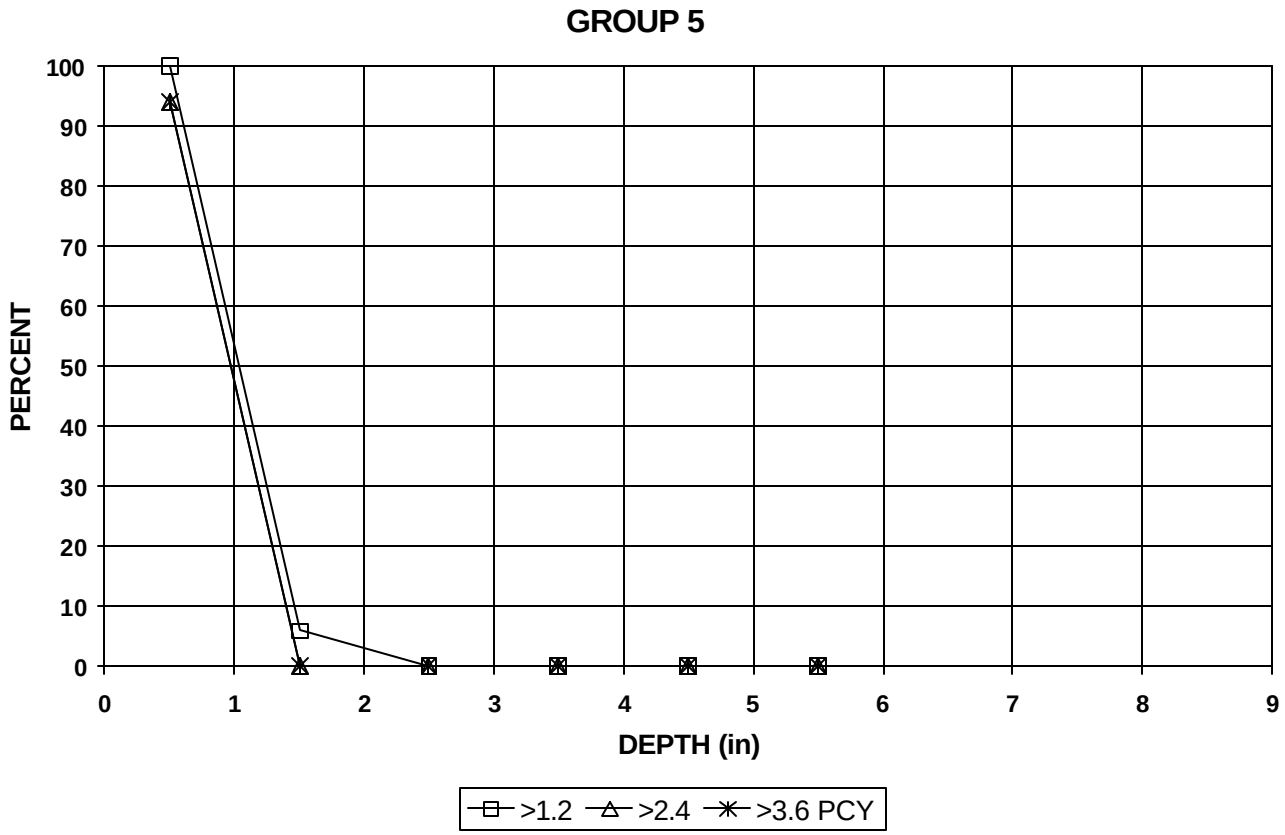

Figure 4.8 Chloride Penetration. Sunshine Skyway Bridge. Percentage of Cores for which the Chloride Content at the indicated Depths Exceeded 1.2, 2.4 and 3.6 pcy.

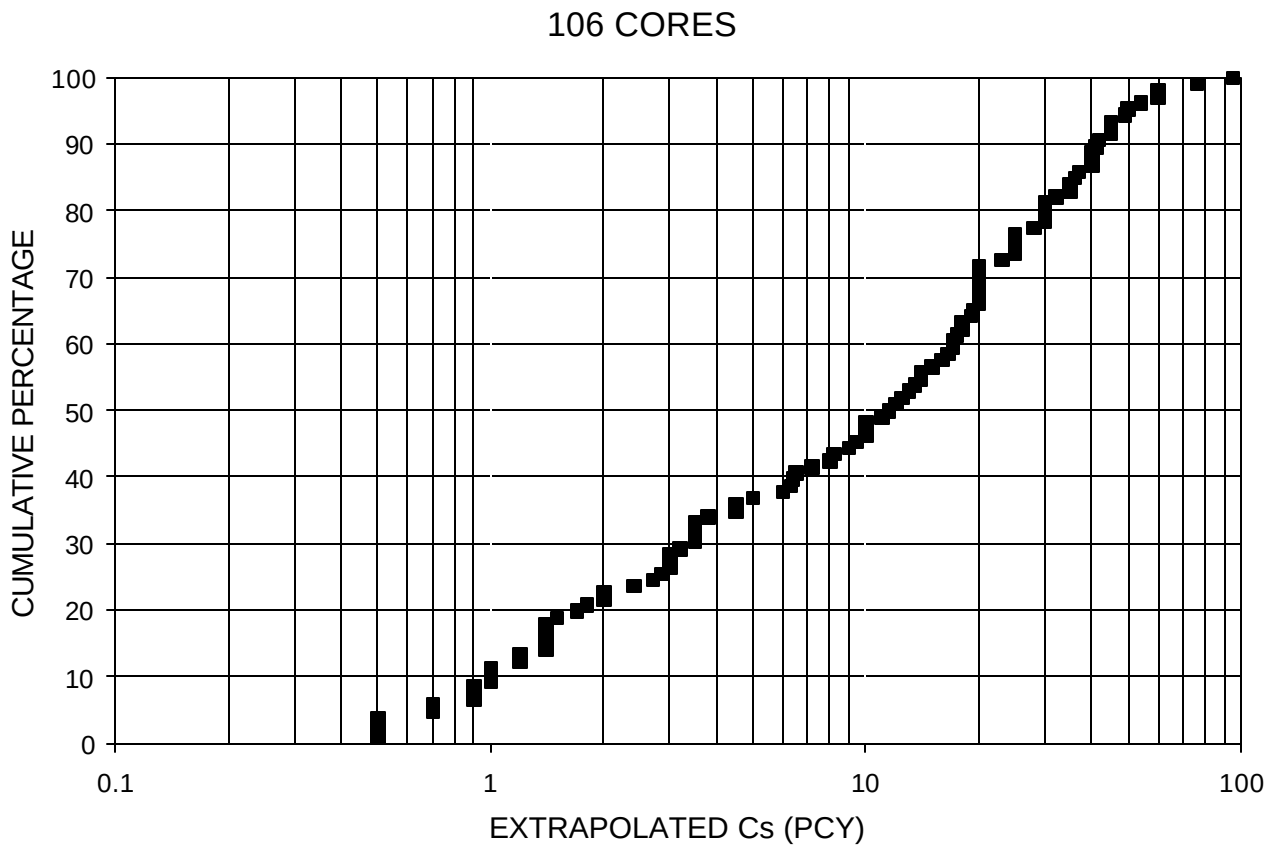

Figure 4.9 Distribution of Calculated Surface Chloride Concentrations

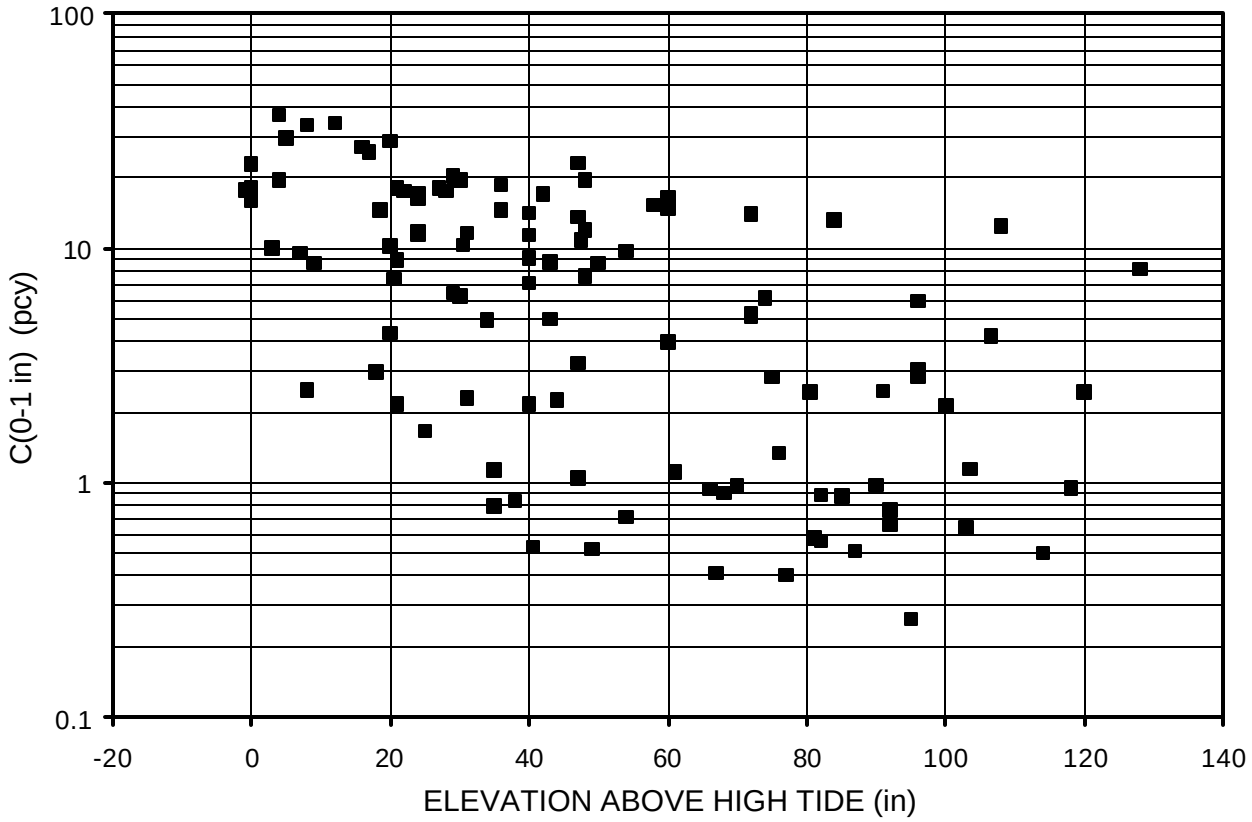

Figure 4.10 Average Chloride Concentration of the First 1-inch Slice of Each Field-extracted Cores vs. Elevation of the Core.

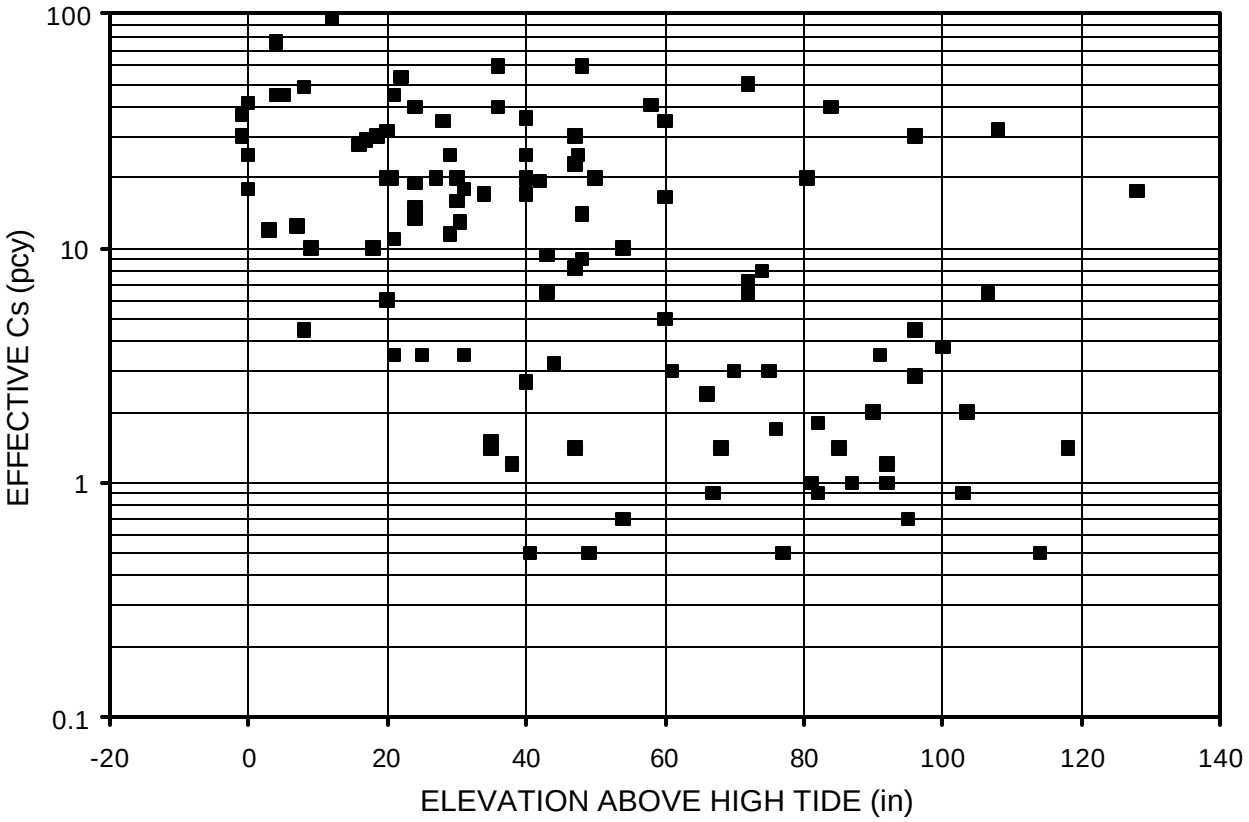

Figure 4.11 Calculated Chloride Concentration at the Surface of the Field-extracted Cores vs. Elevation of the Core.

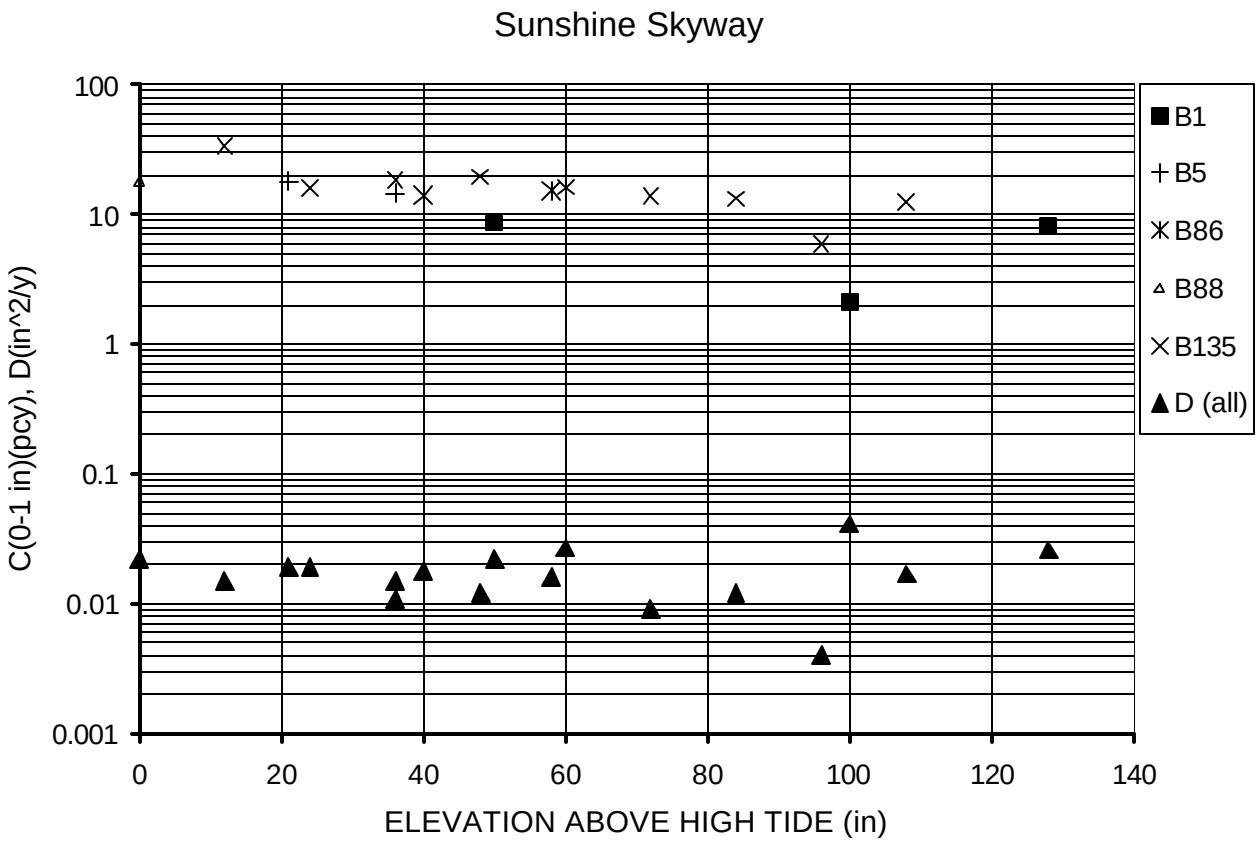

Figure 4.12 Average Chloride Concentration (First 1-inch Slice) and Effective Chloride Diffusion Coefficient for Cores Extracted from the Sunshine Skyway Bridge, as a Function of Elevation of the Core. Individual Bridge Bents are Indicated.

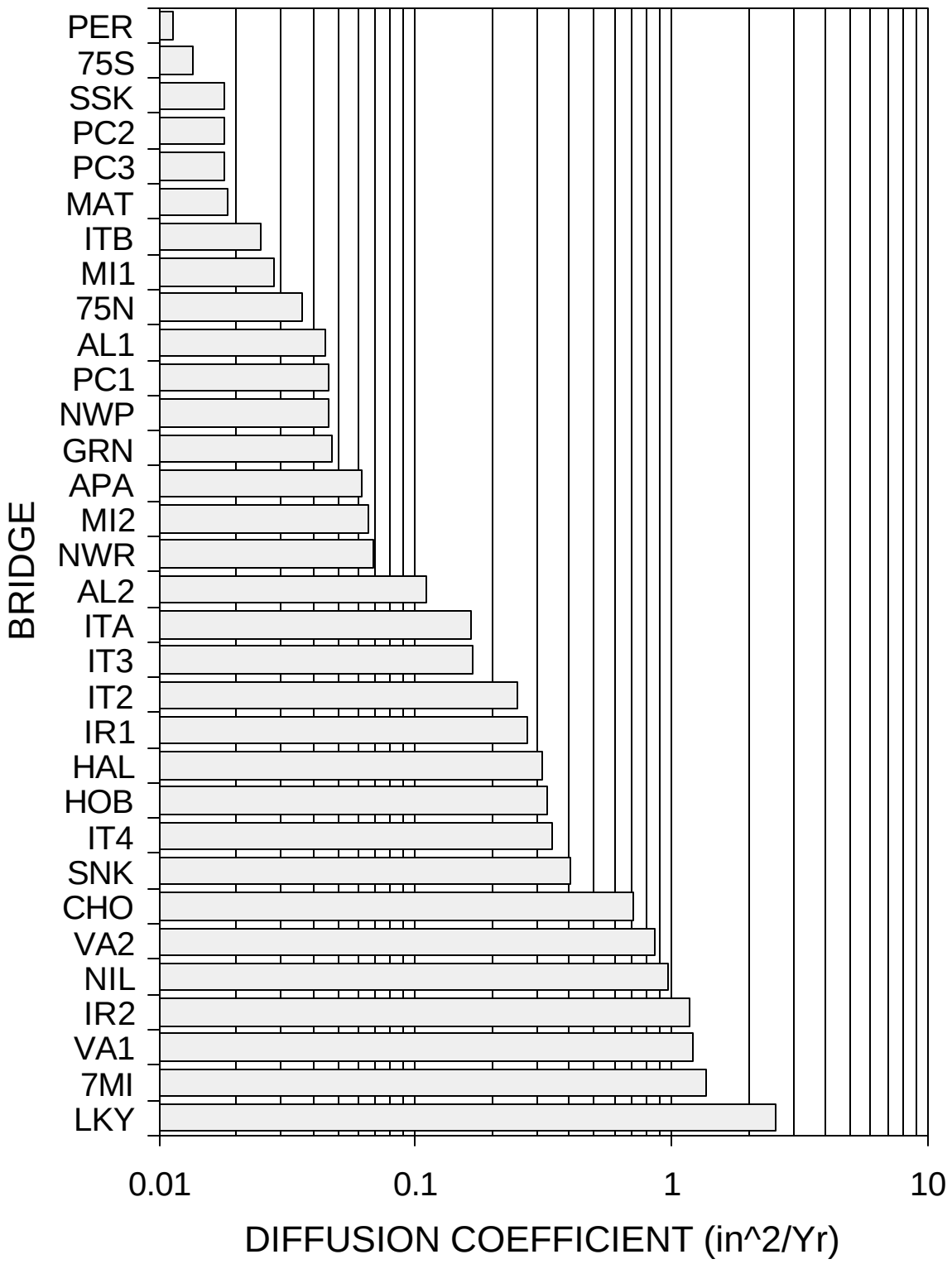

Figure 4.13 Bridge Ranking by Average Effective Diffusion Coefficient (See Table 2.1 for Bridge Code).

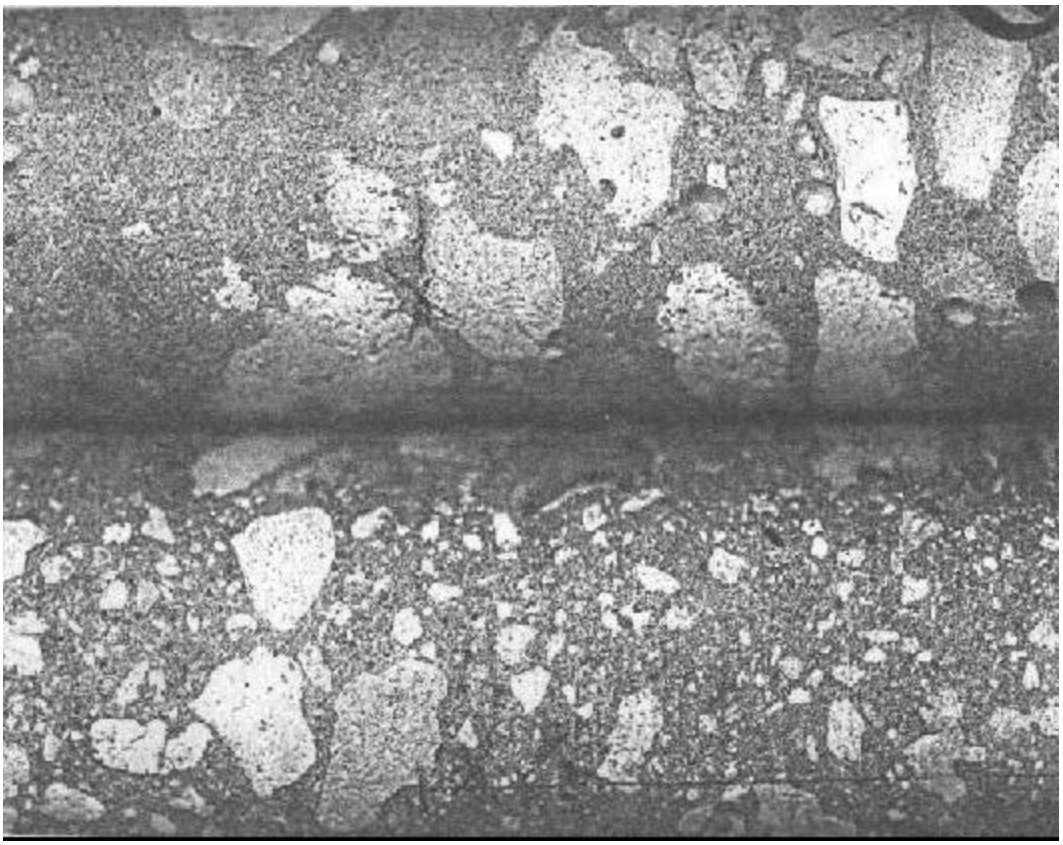

Figure 4.14 Example of two Cores (magnified about 1.3 times) Showing Extremes of Coarse Aggregate Grading.

Top Core: Bridge No.860319, NWR (Low content of fines)

Bottom Core: Bridge No. 900126, VA1 (High content of fines)

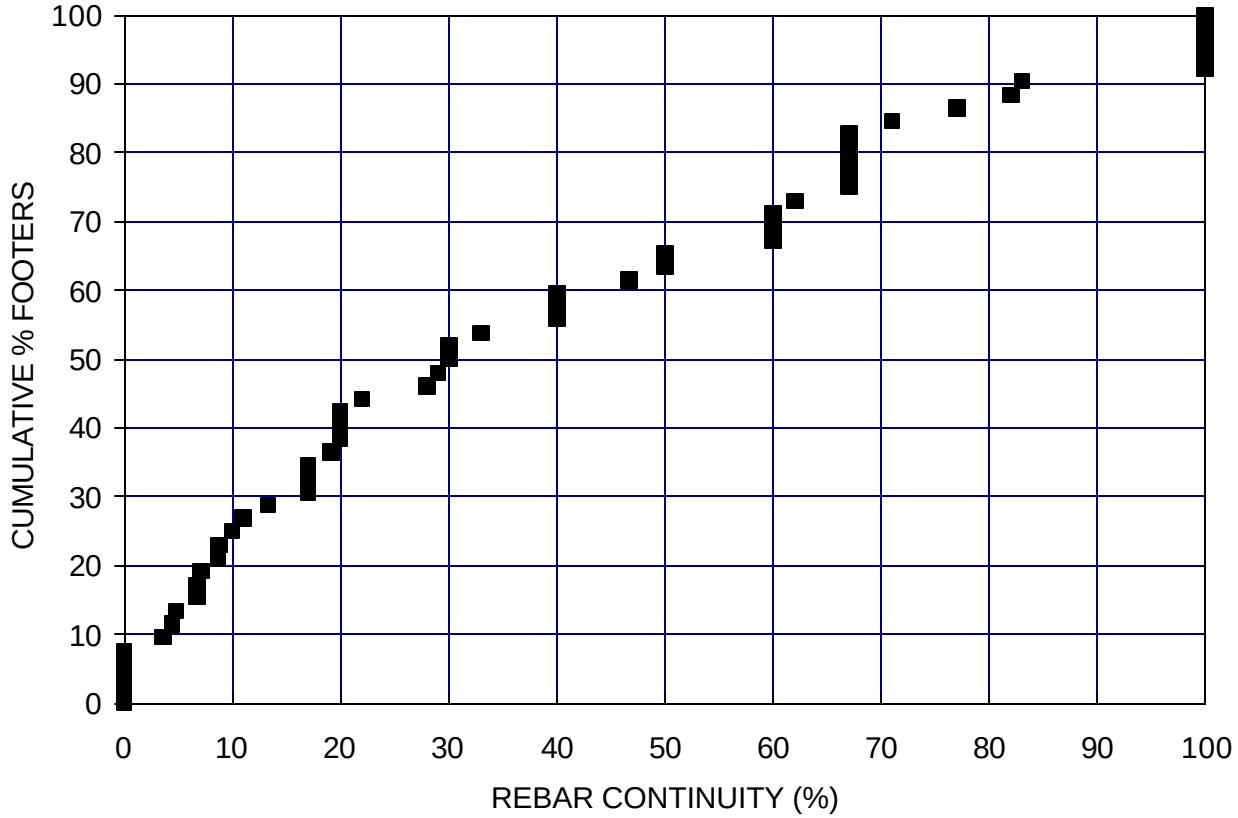

Figure 4.15 Distribution of Degree of Rebar Electric Continuity. Percentage of Bridge Footers Which Have a Degree of Continuity Equal or Less Than the Value Indicated in the Abscissa. The Median Degree of Continuity was Approximately 30%.

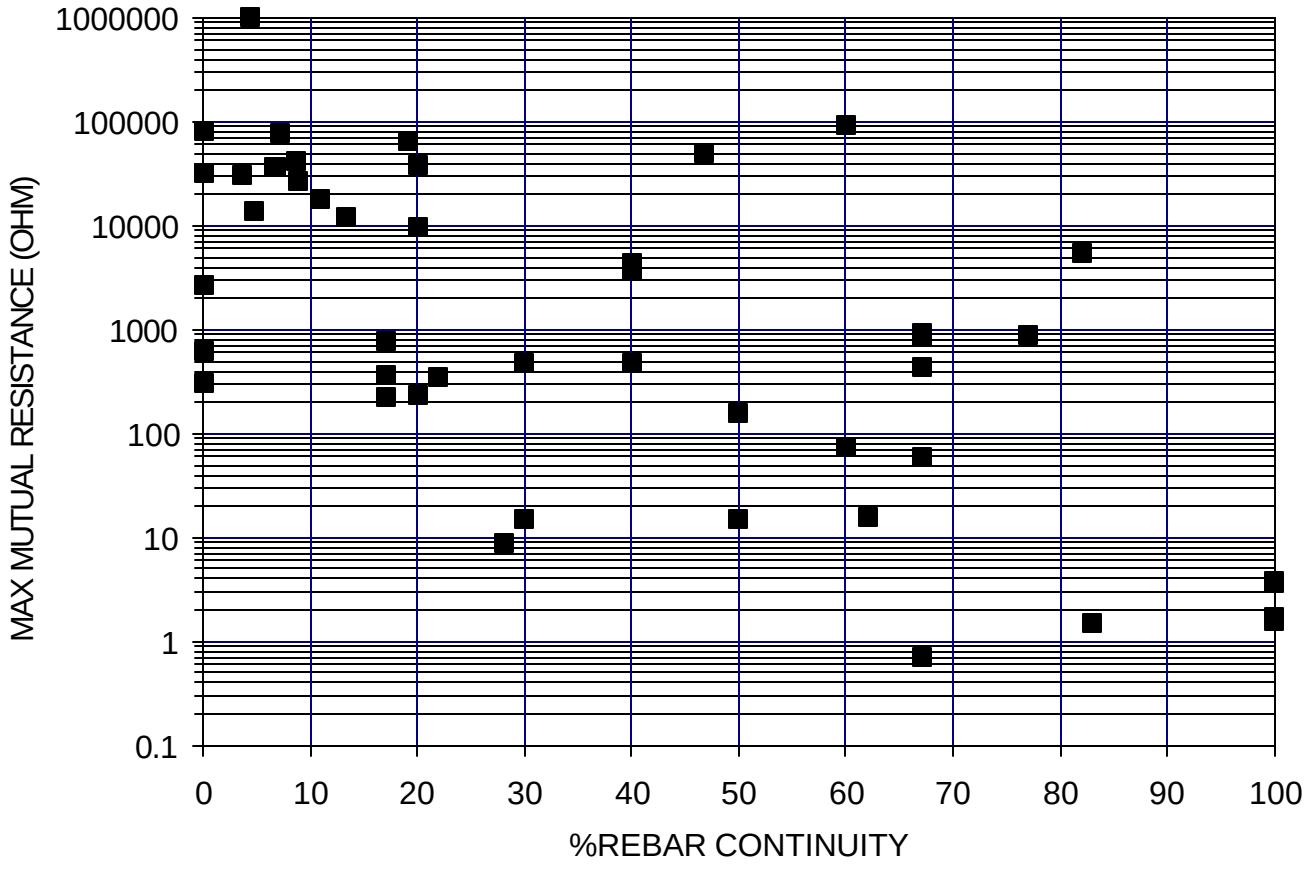

Figure 4.16 Distribution of the Maximum Mutual Resistance in Footers as Function of the Degree of Electric Continuity.

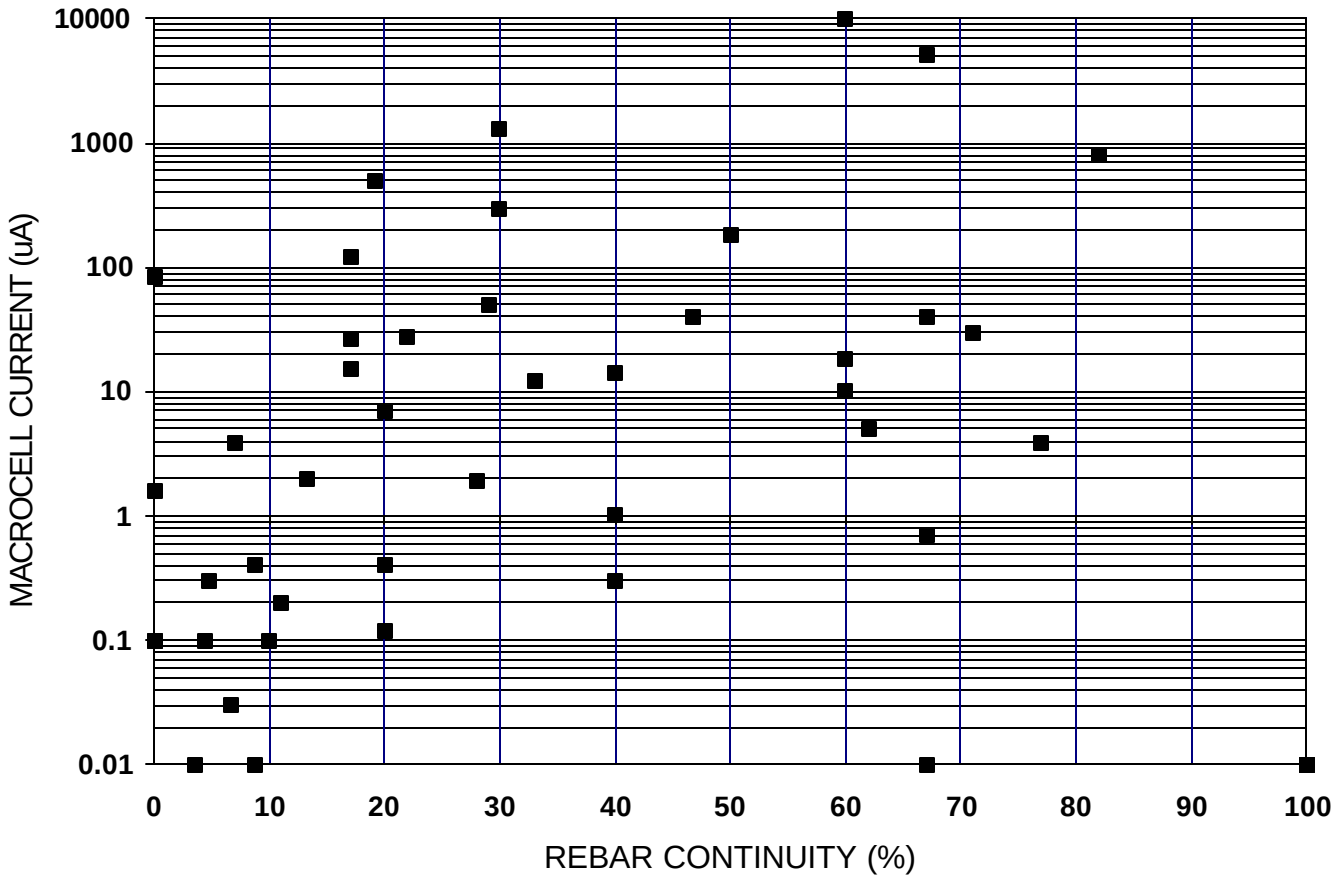

Figure 4.17 Distribution of the 10-Minute Macrocell Current in Footers as a Function of the Degree of Electric Continuity.

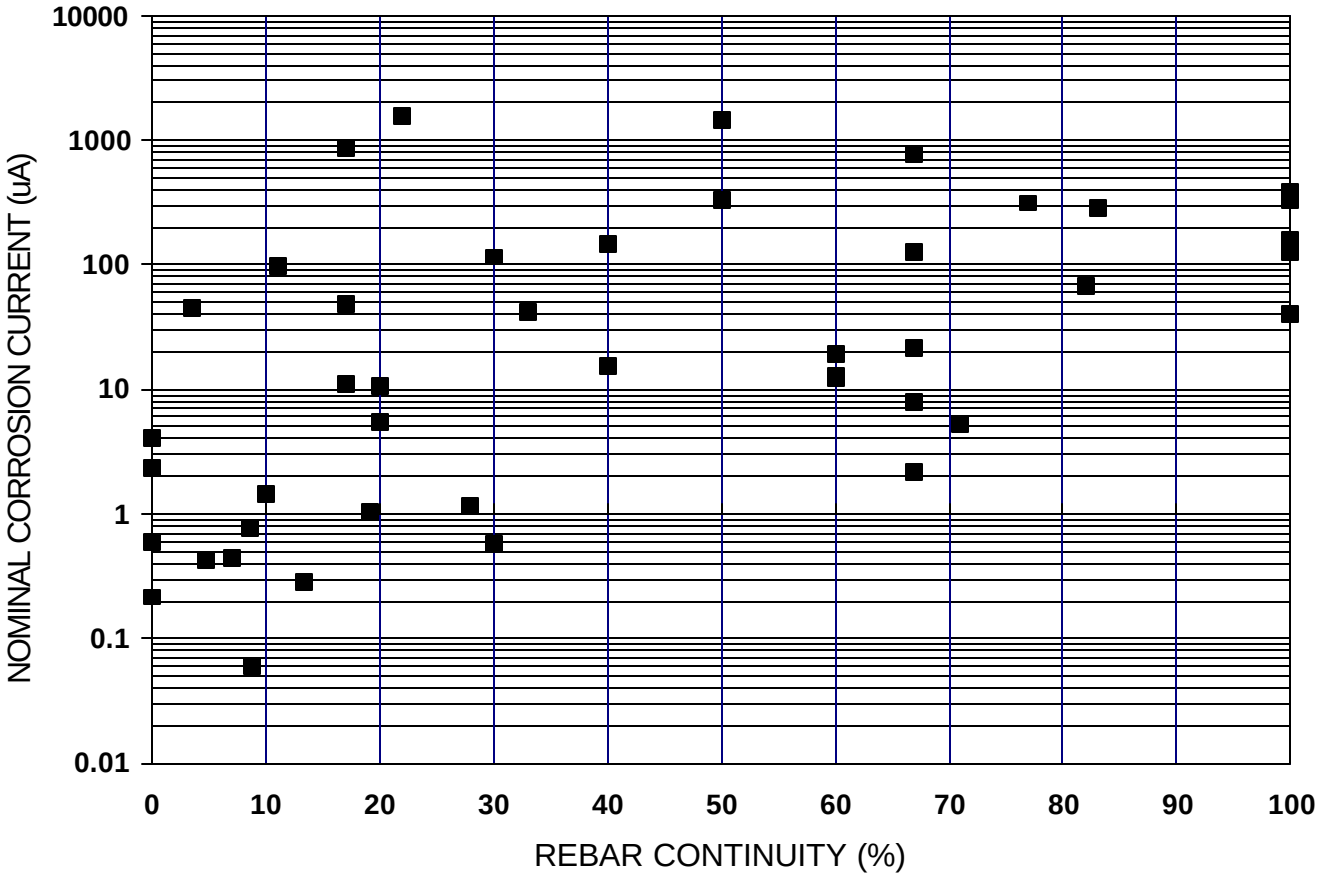

Figure 4.18 Distribution of Nominal Corrosion Current Measurements in Footers as a Function of the Degree of Electric Continuity.

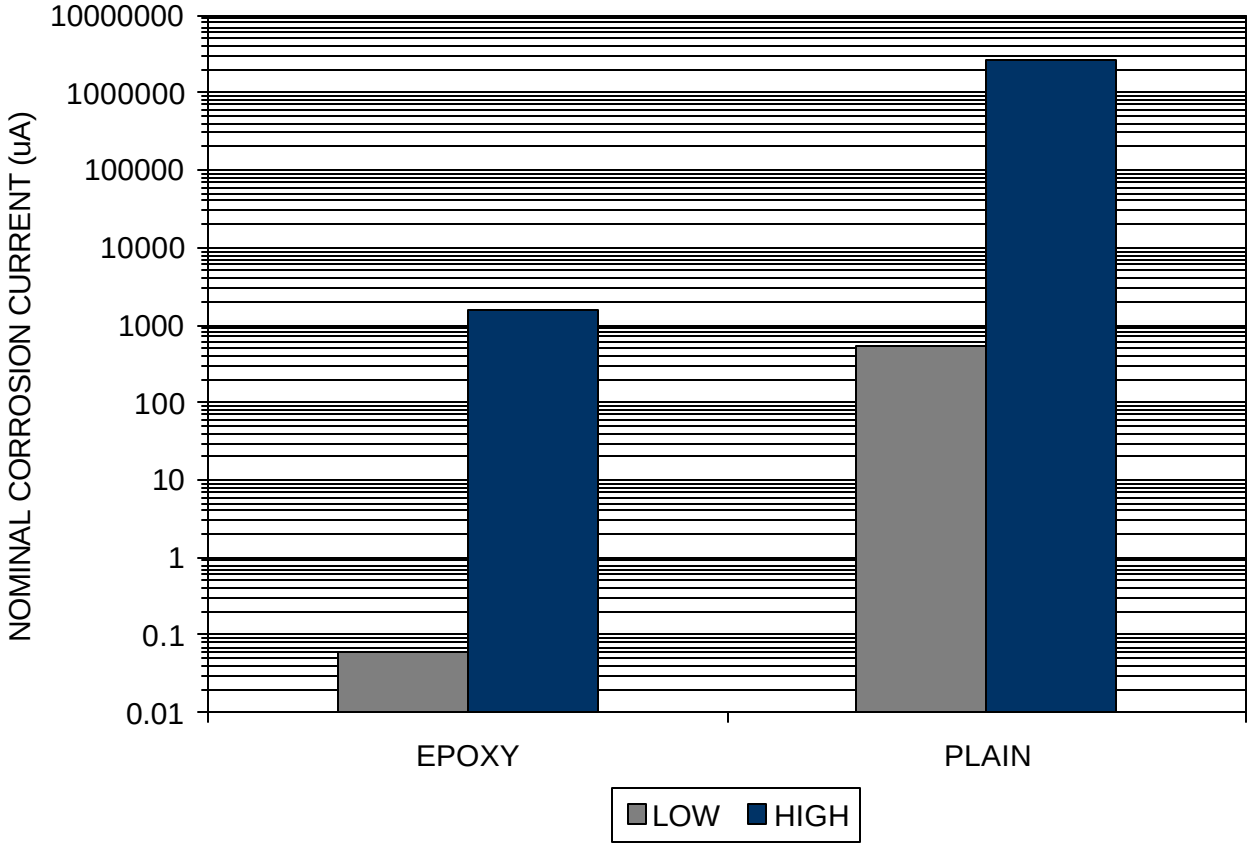

Figure 4.19 Range of Nominal Corrosion Current Measurements in Footers of Structures with ECR and Plain Rebar.

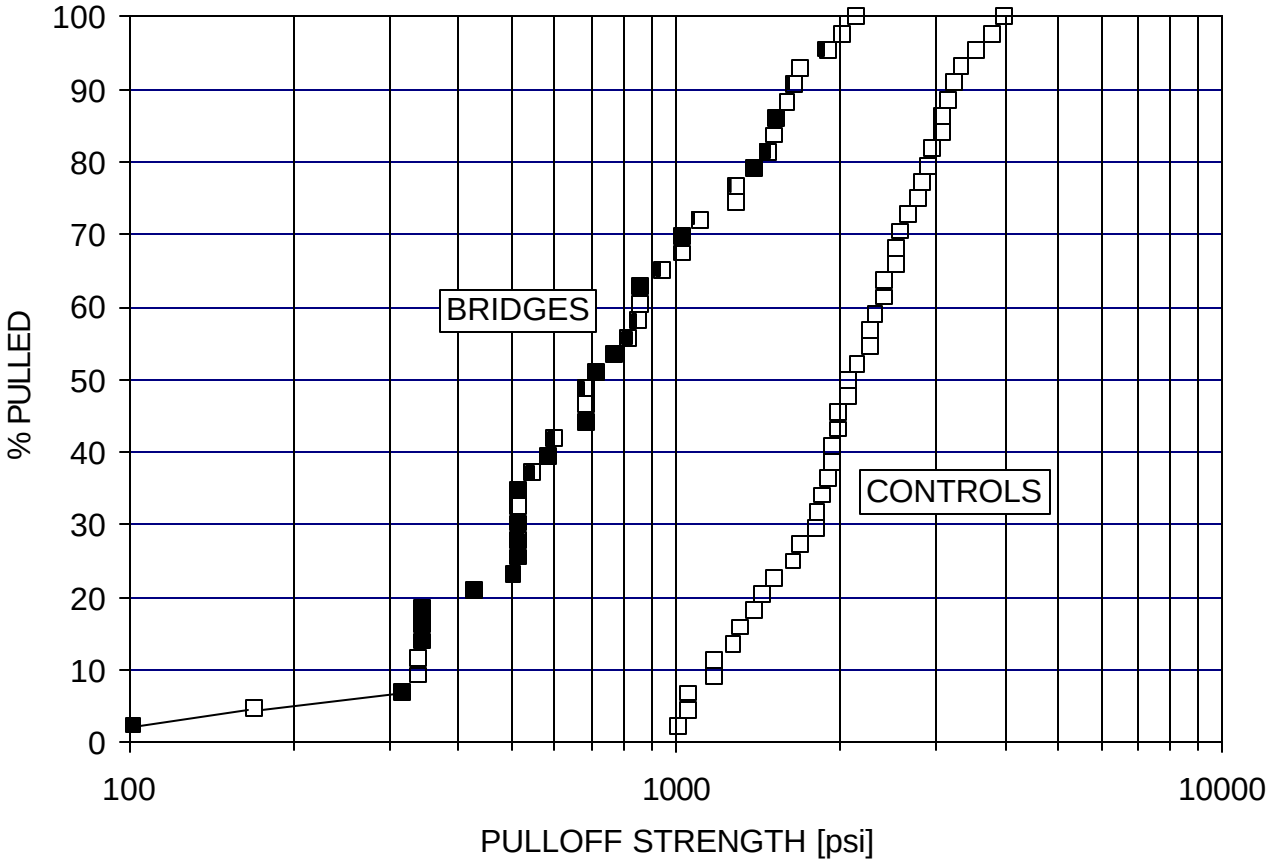

Figure 4.20 Distribution of the Pulloff Strength of ECR Specimens Extracted from the Field Bridge Test Sites and of Unexposed Controls. Completely Filled Symbols Indicate Total Epoxy-Rebar Separation Under the Test Dolly. Partial Filling is Proportional to Fraction Separated.

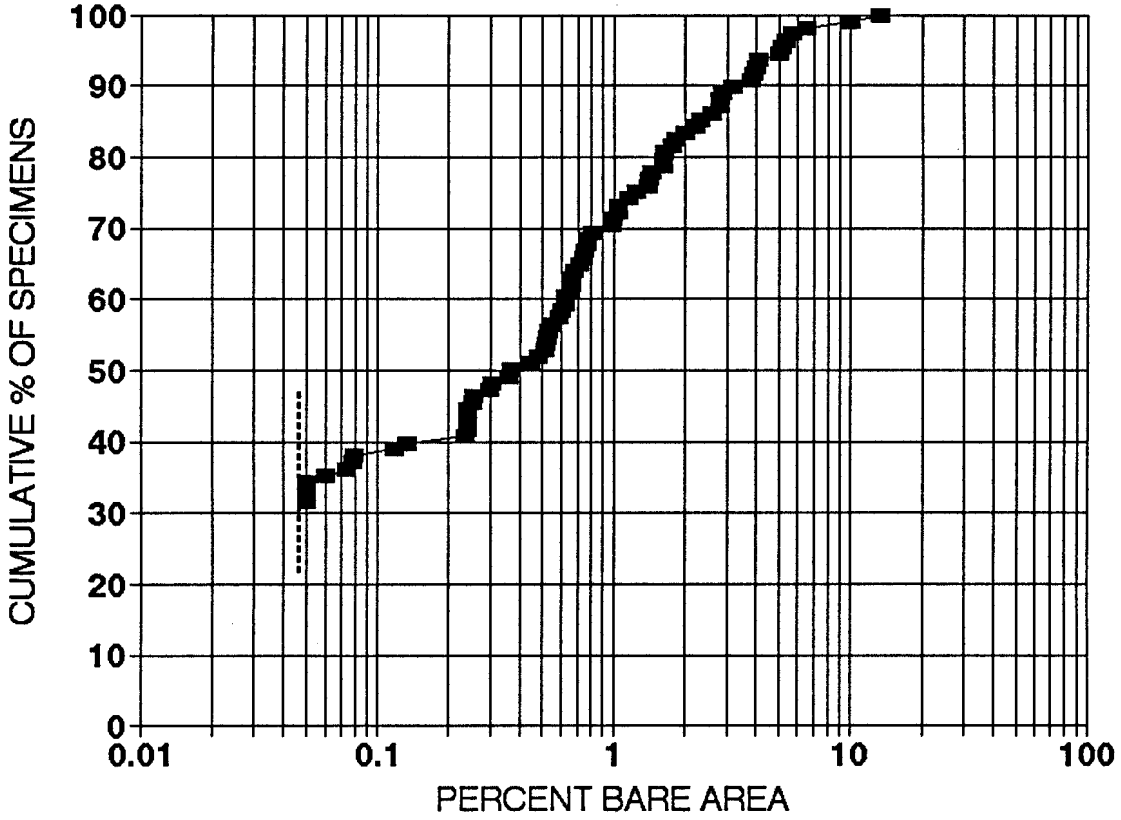

Figure 4.21 Distribution of Percentage of the Surface of Field-extracted ECR Specimens Showing Bare Metal (Unaided Eye). The Dashed Line Indicates the Detection Limit.

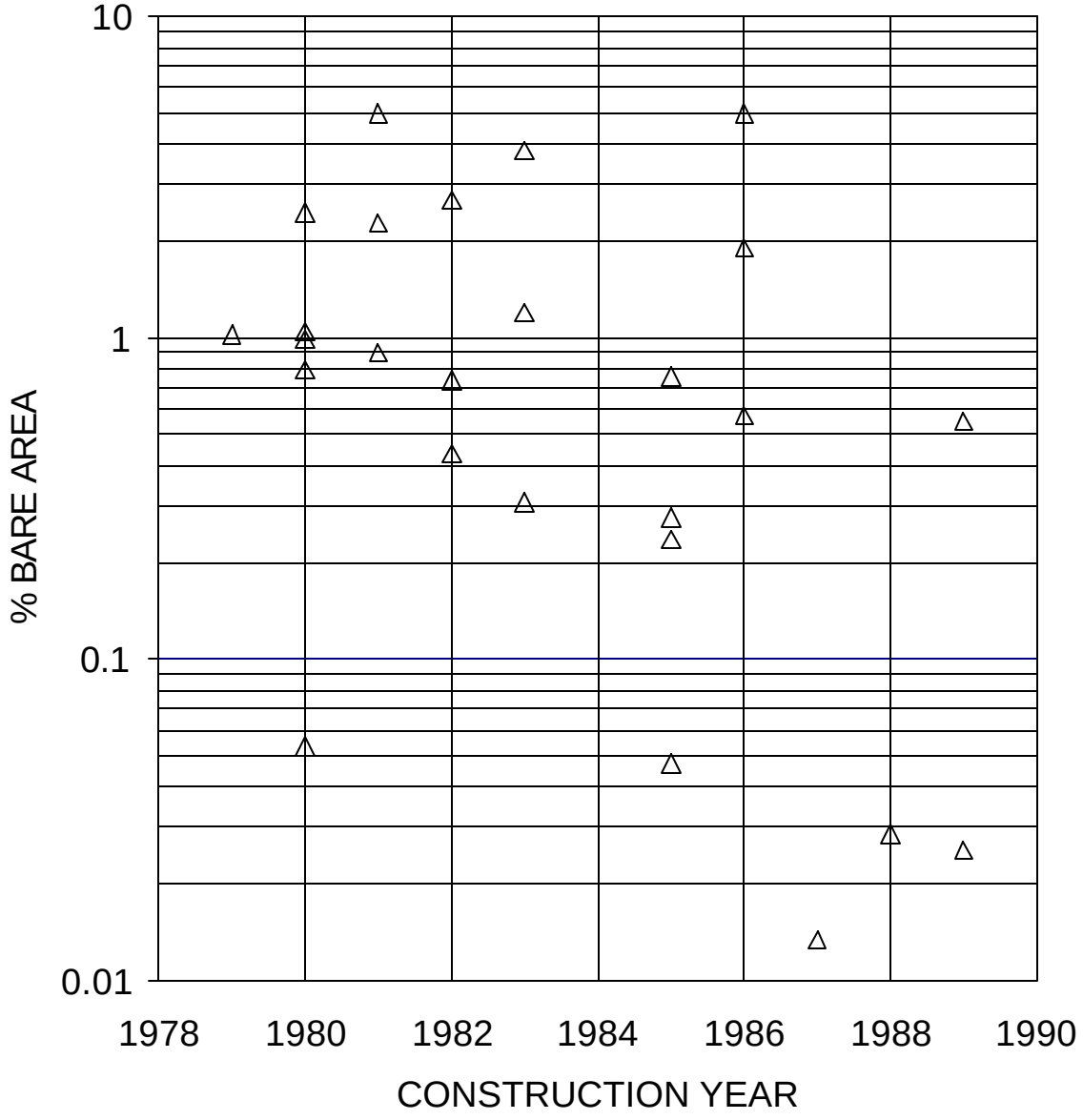

Figure 4.22 Bare Metal (Percentage) Exposed on Field-extracted ECR Specimens vs. Year of Bridge Construction.

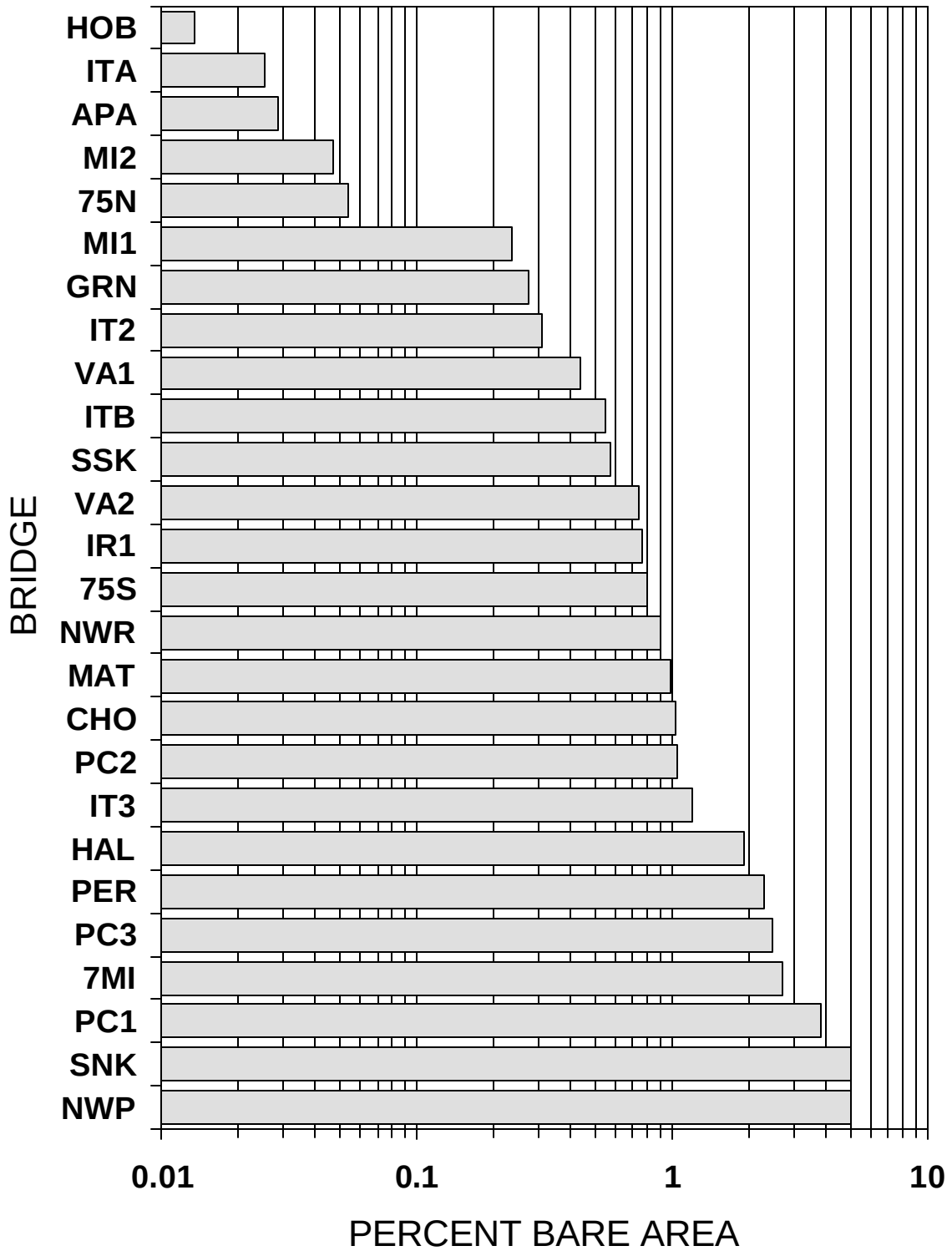

Figure 4.23 Ranking of Bridges by Bare Metal (Percentage) Exposed on Field-extracted ECR Specimens. (See Table 2.1 for Bridge Code).

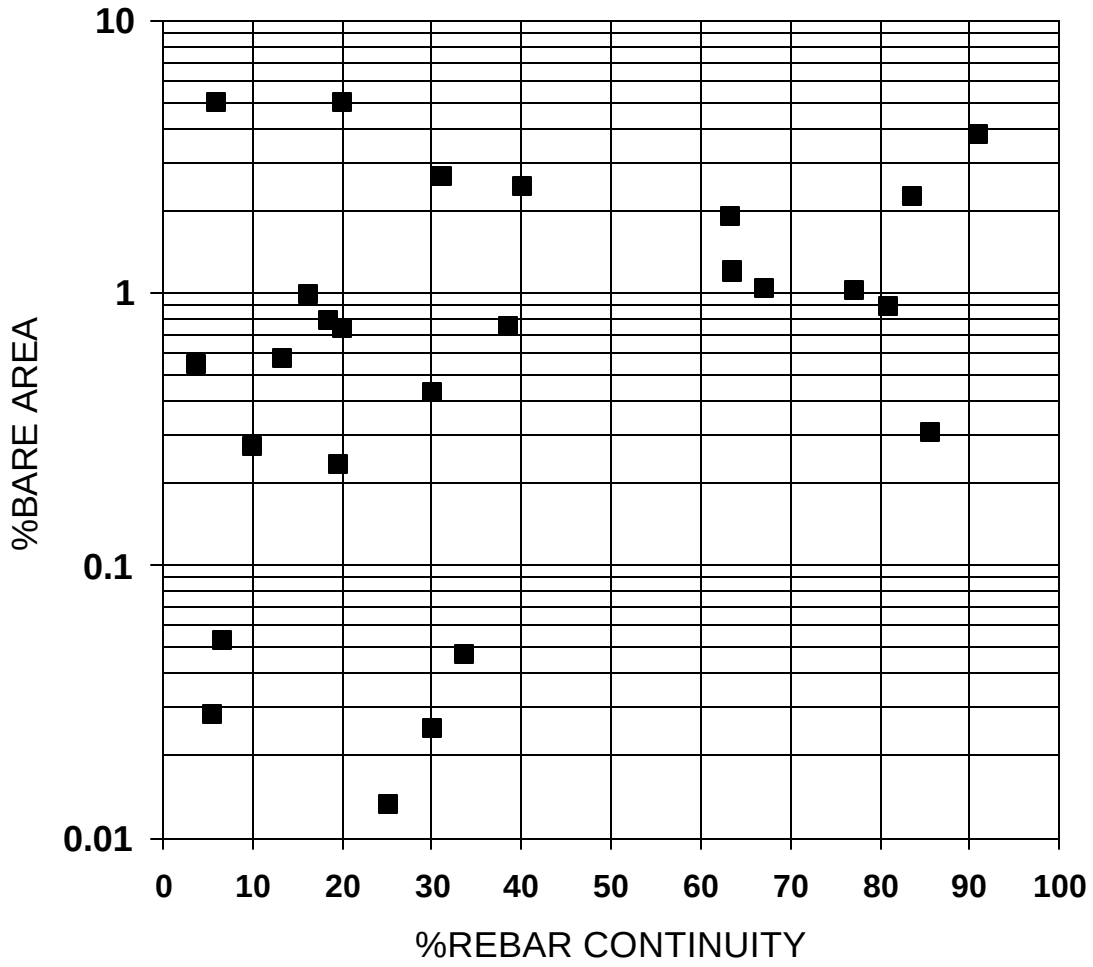

Figure 4.24 Bare Metal (percentage) Exposed on Field-extracted ECR Specimens from Footers vs. Degree of Electric Rebar Continuity.

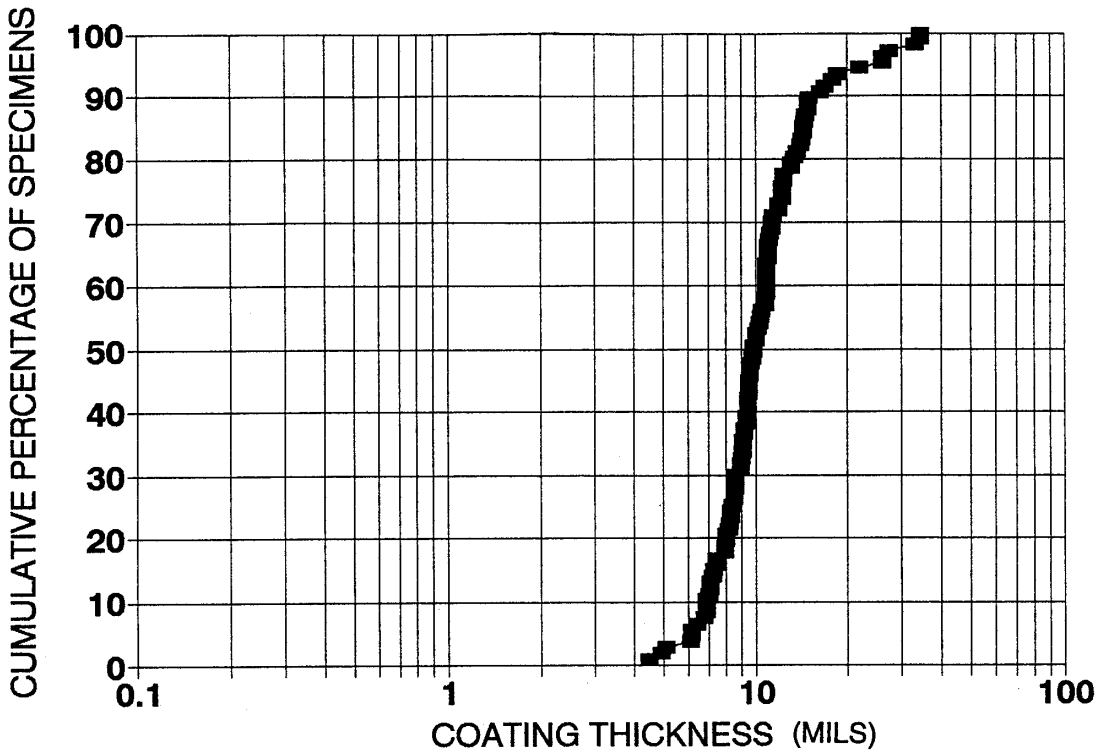

Figure 4.25 Distribution of Coating Thickness of Field-extracted ECR Specimens.

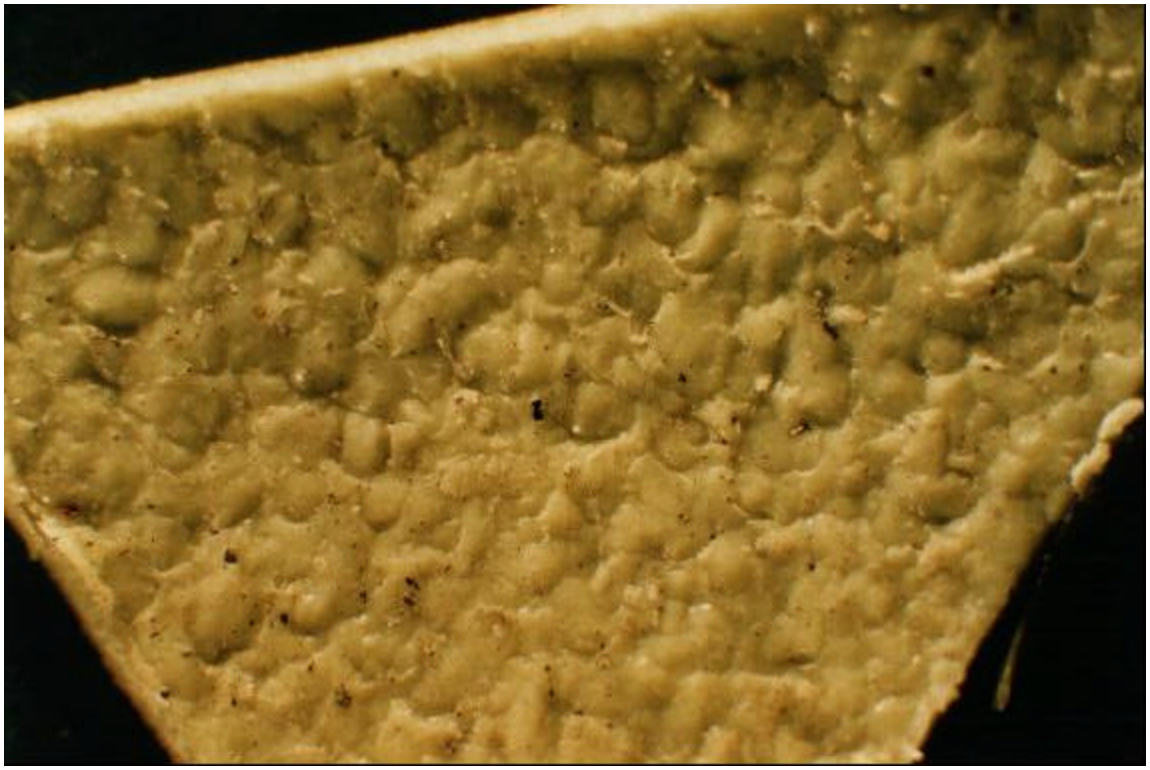

Figure 4.26 Example of Backside Appearance of Coating Removed from Field-extracted ECR Specimens. (~35X)

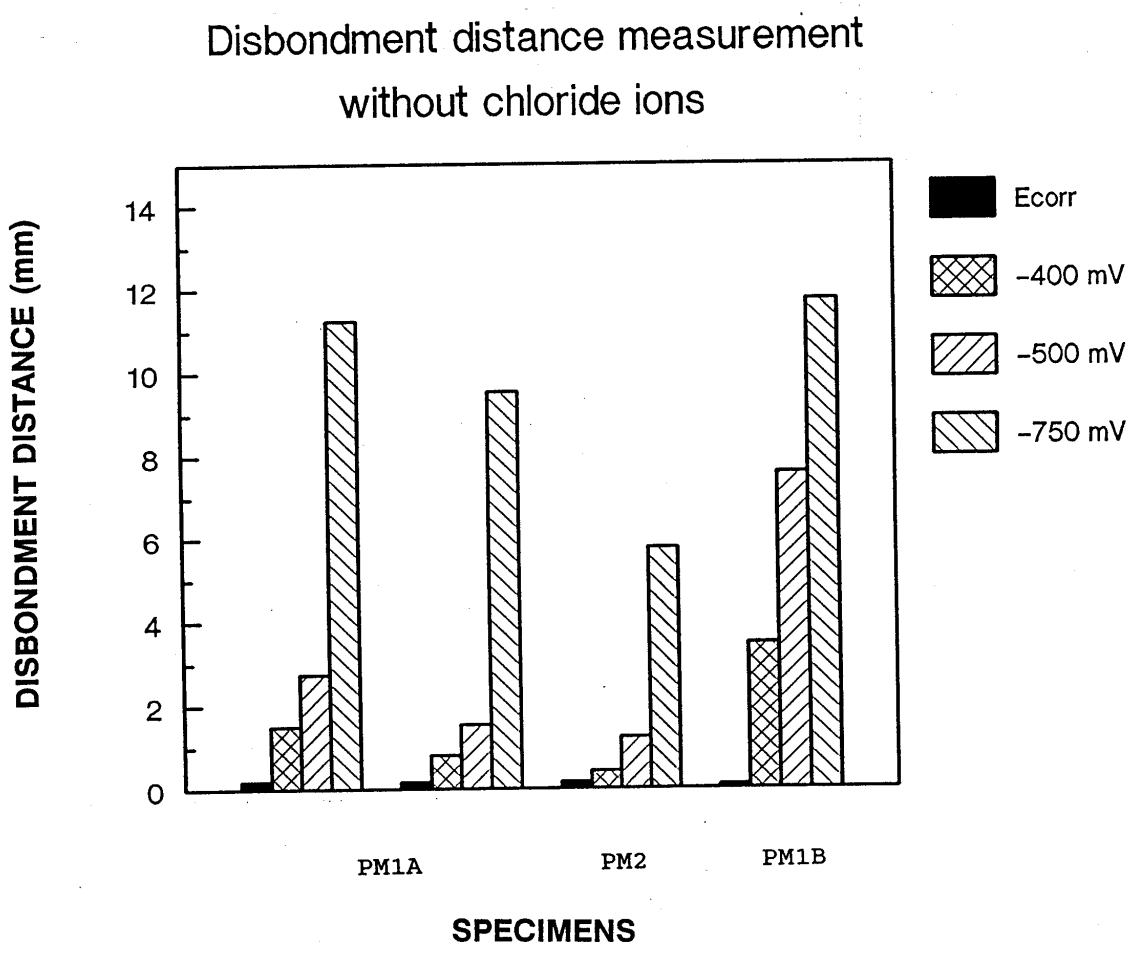

Figure 5.1 Disbondment Distance as Function of Polarization Potential After 30-Day Exposures to Chloride-free SPS (Table 3.1). PM1 (A and B) and PM2 Correspond to ECR Prepared with Powder from Two Different Manufacturers.

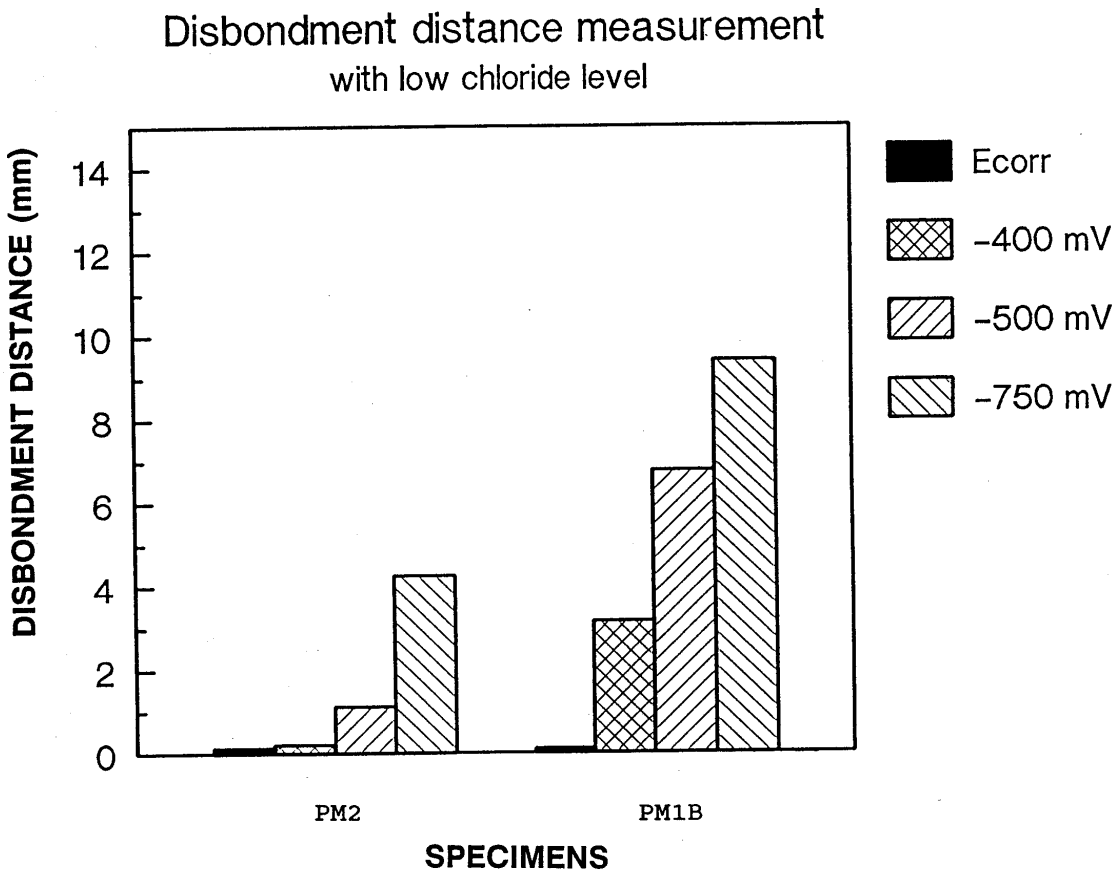

Figure 5.2 Disbondment Distance as Function of Polarization Potential After 30-Day Exposures to SPS with 0.06 M Chloride Addition (Table 3.1). PM1B and PM2 Correspond to ECR Prepared with Powder from Two Different Manufacturers.

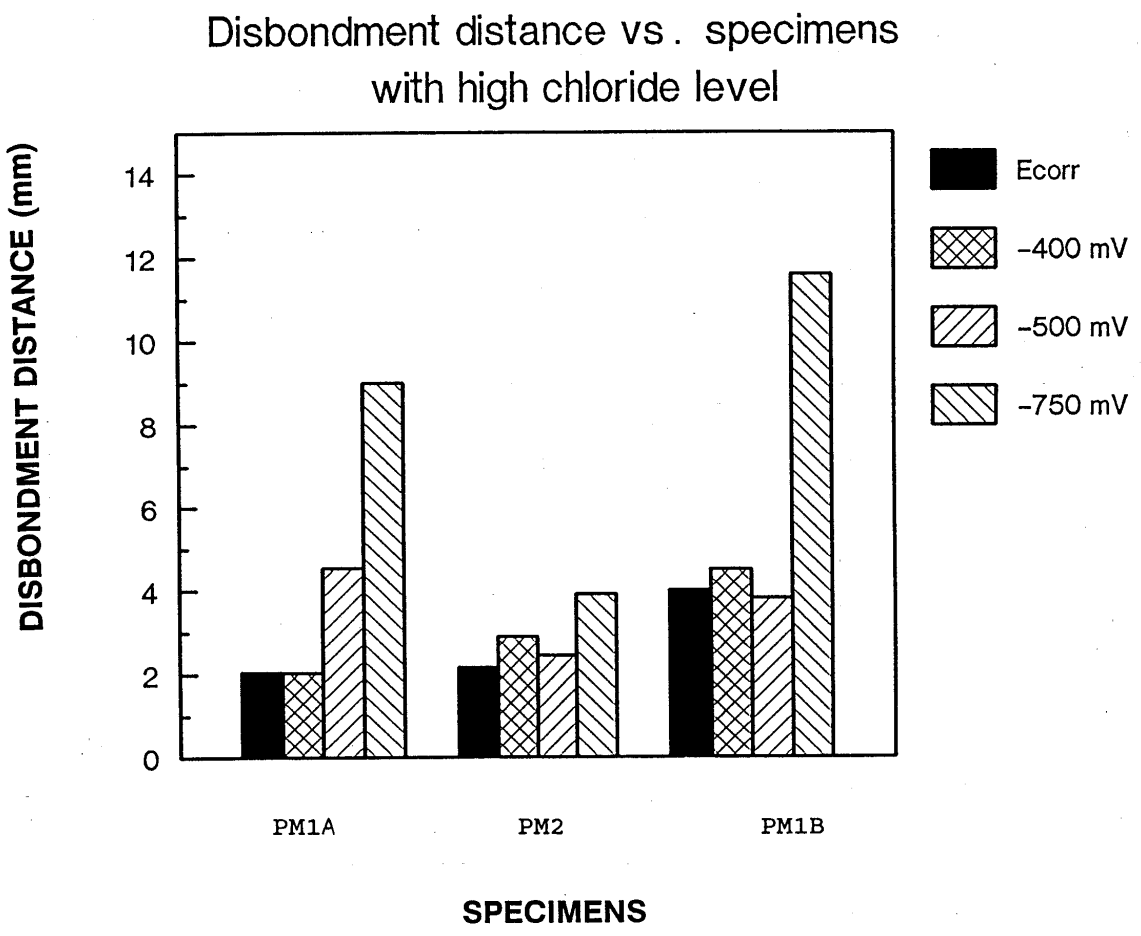

Figure 5.3 Disbondment Distance as Function of Polarization Potential After 30-Day Exposures to SPS with 0.45 M Chloride Addition (Table 3.1). PM1 (A and B) and PM2 Correspond to ECR Prepared with Powder from Two Different Manufacturers.

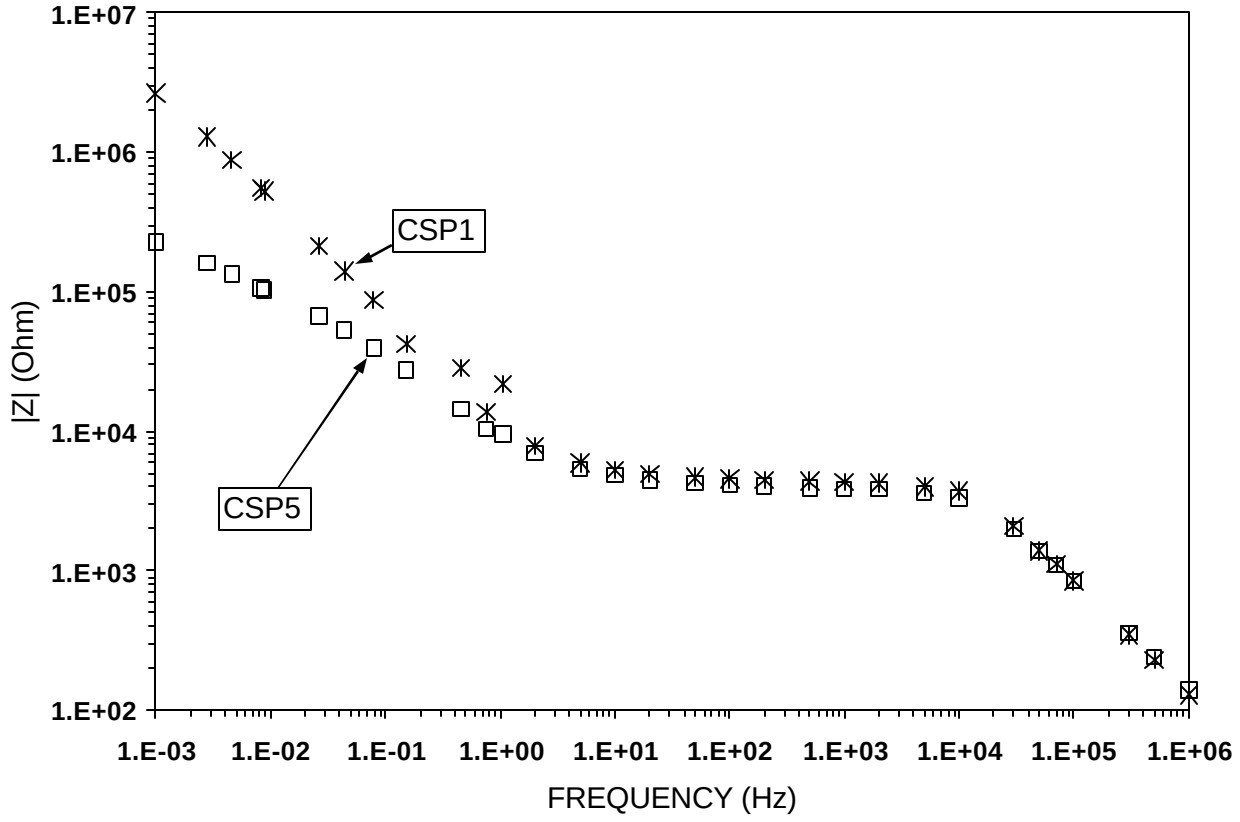

Figure 5.4 Electrochemical Impedance Behavior of ECR in Chloride-free Concrete after 486 Days. CSP1 Corresponds to a Specimen Exposed at its Natural Open Circuit Potential (Near -150 mV SCE); CSP5 Corresponds to Exposure at a Controlled Potential of -500 mV SCE (Specimen Allowed to Depolarize 24 h Before Testing in Open Circuit Conditions).

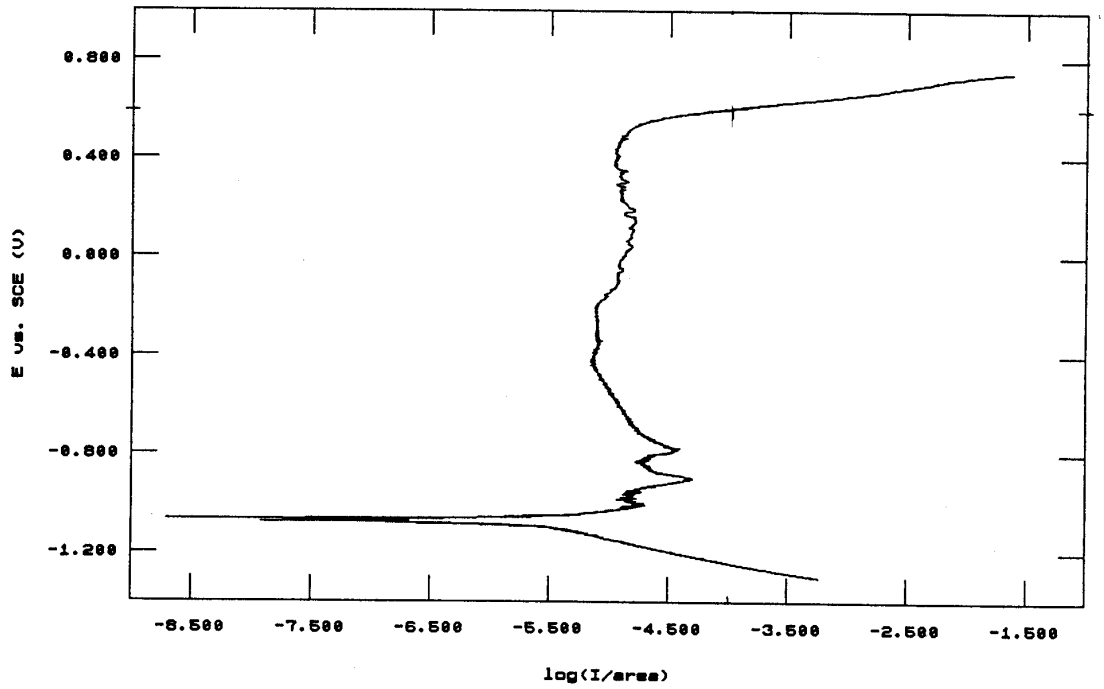

Figure 5.5 Polarization Behavior of a Steel Surface Freely Exposed to a SPS containing 0.1 M Cl^-.

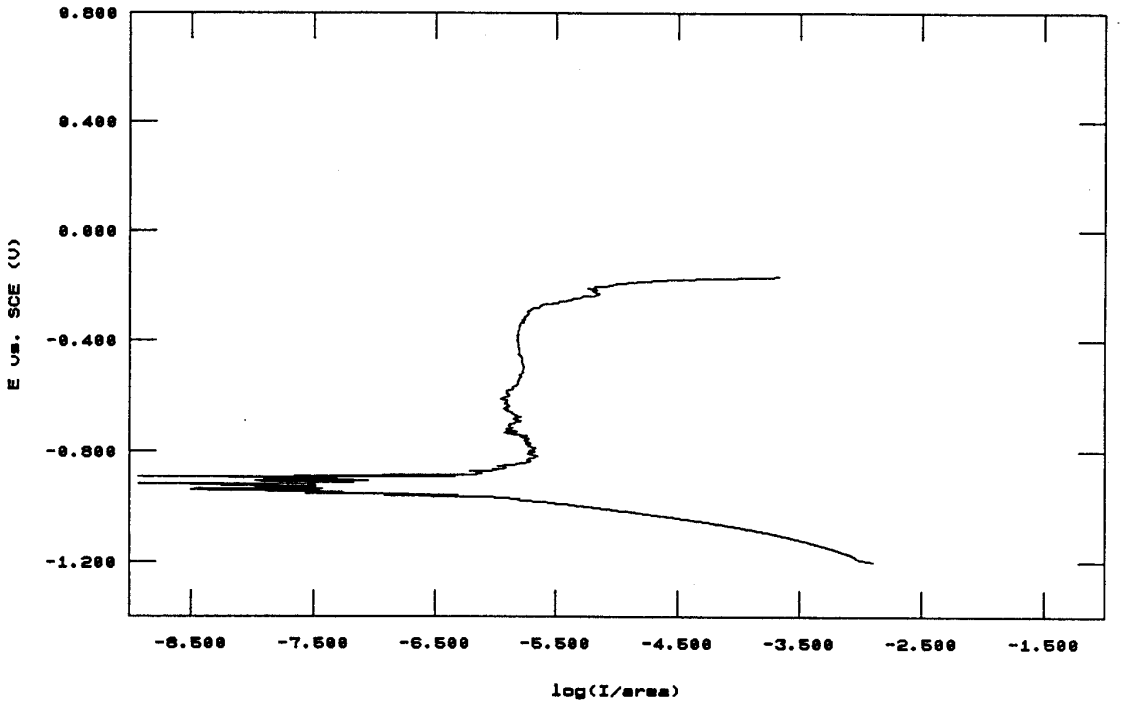

Figure 5.6 Polarization Behavior of a Steel Specimen with Half of its Surface Freely Exposed to a SPS containing 0.1 M Cl^-, and the Other Half Loosely Covered by Plexiglas.

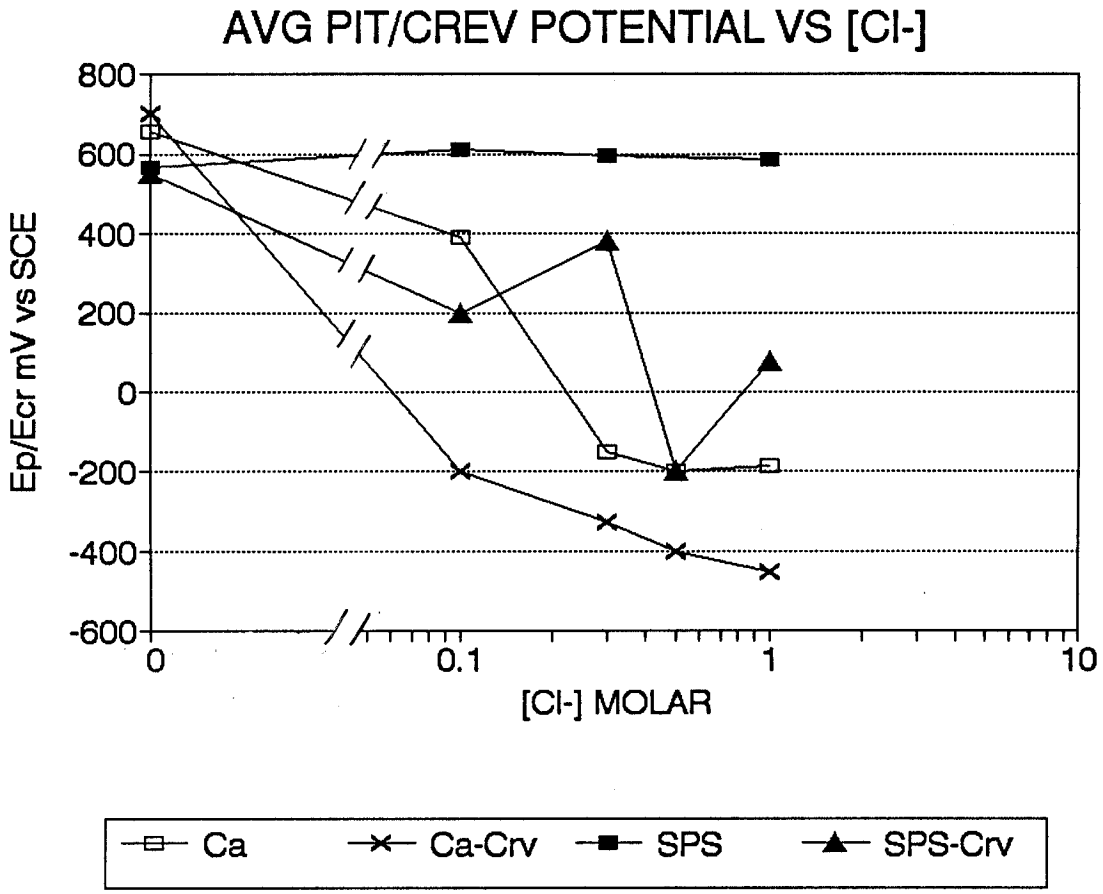

Figure 5.7 Average Pitting (or Crevicing) Potentials for Freely Exposed and Creviced Specimens in $Ca(OH)_2$ (Ca) and SPS Solutions as a Function of Cl^- Content.

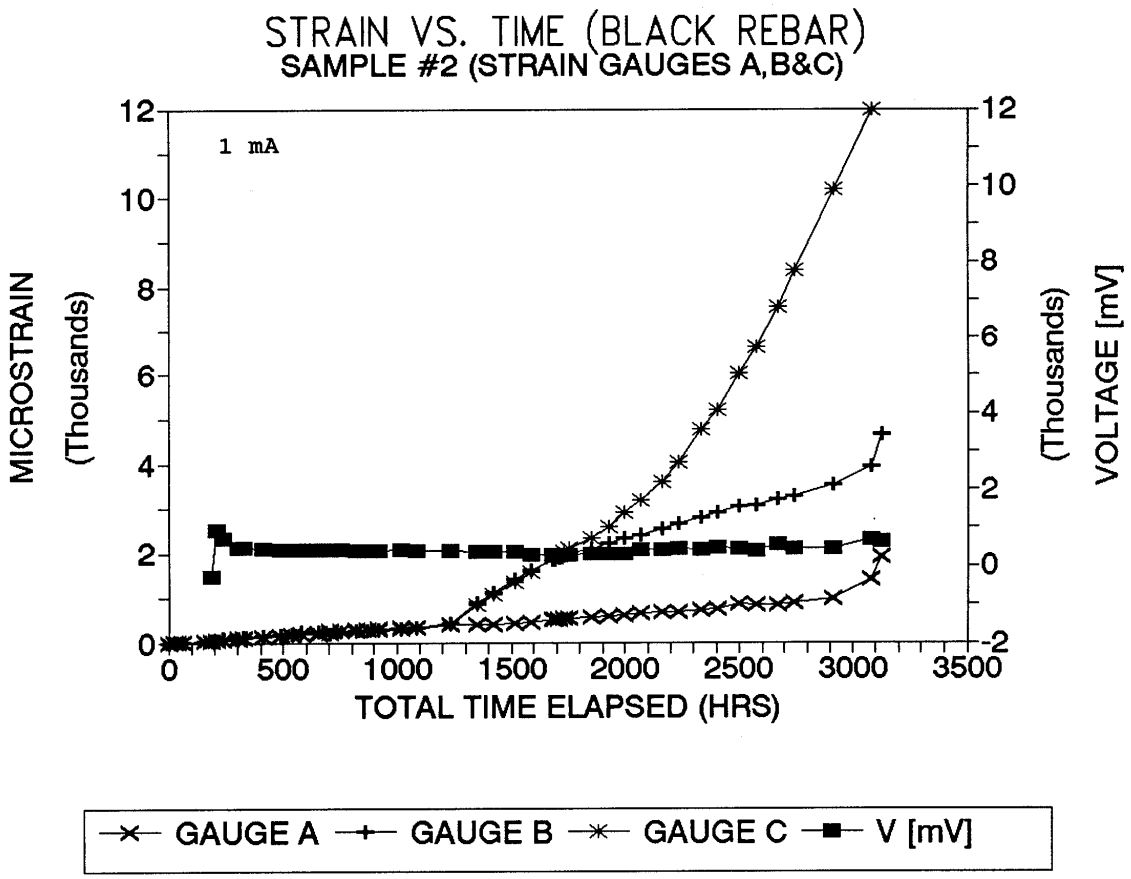

Figure 5.8 Example of Strain Gage Readings and Driving Potential as Function of Exposure Time for a Plain Rebar Specimen with 1mA Impressed Current. The Time to Cracking per Gage Reading was 1200 h.

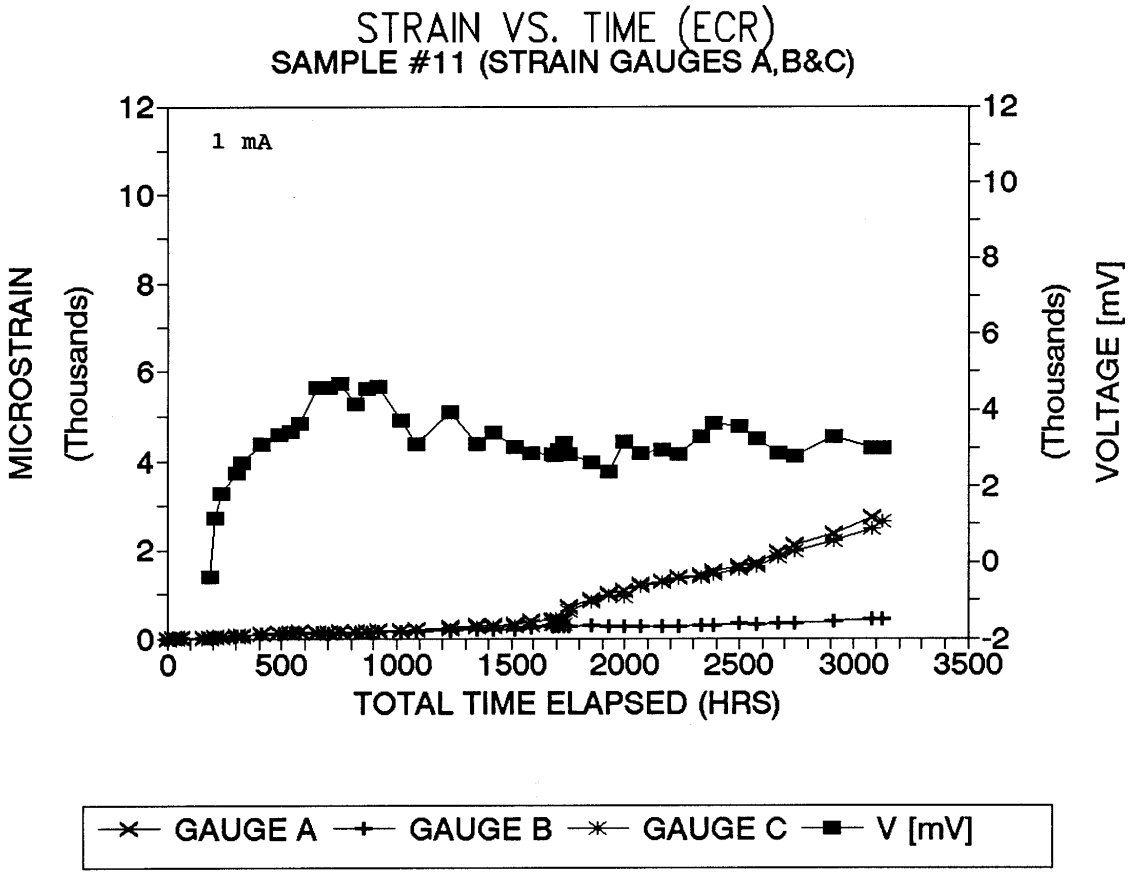

Figure 5.9 Example of Strain Gage Readings and Driving Potential as Function of Exposure Time for an ECR Specimen with 1mA Impressed Current. The Time to Cracking per Gage Reading was 1700 h.

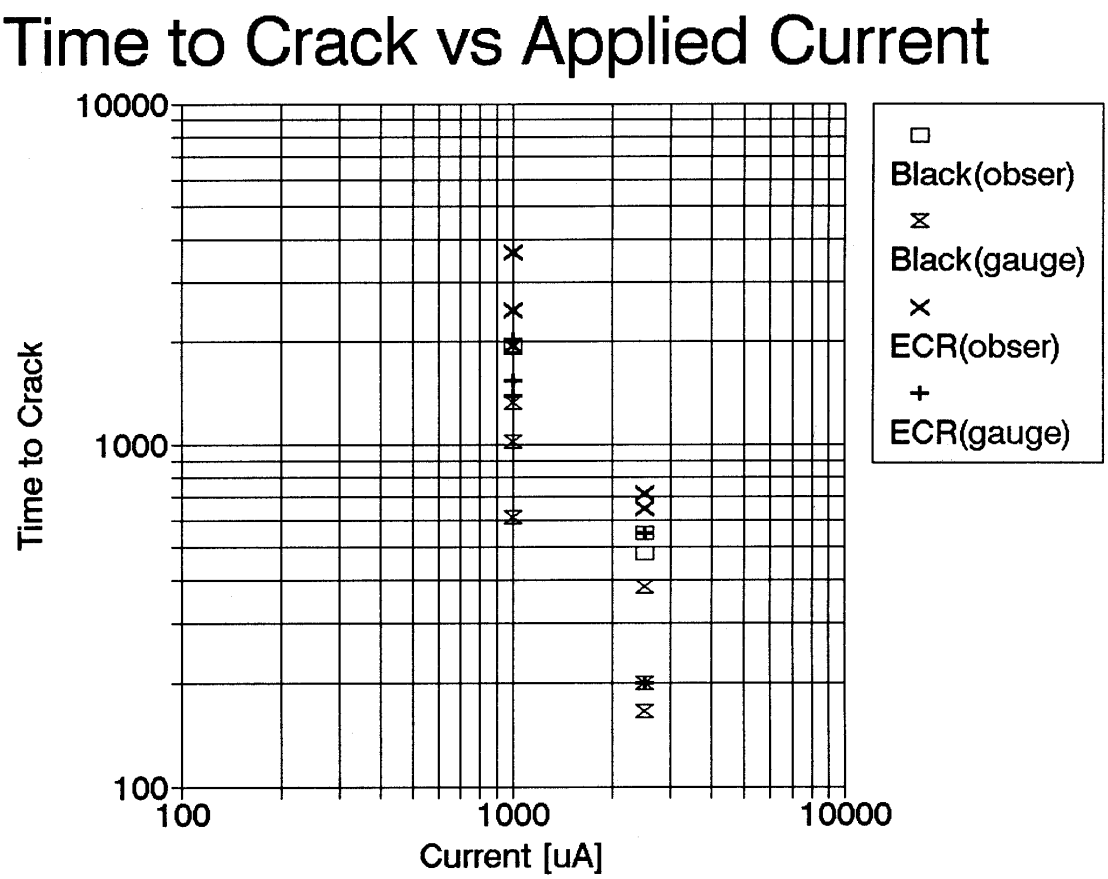

Figure 5.10 Summary of Time-to-cracking Results (Based on Gauge Readings and Direct Surface Observation) of Plain Rebar and ECR Under Two Impressed Current Levels.

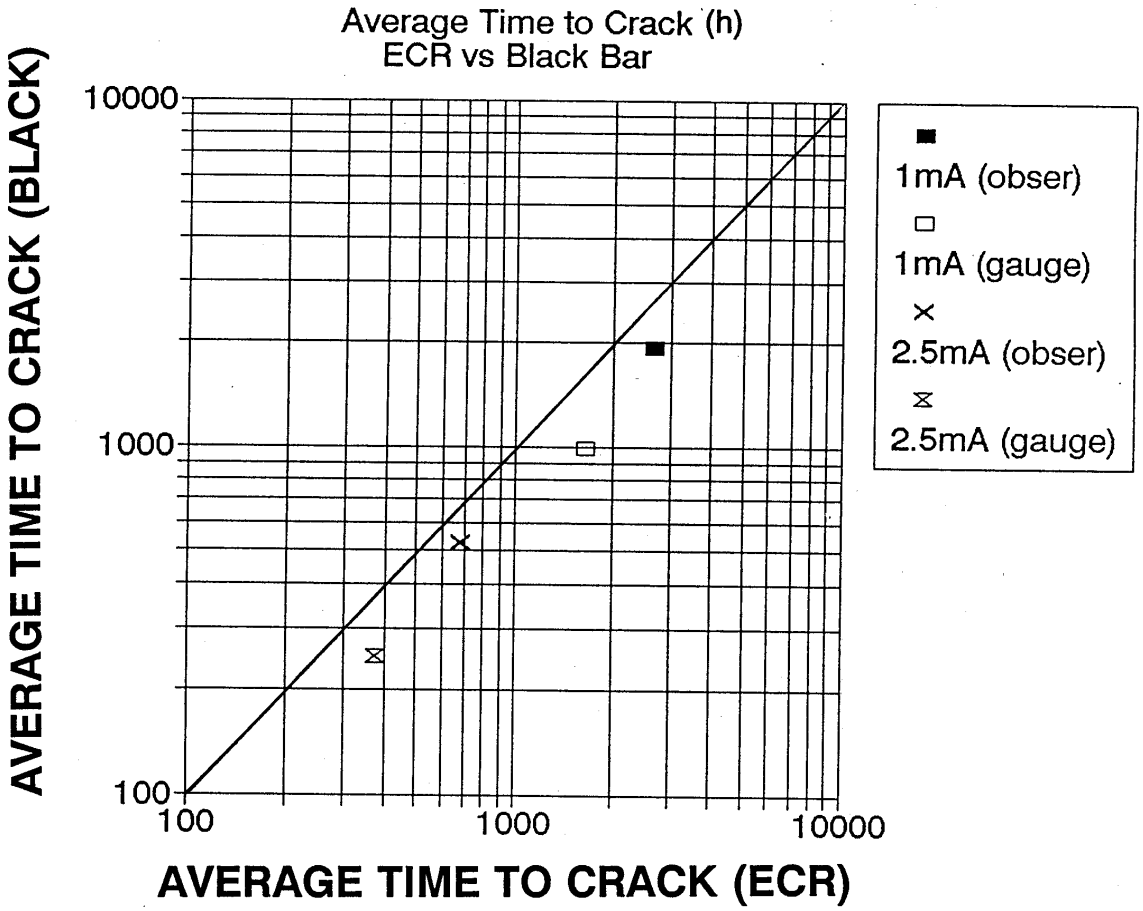

Figure 5.11 Average Time-to-cracking (For Both Gauge and Direct Observation) of Plain Rebar and ECR Under Two Impressed Current Levels.

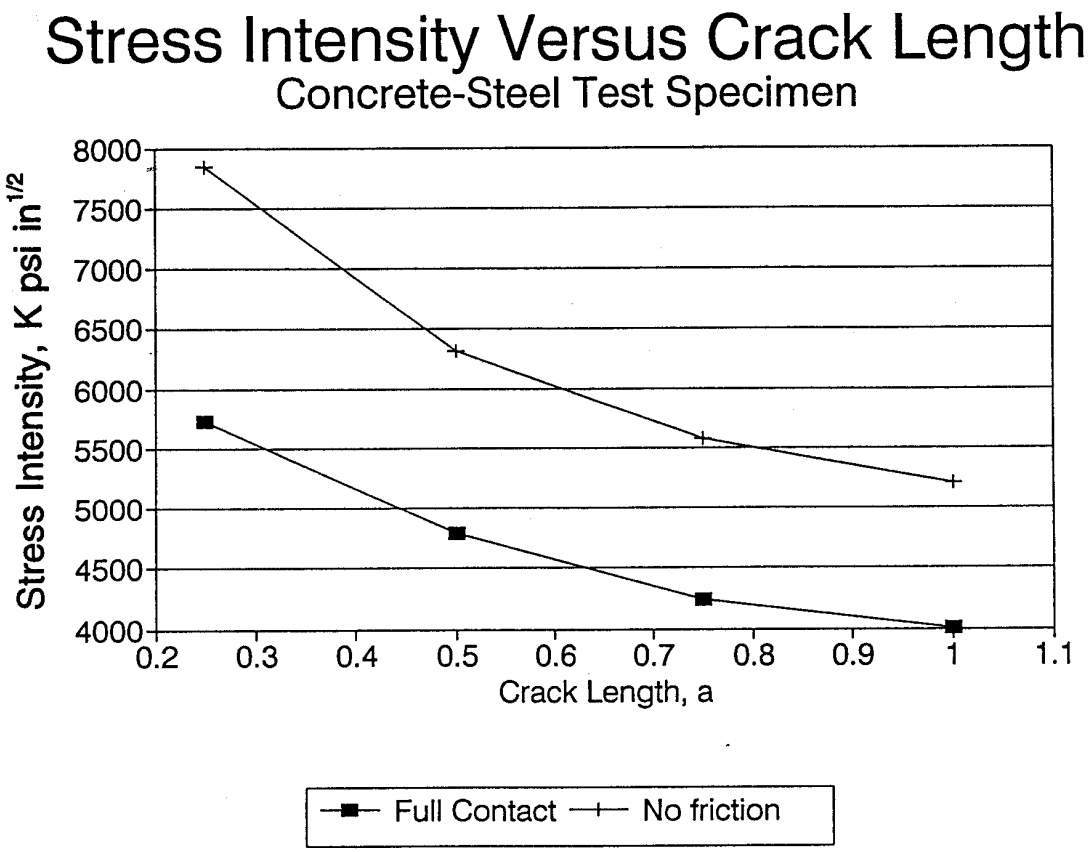

Figure 5.12 Computed Stress Intensity at the Tip of a Propagating Crack for the Cases of Full Rebar-Concrete Contact (Simulating Plain Rebar) and No Friction (ECR) as a function of Crack Length.

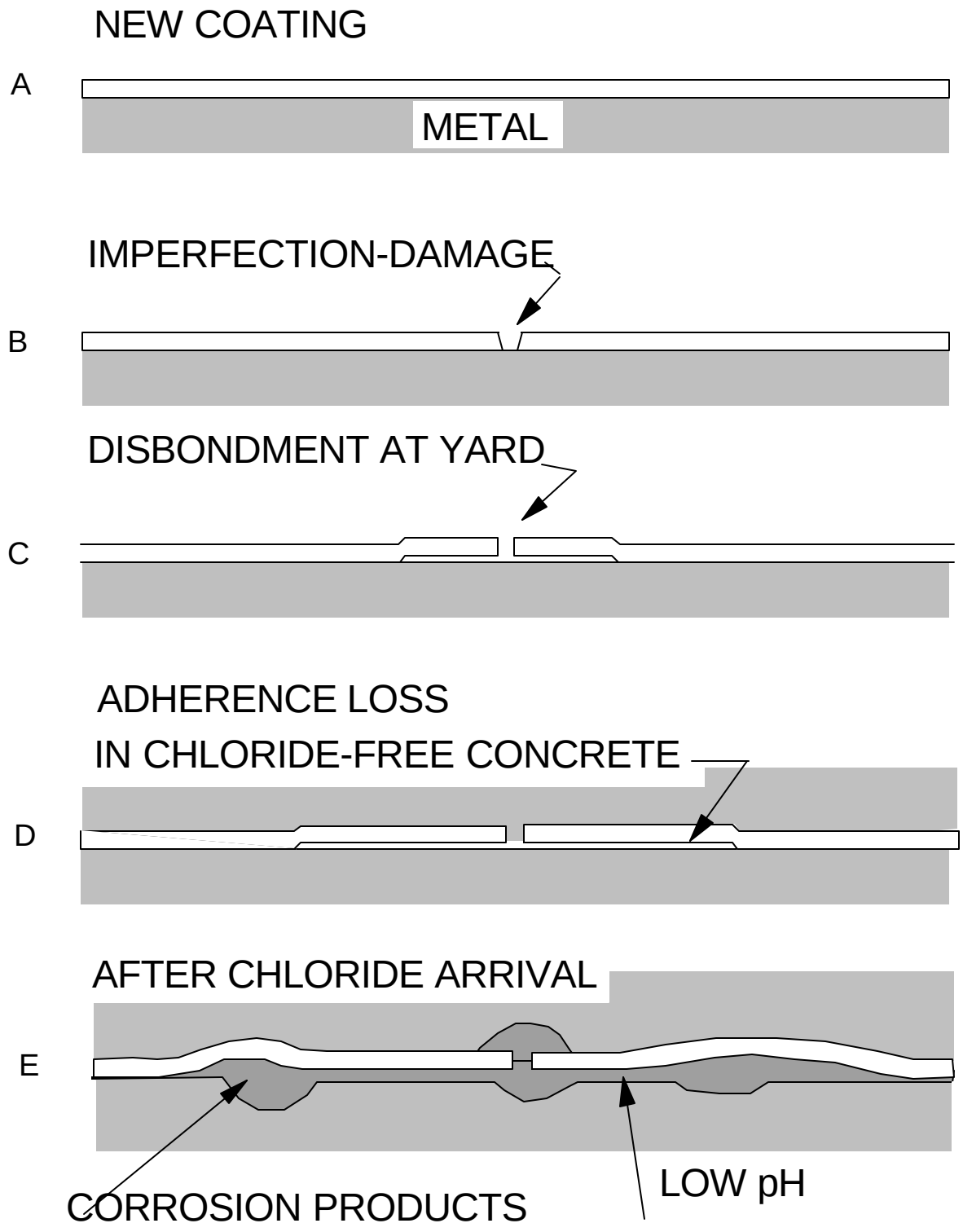

Figure 6.1 Summary of Steps in the Proposed Corrosion Mechanism.

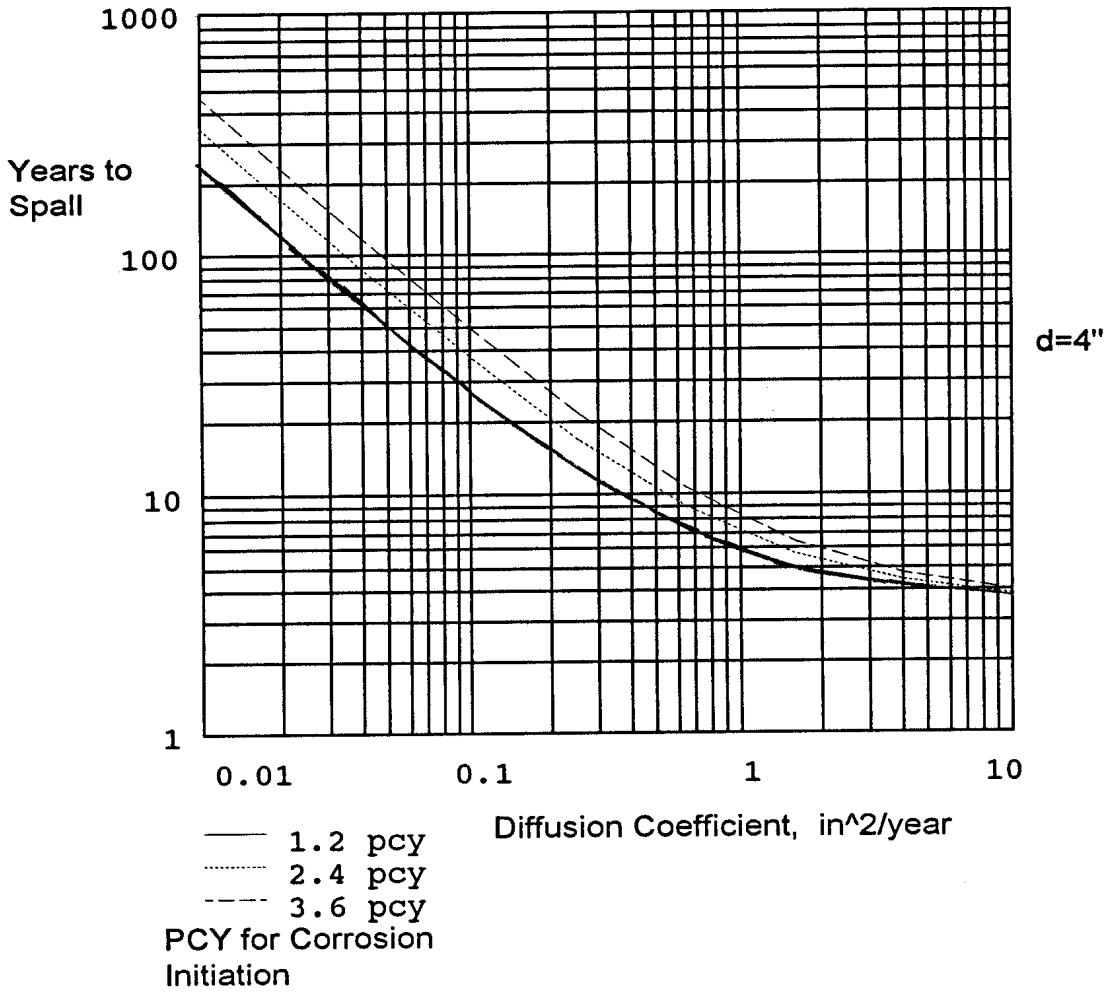

Figure 6.2 Computed Time to Appearance of a Concrete Spall for a Rebar Cover of 4 in, a Chloride Surface Concentration of 20 pcy, and Various Levels of Chloride Concentration Threshold as a Function of Effective Chloride Diffusivity. The Assumed Length of the Propagation Period is 3.5 Years.

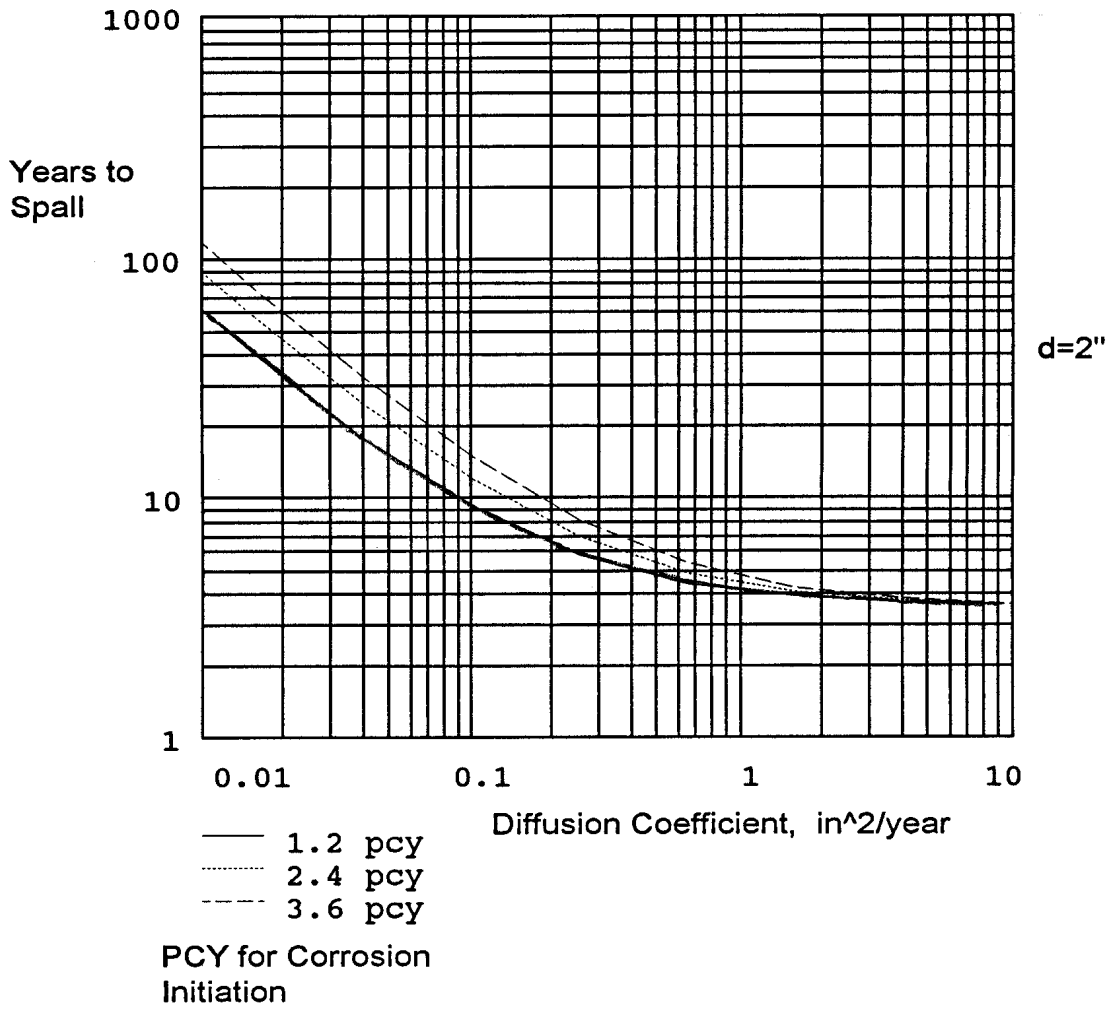

Figure 6.3 Computed Time to Appearance of a Concrete Spall for a Rebar Cover of 2 in, a Chloride Surface Concentration of 20 pcy, and Various Levels of Chloride Concentration Threshold as a Function of Effective Chloride Diffusivity. The Assumed Length of the Propagation Period is 3.5 Years.

APPENDIX 1. COMPUTATION OF EFFECTIVE CHLORIDE DIFFUSION COEFFICIENTS

The chloride concentration profiles were obtained from the field-extracted cores in the manner indicated in Section 2.3.4 and arranged as shown in Figure A1. The results were input to a MATHCAD 4.0 calculation sheet in the form of distance (slice centers) and concentration vectors as shown in Figure A2 (top). The time of exposure (six year in the example of Figure A2) was entered as the value of the variable t. The background concentration was estimated from the value of the chloride concentrations of the slices furthest away from the surface, and entered as the value of the variable c0. Because the slices were relatively thick, the concentration of each slice was expressed as the average indicated by the integral of the function F(d,D,cs). The calculation assumed that the concentration was related to distance from the surface d, surface concentration cs, effective diffusion coefficient D, base concentration c0 and exposure time t, by means of Eq.(2), Section 6.3.3.

The function F described the estimated concentration at the center of the slice. A deviation function s(D,cs) was defined as the sum of the squares of the differences between estimated and measured concentrations. The s function was minimized by choice of the optimal D and cs values, using the MATHCAD operation Minerr for D and sweeping through a range of cs values chosen by trial and error. The choice of cs was refined manually (usually involving two or three iterations) until an absolute minimum of cs (ERR) was identified. The graphic display of the possible values of D aided in establishing the minimum and in indicating sensitivity of results to parameter choices. The bottom graph displayed the fit and measured values to further aid in assessing the adequacy of the fit. The values of cs, c0 and D were the sheet output.

FLORIDA DEPARTMENT OF TRANSPORTATION

LAWTON CHILES
GOVERNOR

BEN G. WATTS
SECRETARY

CORROSION RESEARCH

LABORATORY

MISCELLANEOUS TEST REPORT

Bridge: 700181
Report Date: 8/23/91

Core No: 079
Lab No: 692

Submitted By: Ivan Lasa

SAMP	CORE NO	PIER NO	ELEV AHT	INCH MARK 0-1	1-2	2-3	3-4	4-5	5-6	6-7	7-8	8-9
A	79	05	24	11.60	5.64	2.76	.63	.28	.26	.04	.21	.20

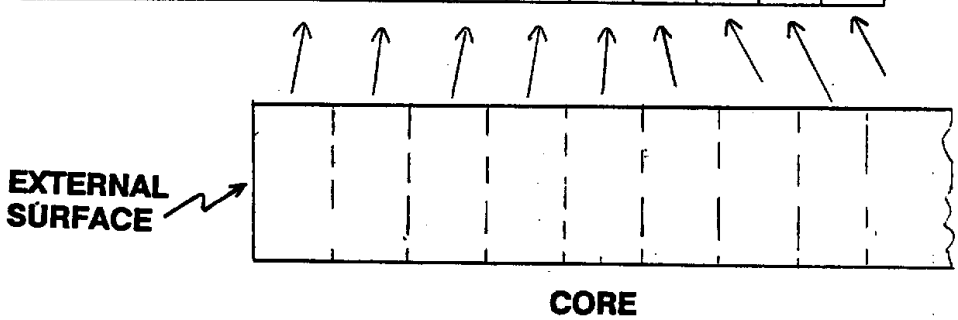

Figure A1 Example of Chloride Profile Data Sheet for a Field-extracted Core.

Bridge 700181 INDIAN RIVER
Core No. 79 24" AHT
Pier No. 5
File chlori 14

$$c := \begin{bmatrix} 11.6 \\ 5.64 \\ 2.76 \\ 0.63 \\ 0.28 \\ 0.26 \\ 0.04 \\ 0.21 \\ 0.2 \end{bmatrix} \quad d := \begin{bmatrix} 0.5 \\ 1.5 \\ 2.5 \\ 3.5 \\ 4.5 \\ 5.5 \\ 6.5 \\ 7.5 \\ 8.5 \end{bmatrix}$$

$t := 6$

$c0 := .16$

$$F(d, D, cs) := cs - (cs - c0) \cdot \left[\int_{d-0.5}^{d+.5} \operatorname{erf}\left[\frac{d}{\left[2\sqrt{(|D|t)}\right]} \right] dd \right]$$

$i := 0..8$

$$s(D, cs) := \sum_i \left(c_i - F(d_i, D, cs)\right)^2$$

$D := .1$

Given

$s(D, cs) = 0$

$f(cs) := \text{Minerr}(D)$

$j := 0..3 \quad cs_j := 11 + 3j$

$f_j := f(cs_j) \quad DC_j := |f_j| \quad g_j := s(f_j, cs_j)$

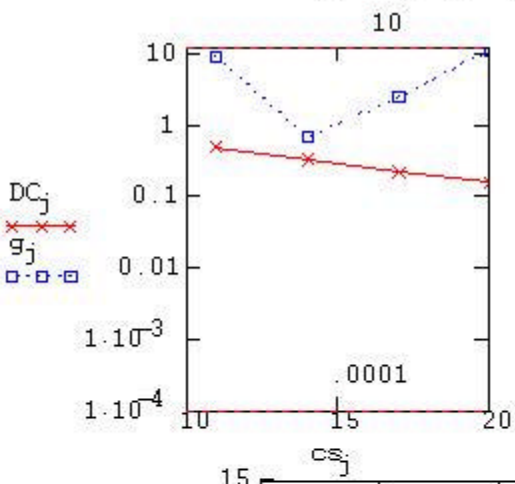

$j := 1$

$Dc := |f_j|$

$CS := cs_j$

$ERR := g_j$

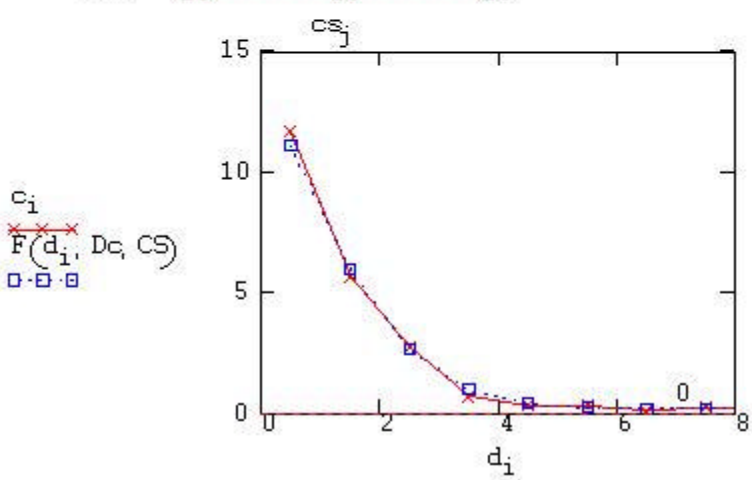

$Dc = 0.274$

$ERR = 0.556$

$CS = 14$

$c0 = 0.16$

Figure A2 Example of Computation of Effective Chloride Diffusion Coefficient From Profile Data